Watching Nanomaterials with X-rays Eyes

Consiglio Nazionale delle Ricerche
Dipartimento Scienze Chimiche e Tecnologie dei Materiali

DSCTM
Dipartimento Scienze Chimiche e Tecnologie dei Materiali

Dr. Cinzia Giannini
CNR - **Istituto di Cristallografia BARI**
Email: cinzia.giannini@ic.cnr.it

ICCI
CNR Istituto di Cristallografia

DSCTM
Dipartimento Scienze Chimiche e Tecnologie dei Materiali

xmi l@b

A NANOMATERIALS ROADMAP

2000 2005 2010 2015 2020 2025

Complexity

Nanoscale Building Blocks – variety of shape, size, composition

SCIENCE

Specialty Coatings

Surface/Interface Control

Mechanical properties at nanoscale

Lightweight Structures

Nanostructured Polymers

Selectively Permeable Membranes

Nanostructure in metals

Directed, Self Assembled Materials

Fuel Cell/Solar Cell

Hierarchically-Structured Materials

High Power Ceramic

DEVICE/APPLICATION

Laser

3-D Nanofabrication

Multifunction composites

Integrated model nano-macro

Smart/Interactive Textiles

Biointeractive

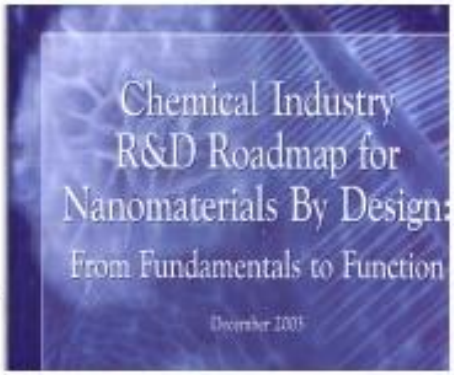

"Aldrich" catalog of nanostructures

Cost effective 3-D nanoassembly

Plethora of systems with "Nano inside"

http://www.chemicalvision2020.org/nanomaterialsroadmap.html

Slide Provided by Jim Murday, NRL

APPLICATIONS

Nanoelectronics

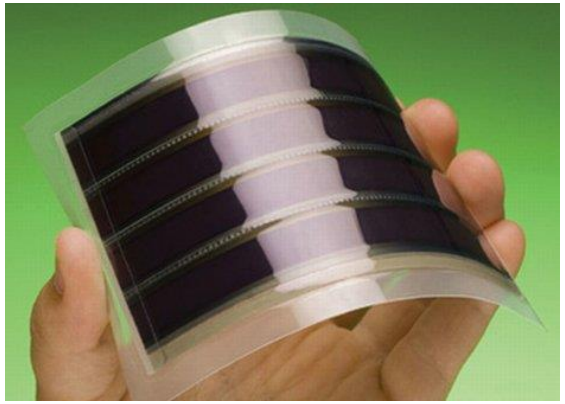

Flexible screens

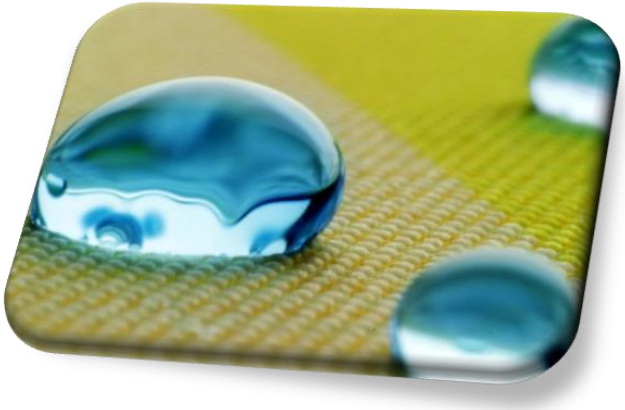

Smart Surfaces

Health

Health

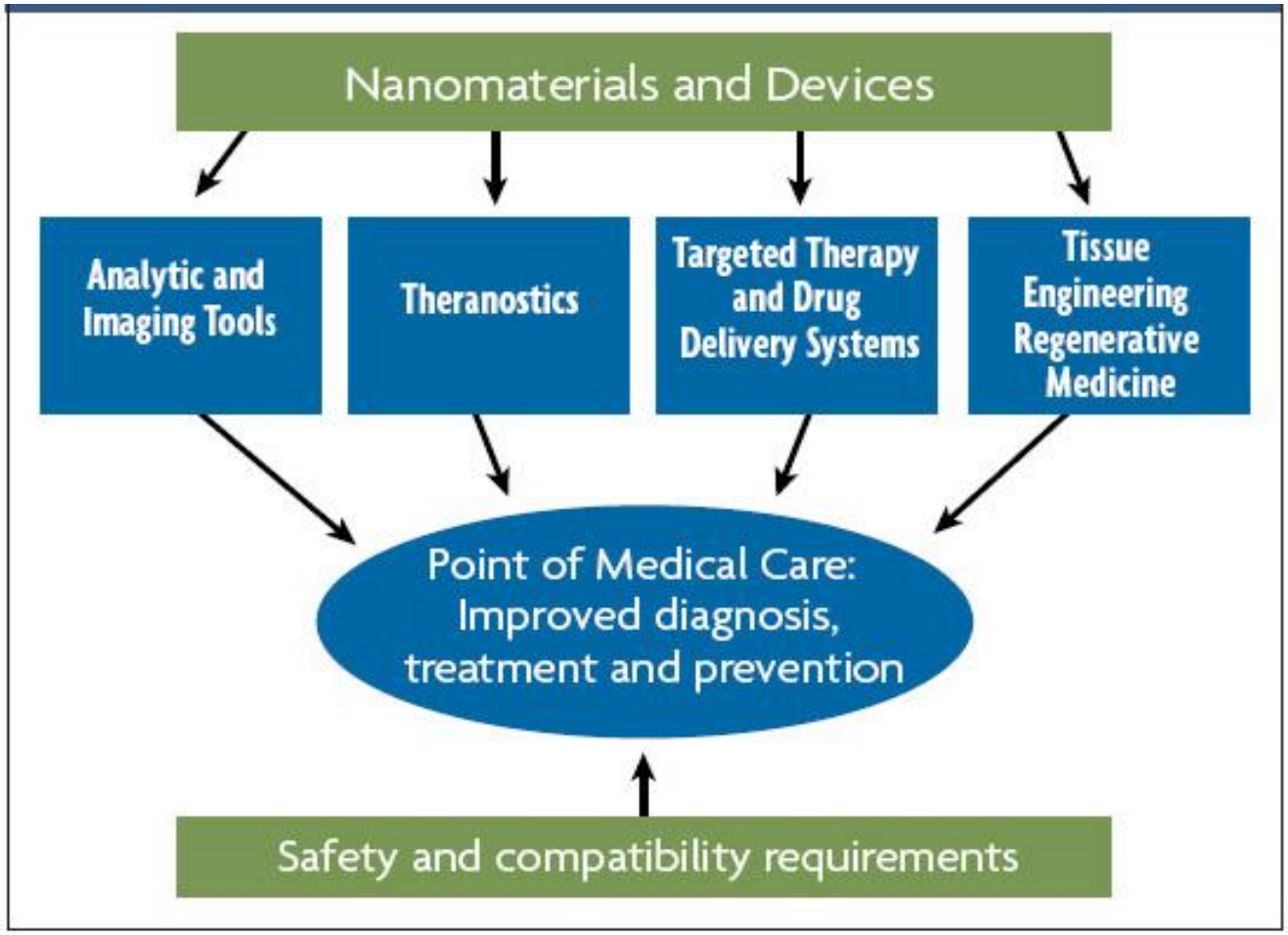

MC Rocho et al. US National Science Foundation. Science Policy Report, 2011.

Pharmaceutic industrial applications

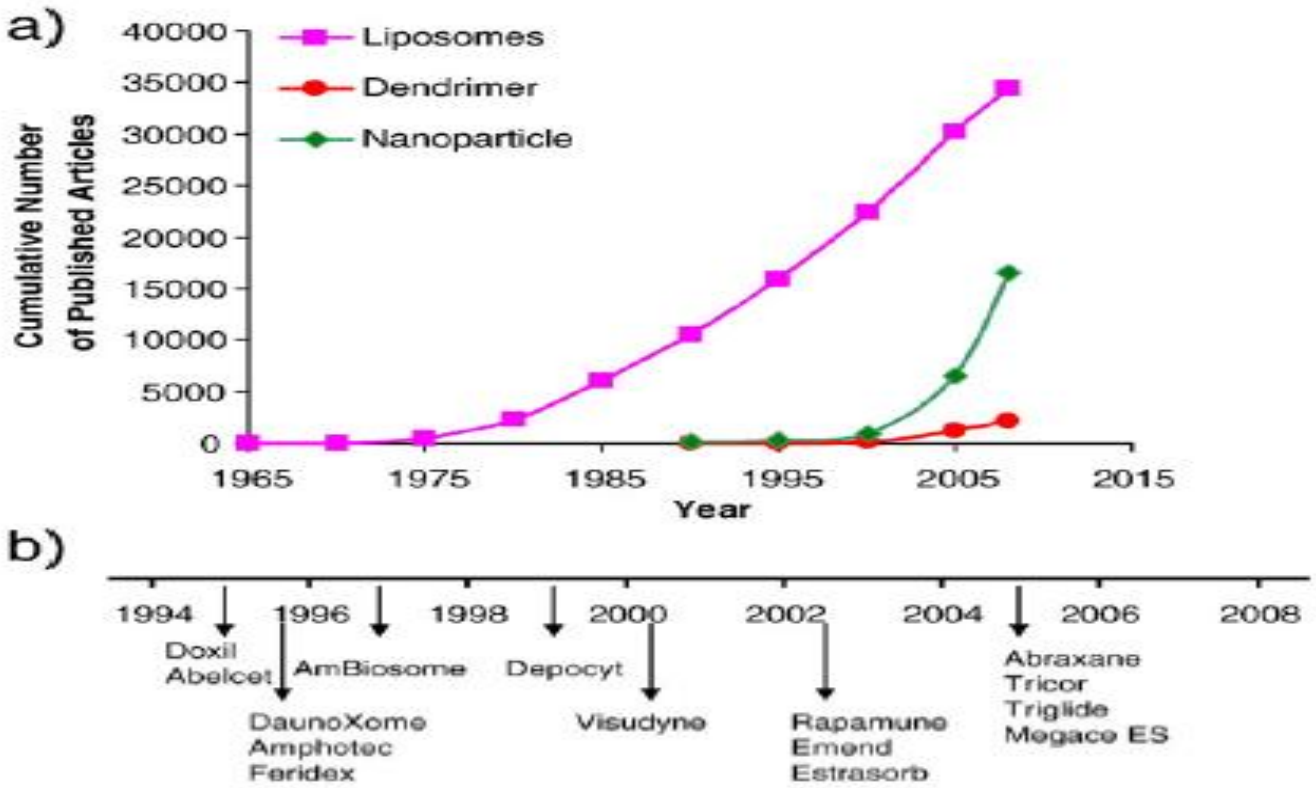

Fig. 1. a) The number of published nanomedicine related articles since 1965. b) Timeline of the FDA approved drugs in nanometer size range.

MC Rocho et al. US National Science Foundation. Science Policy Report, 2011.

Pharmaceutic industrial applications

Table 1 | **Nanoscaled systems for systemic cancer therapy**

Platform	Latest stage of development	Examples
Liposomes	Approved	DaunoXome, Doxil
Albumin-based particles	Approved	Abraxane
PEGylated proteins	Approved	Oncospar, PEG-Intron, PEGASYS, Neulasta
Biodegradable polymer–drug composites	Clinical trials	Doxorubicin Transdrug
Polymeric micelles	Clinical trials	Genexol-PM*, SP1049C, NK911, NK012, NK105, NC-6004
Polymer–drug conjugate-based particles	Clinical trials	XYOTAX (CT-2103), CT-2106, IT-101, AP5280, AP5346, FCE28068 (PK1), FCE28069 (PK2), PNU166148, PNU166945, MAG-CPT, DE-310, Pegamotecan, NKTR-102, EZN-2208
Dendrimers	Preclinical	Polyamidoamine (PAMAM)
Inorganic or other solid particles	Preclinical (except for gold nanoparticle that is clinical)	Carbon nanotubes, silica particles, gold particles (CYT-6091)

*Approved in South Korea. PEG, polyethylene glycol.

Key properties of anticancer nanoparticles: nanoparticle **4S**

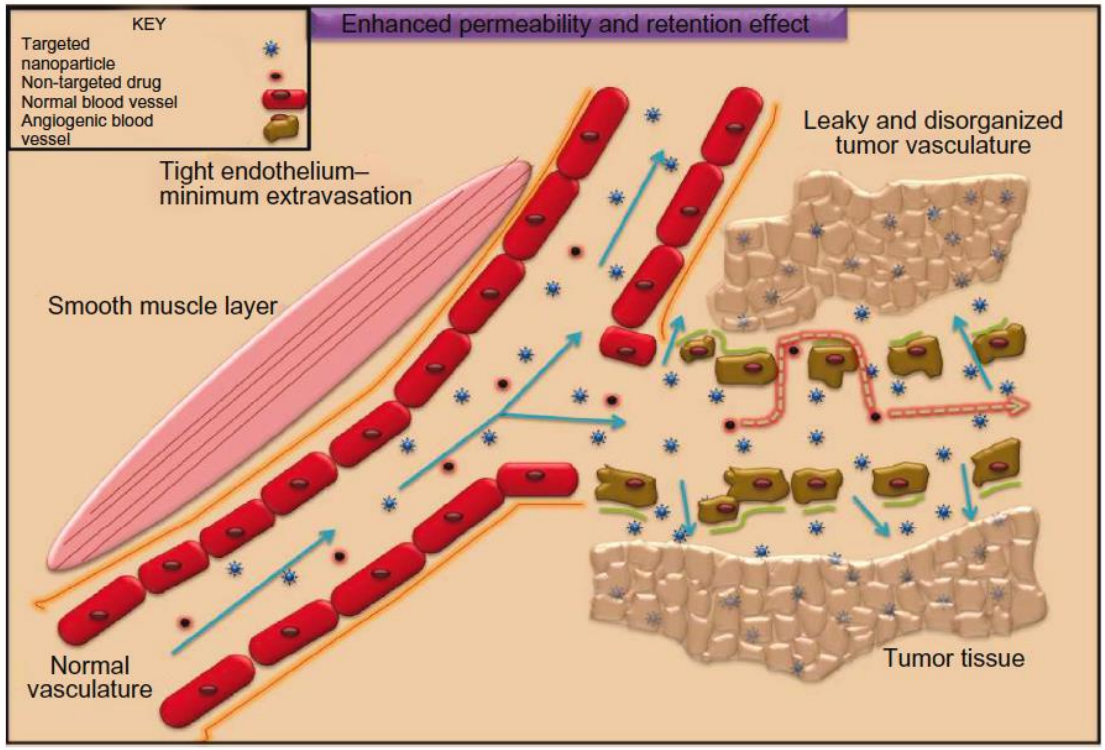

- Nanoparticles can be tuned to provide long or short **circulation times** by careful control of **size/shape** and **surface/stiffness** properties

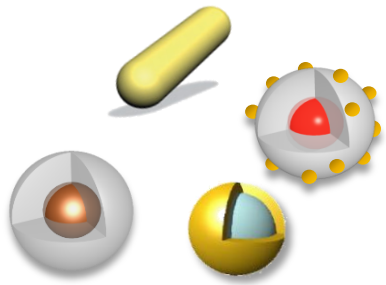

nanocrystals and nanoparticles share the same size regime of biologically relevant systems and components

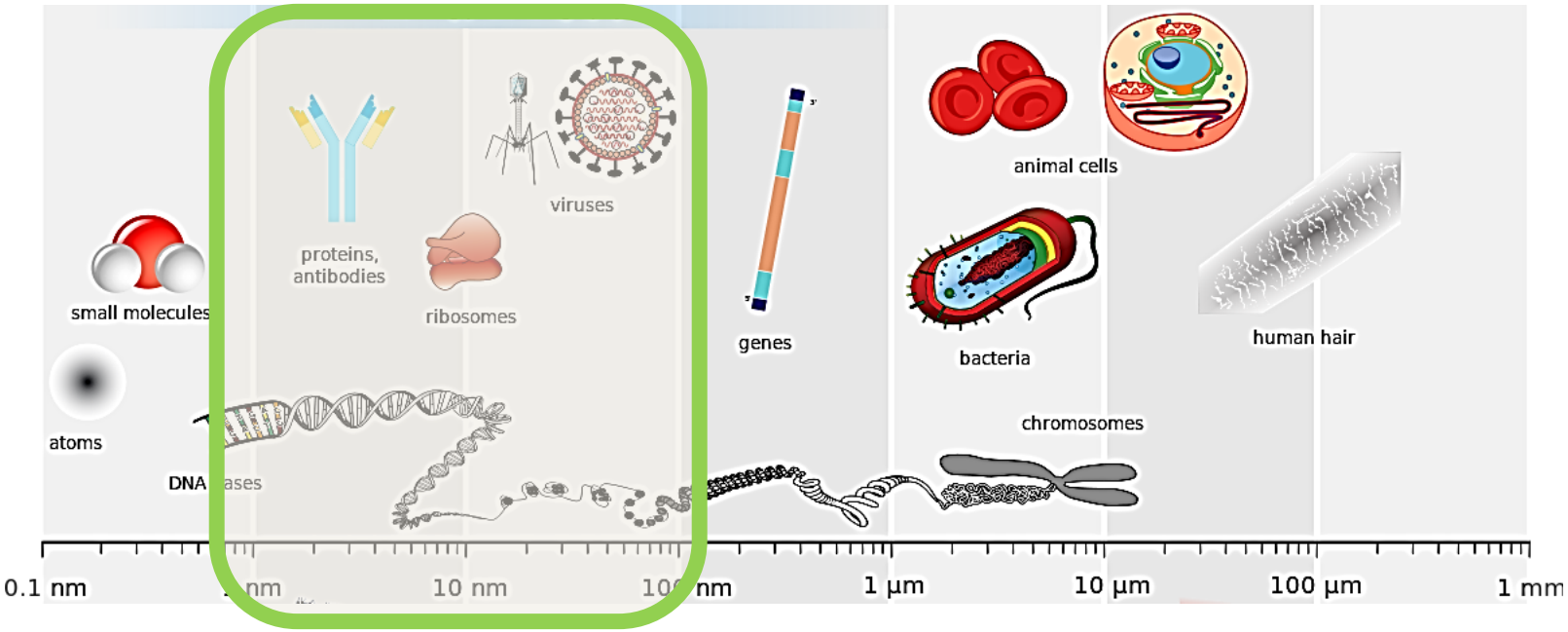

Percentage of Surface Atoms

Surface to Bulk Atom Ratio

Full-shell Clusters		Total Number of Atoms	Surface Atoms (%)
1 Shell		13	92
2 Shells	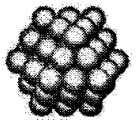	55	76
3 Shells	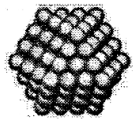	147	63
4 Shells	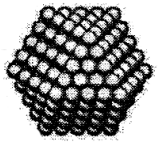	309	52
5 Shells	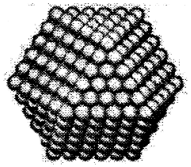	561	45
7 Shells	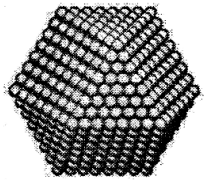	1415	35

Nanoscale Materials in Chemistry, Ed. K.J. Klabunde, Wiley, 2001

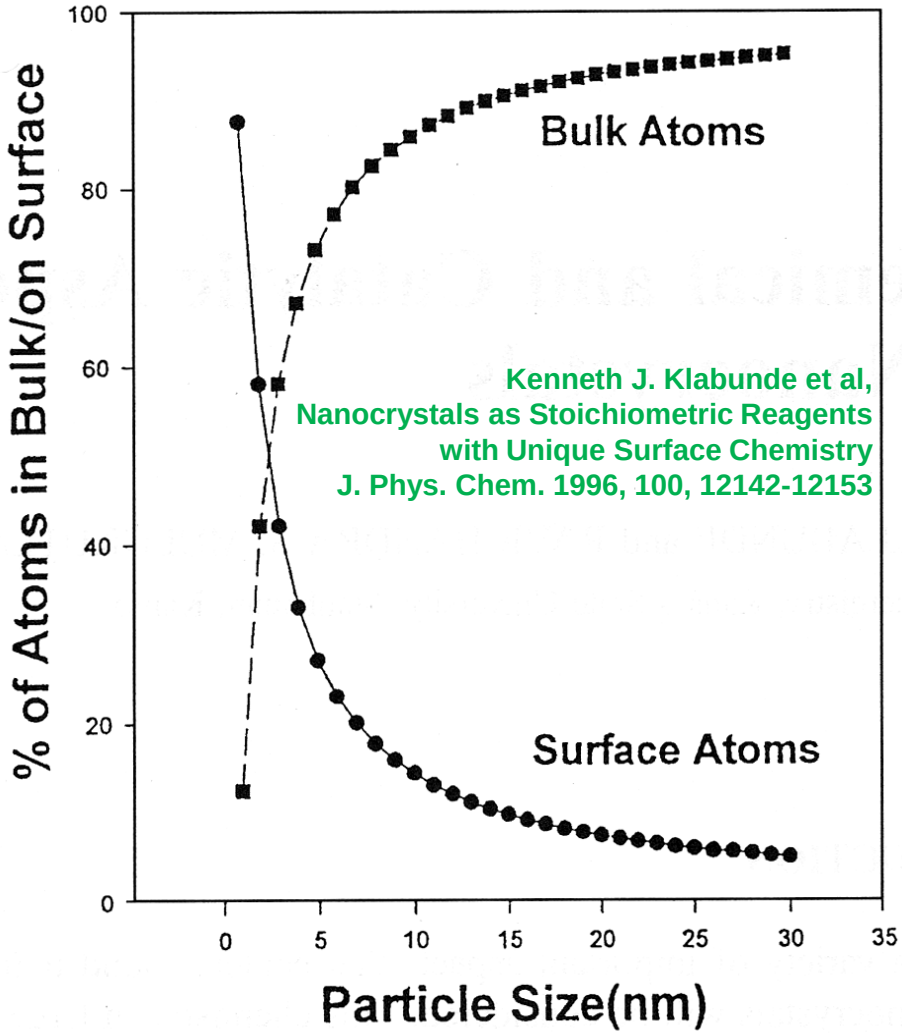

Kenneth J. Klabunde et al,
Nanocrystals as Stoichiometric Reagents
with Unique Surface Chemistry
J. Phys. Chem. 1996, 100, 12142-12153

PASSIVE/ACTIVE Nanomaterials: chemistry & morphology

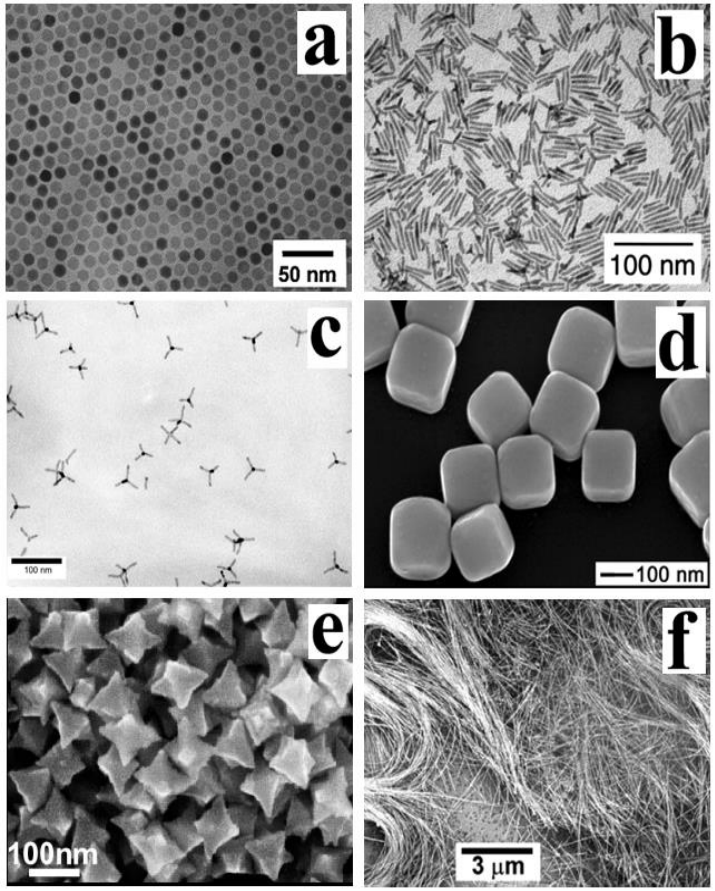

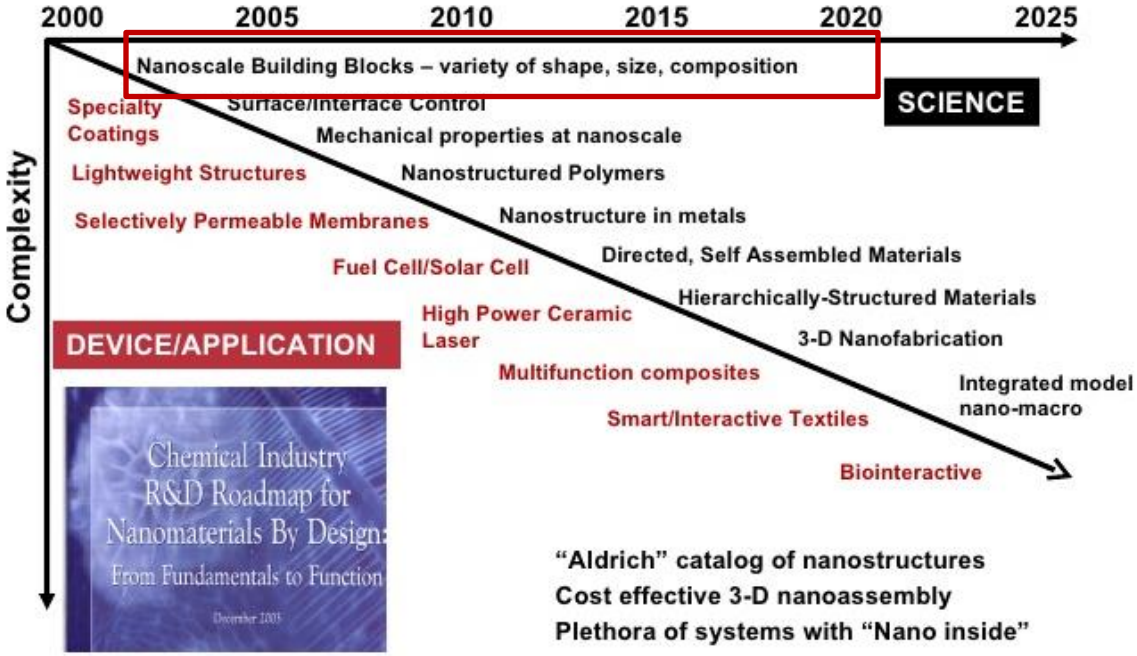

http://www.chemicalvision2020.org/nanomaterialsroadmap.html

Slide Provided by Jim Murday, NRL

What is the structure?

crystals

MDPI

Review

X-ray Diffraction: A Powerful Technique for the Multiple-Length-Scale Structural Analysis of Nanomaterials

Cinzia Giannini *, Massimo Ladisa, Davide Altamura, Dritan Siliqi, Teresa Sibillano and Liberato De Caro

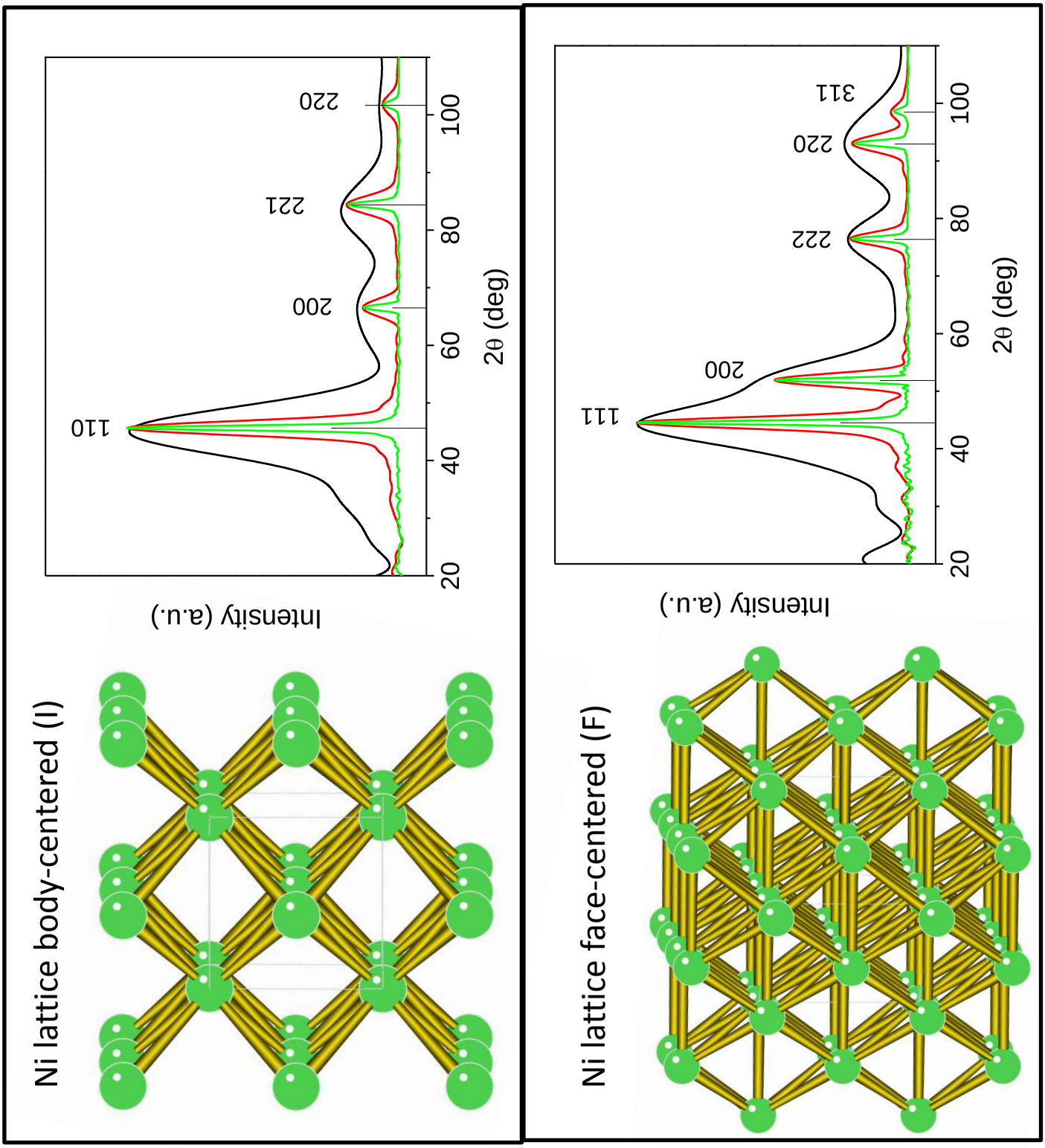

What is the structure?

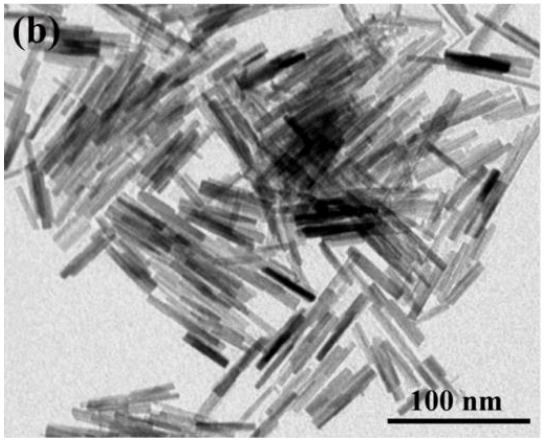

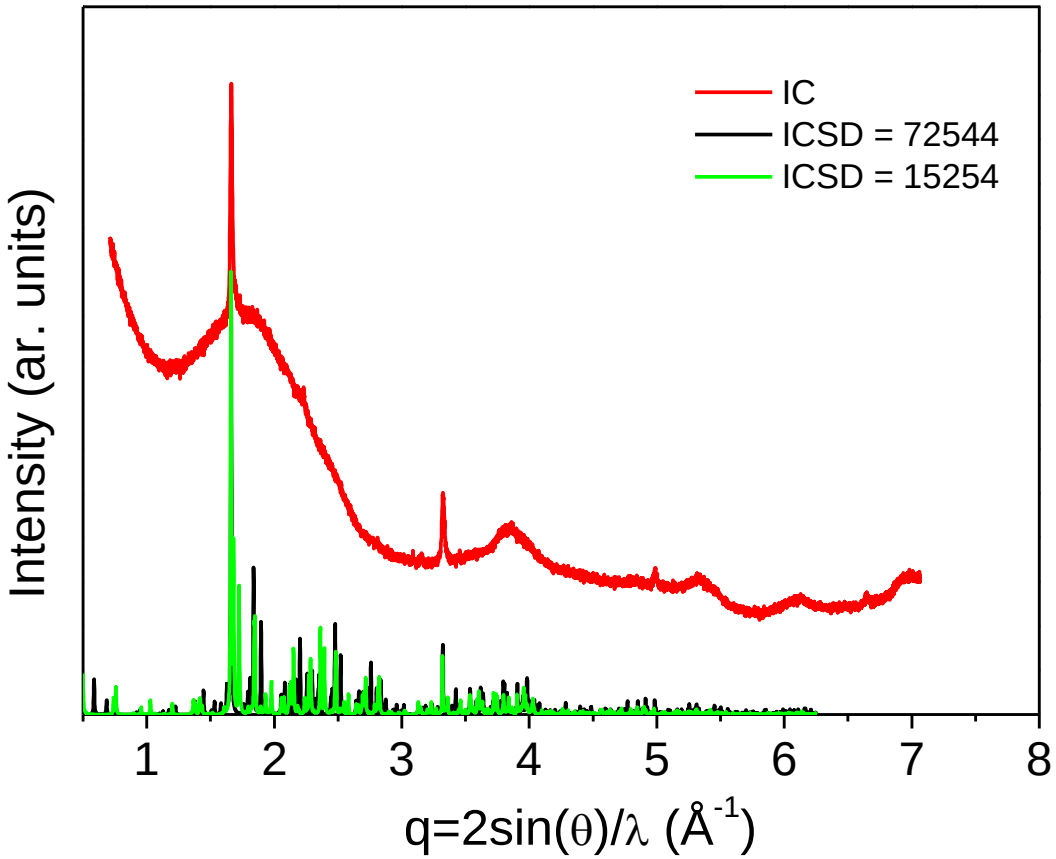

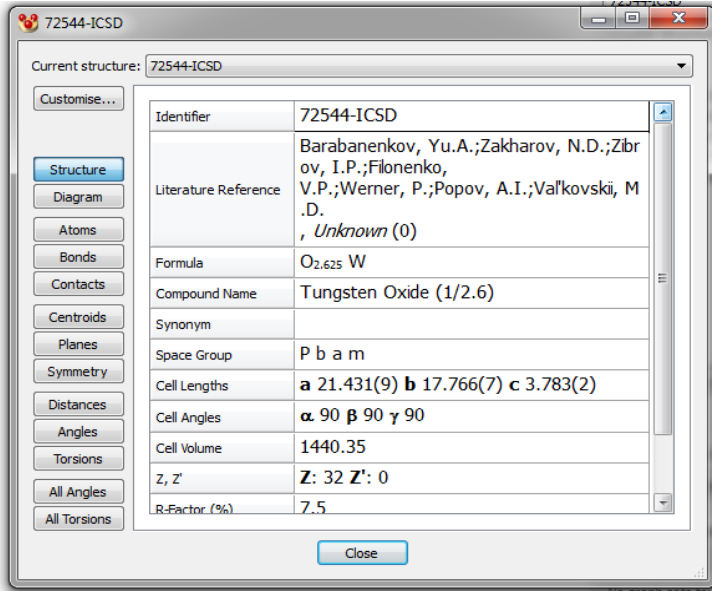
72544-ICSD
Current structure: 72544-ICSD
Customise...
Structure
Diagram
Atoms
Bonds
Contacts
Centroids
Planes
Symmetry
Distances
Angles
Torsions
All Angles
All Torsions
Identifier 72544-ICSD
Literature Reference Barabanenkov, Yu.A.;Zakharov, N.D.;Zibrov, I.P.;Filonenko, V.P.;Werner, P.;Popov, A.I.;Val'kovskii, M.D. , Unknown (0)
Formula O2.625 W
Compound Name Tungsten Oxide (1/2.6)
Synonym
Space Group P b a m
Cell Lengths a 21.431(9) b 17.766(7) c 3.783(2)
Cell Angles α 90 β 90 γ 90
Cell Volume 1440.35
Z, Z' Z: 32 Z': 0
R-Factor (%) 7.5
Close

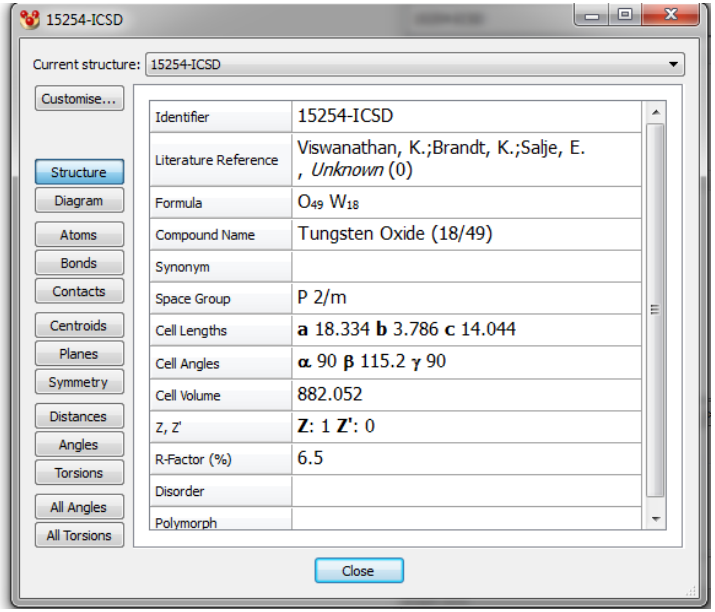
15254-ICSD
Current structure: 15254-ICSD
Customise...
Structure
Diagram
Atoms
Bonds
Contacts
Centroids
Planes
Symmetry
Distances
Angles
Torsions
All Angles
All Torsions
Identifier 15254-ICSD
Literature Reference Viswanathan, K.;Brandt, K.;Salje, E. , Unknown (0)
Formula O49 W18
Compound Name Tungsten Oxide (18/49)
Synonym
Space Group P 2/m
Cell Lengths a 18.334 b 3.786 c 14.044
Cell Angles α 90 β 115.2 γ 90
Cell Volume 882.052
Z, Z' Z: 1 Z': 0
R-Factor (%) 6.5
Disorder
Polymorph
Close

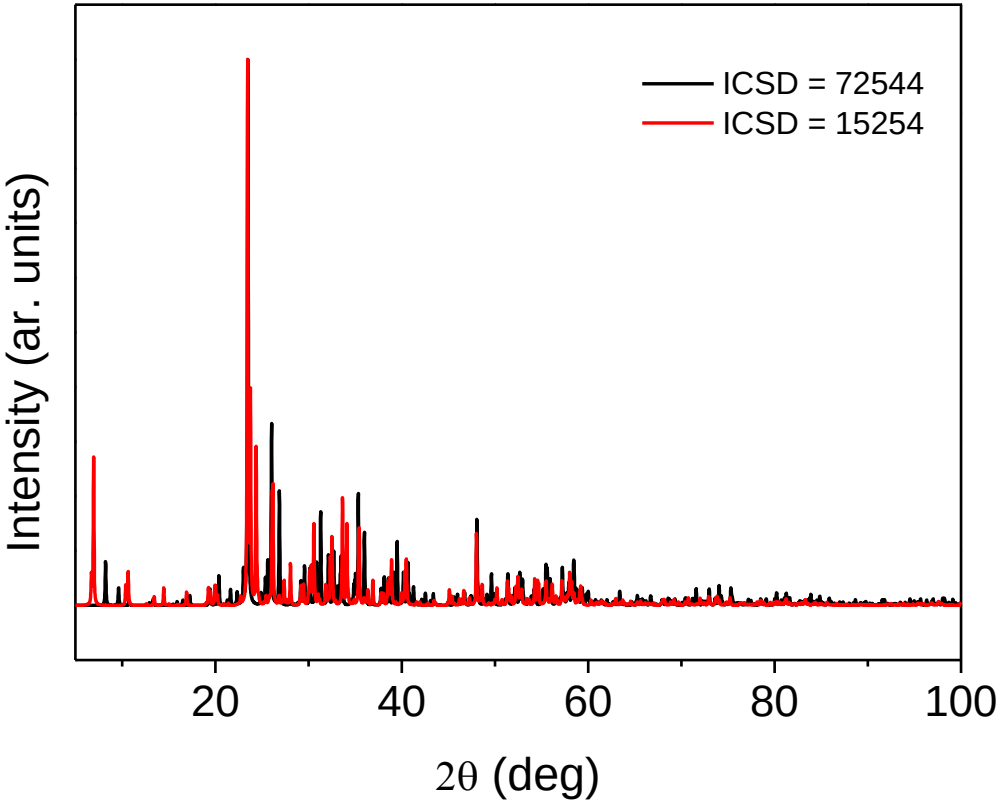
ICSD = 72544
ICSD = 15254
Intensity (ar. units)
20
40
60
80
100
2θ (deg)

What is the structure?

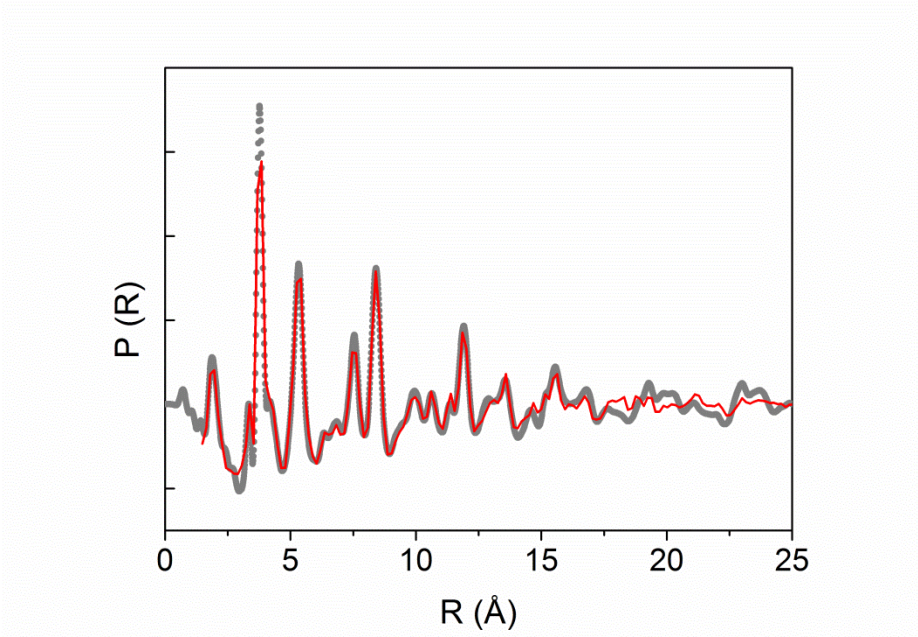

$W_{32}O_{84}$ (ICSD=72544)

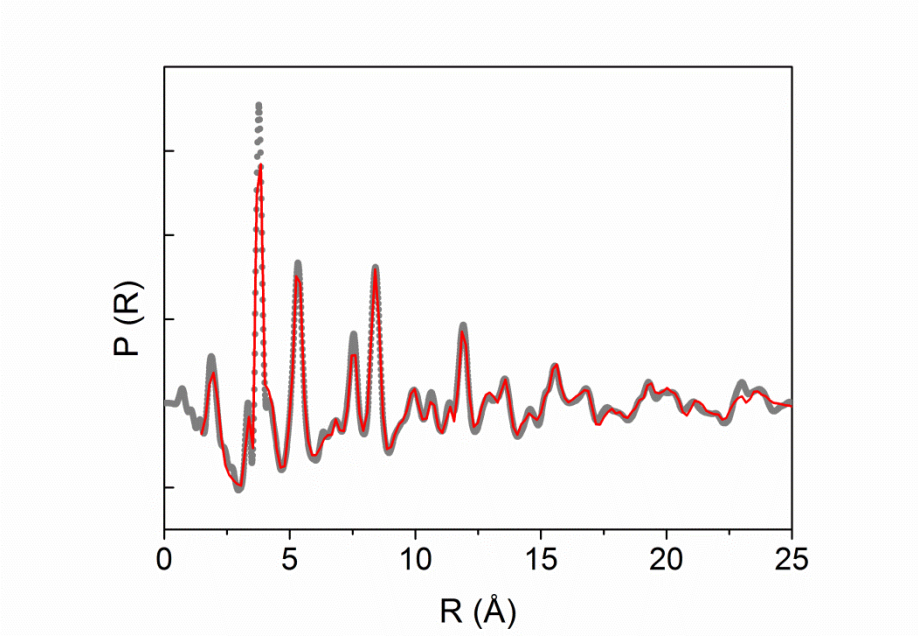

$W_{18}O_{49}$ (ICSD=15254)

Results of the PDF data allowed to identify the **monoclinic $W_{18}O_{49}$ crystal phase** (ICSD # 15254); fitting proved that the actual stoichiometry was **$W_{16\pm0.4}O_{45\pm3}$**


ChemPubSoc Europe
DOI: 10.1002/cphc.201501175
CHEMPHYSCHEM Articles

Static and Dynamical Structural Investigations of Metal-Oxide Nanocrystals by Powder X-ray Diffraction: Colloidal Tungsten Oxide as a Case Study

Rocco Caliandro,*[a] Teresa Sibillano,[a] B. Danilo Belviso,[a] Riccardo Scarfiello,[b, c, f] Jonathan C. Hanson,[d] Eric Dooryhee,[e] Michele Manca,[c] P. Davide Cozzoli,[b, f] and Cinzia Giannini*[a]

What is the size?

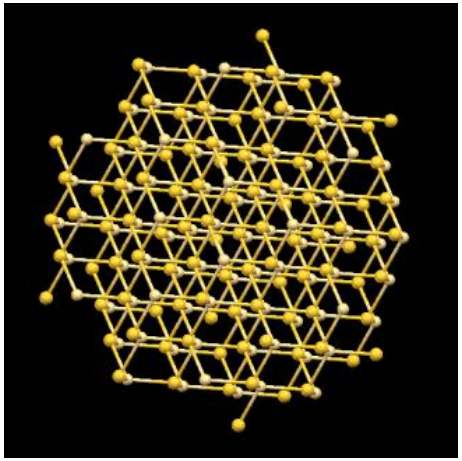

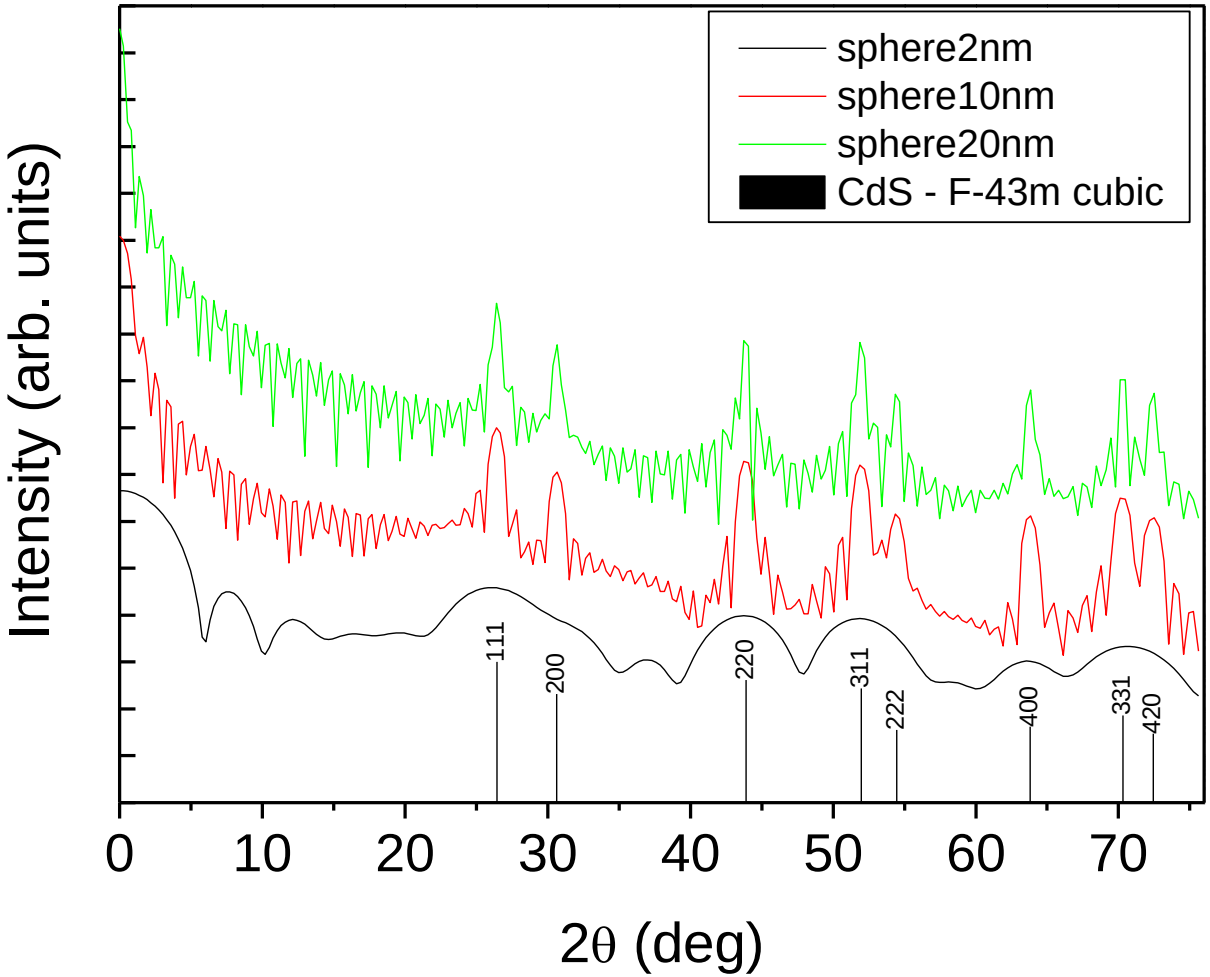

Crystal domain

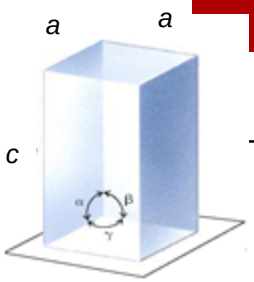

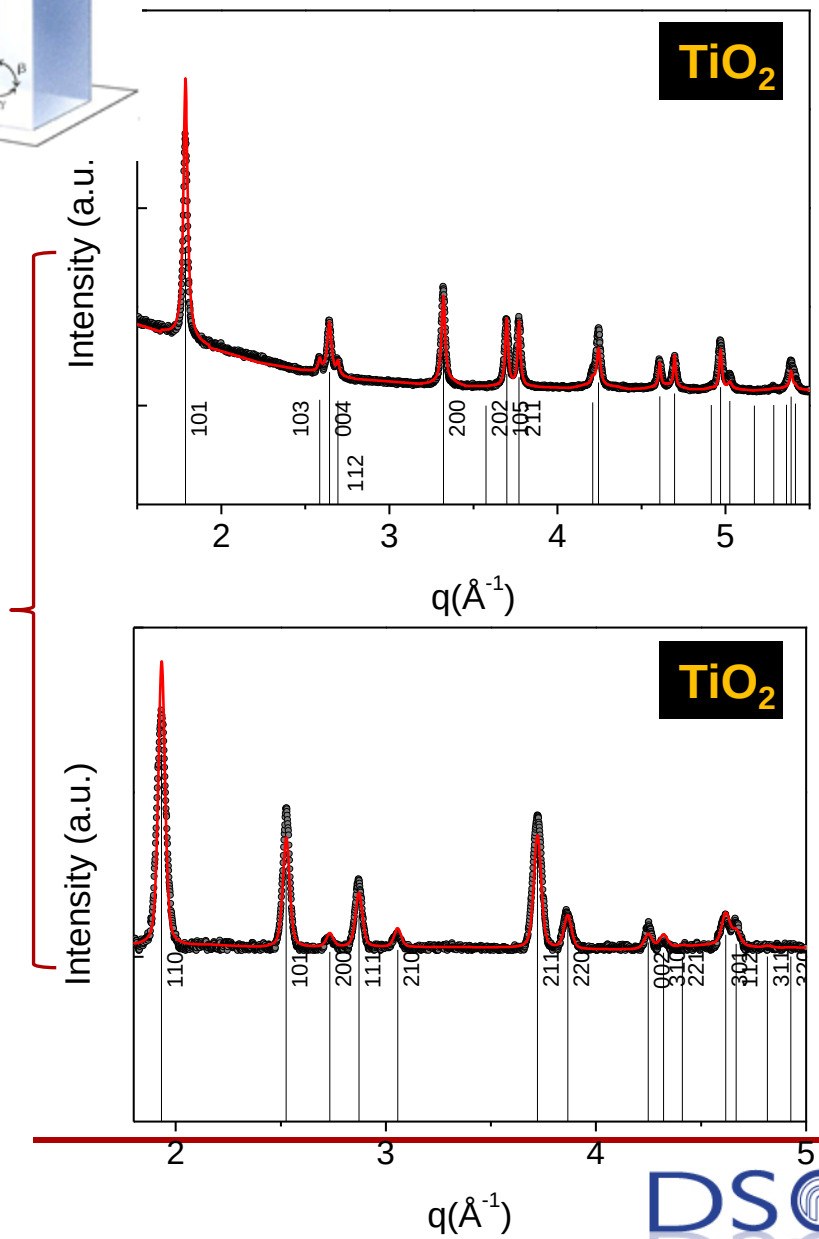

Three-step procedure:

1. **the instrumental resolution function (IRF)**

was evaluated by fitting the XRD pattern of a LaB_6 NIST standard recorded under the same experimental conditions.

2. **the crystal structure models** of the crystalline phases previously identified, here tetragonal TiO2 anatase (space group I41/amd; cell parameters: a=b=3.7835430 Å and c =9.614647 Å; α=β=γ=90°) and tetragonal TiO2 rutile (space group p 42/m n m; cell parameters: a=b = 4.59365Å; c=2.95874 Å; α= β =γ=90°) were provided to the program.

Crystal domain

Three-step procedure:

3. the inhomogeneous peak broadening of the XRD pattern reflections was described by a phenomenological model based on a modified Scherrer formula:

$$\beta_{h,k,l} = \frac{\lambda}{h\cos\theta} = \frac{\lambda}{\cos\theta}\sum_{imp} a_{imp} y_{imp}(\theta_h, \Phi_h)$$

size contribution to the integral width of the (h,k,l) reflection

real spherical harmonics

Crystal Lattice	Material	Space Group	a,b,c [Å]	Size [Å]	Size [Å]
Cubic	Cu-copper	F m−3 m	a = b = c = 3.623	159 [111]	95 [200]
Monoclinic	CuO-tenorite	C 2/c	a = b = 4.685 c = 5.128	244	244
Tetragonal	TiO_2-anatase	I 41/a m d	a = b = 3.784 c = 9.508	162 [200]	139 [004]
Tetragonal	TiO_2-rutile	P 42/m n m	a = b = 4.597 c = 2.958	233	233
Hexagonal	$Ca_5(PO_4)_3(OH)$-hydroxyapatite	P 63/m	a = b = 9.465 c = 6.9095	210 [002]	25 [110]

What is the size/shape?

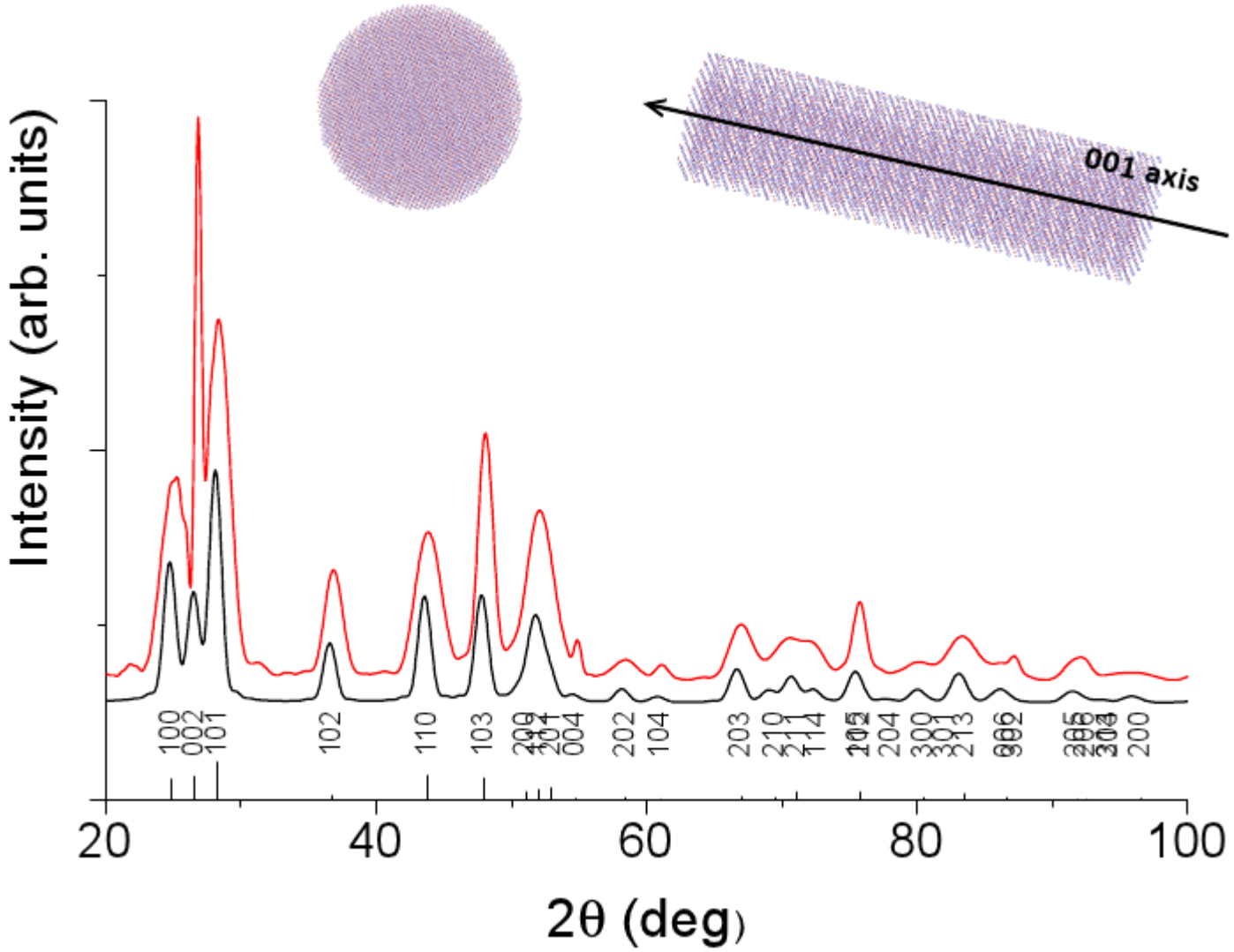

What is the size/shape?

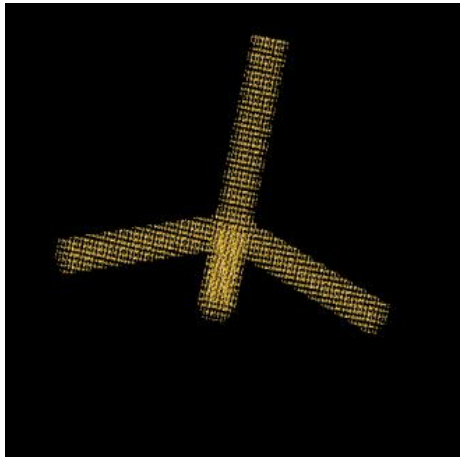

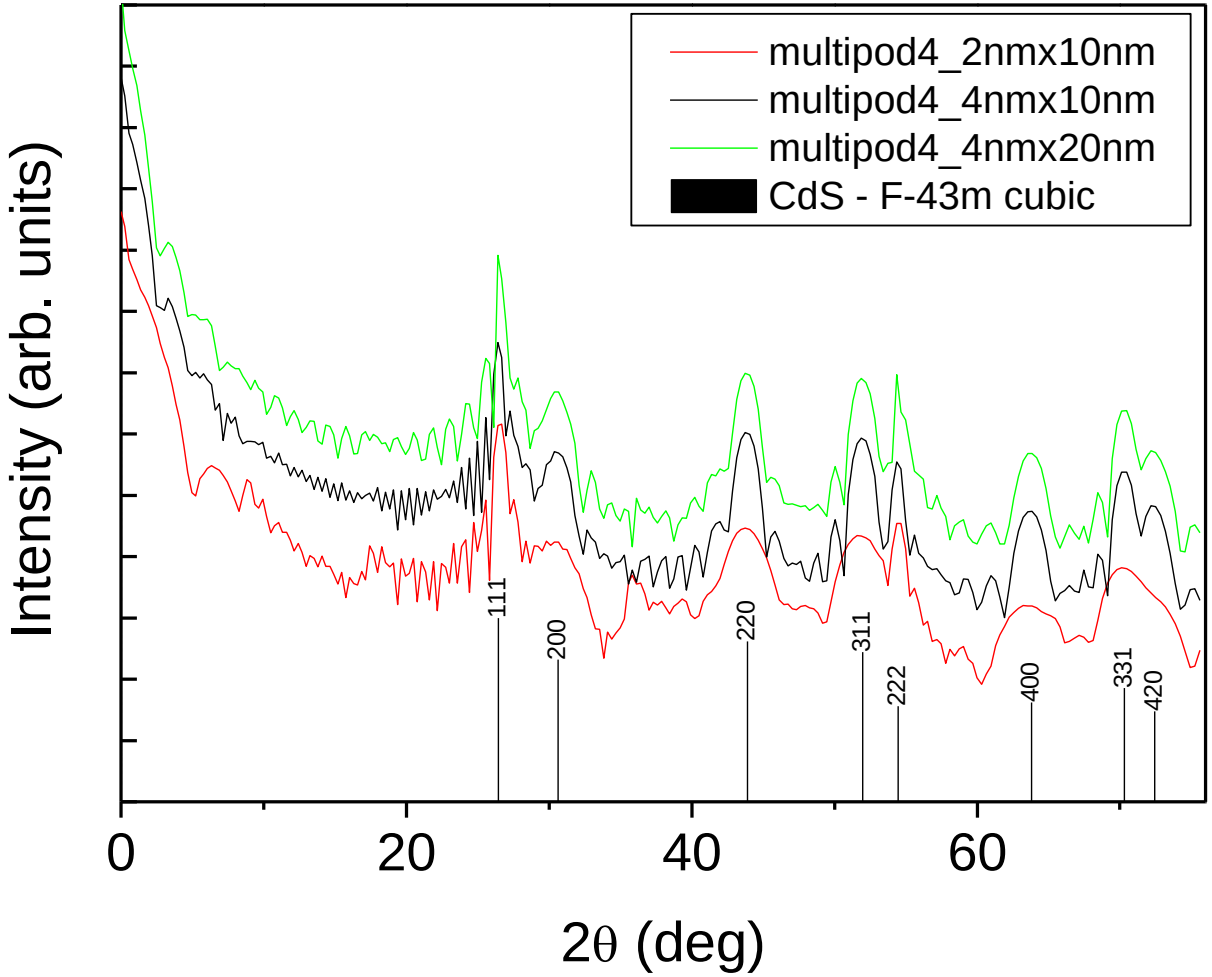

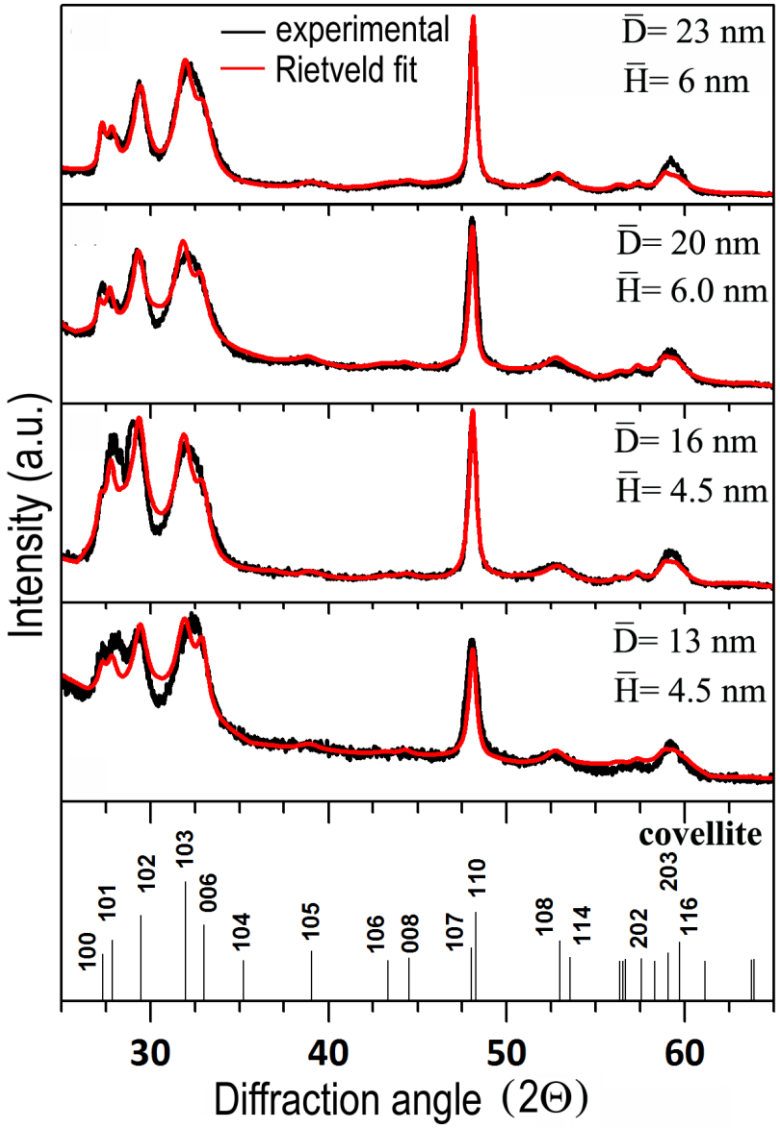

ACS NANO

Metallic-like Stoichiometric Copper Sulfide Nanocrystals: Phase- and Shape-Selective Synthesis, Near-Infrared Surface Plasmon Resonance Properties, and Their Modeling

Yi Xie †, Luigi Carbone §*, Concetta Nobile §, Vincenzo Grillo ⊥‖, Stefania D'Agostino †#, Fabio Della Sala †§, Cinzia Giannini Δ, Davide Altamura Δ, Christian Oelsner ⊗, Carola Kryschi ⊗, and P. Davide Cozzoli §¶*

ACS Nano, **2013**, *7* (8), pp 7352–7369
DOI: 10.1021/nn403035s
Publication Date (Web): July 16, 2013

TABLE 1. Mean Coherent Domain Size, D_{hkl}, Estimated upon Rietveld-Fitting the XRD Patterns Shown in Figure 2

$\bar{D}$ (nm)[a]	$\bar{H}$ (nm)[a]	D_{110} (nm)[c]	D_{100} (nm)[c]	D_{006} (nm)[c]
13 ± 2	4.5 ± 0.5	15 ± 1	15 ± 2	8 ± 2
16 ± 2	5.5 ± 0.5	16 ± 1	16 ± 1	6 ± 1
20 ± 2	6.0 ± 0.5	20 ± 1	20 ± 1	6 ± 1
23 ± 2	6.0 ± 0.5	21 ± 1	22 ± 1	6 ± 1

[a] Mean sizes estimated by TEM by statistical analysis. [c] Minor discrepancies between the XRD-derived and TEM-measured sizes can be attributed to the presence of self-organized ND superstructures within the ND powders deposited on the silicon substrates for analysis. Micrometer-size domains of columnar face-to-face stacked NDs, in which the degree of intracolumnar ND ordering along the *c*-axis direction prevailed over the degree of intercolumnar alignment in the perpendicular orientations (Figure 1g—i), can be expected to hold higher structural coherence along the [001] and, to a lower extent, along the [010] and [110], relative to their fully disordered ND ensemble counterparts.

What is the effect of defects?

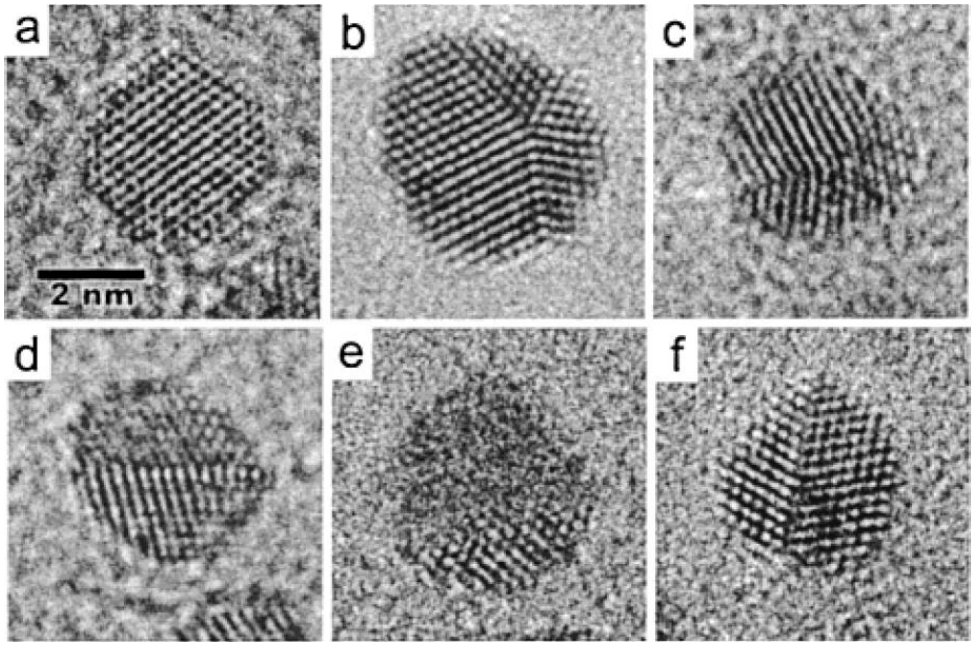

Typical HRTEM micrographs of gold NPs from a thiol-capped 4.1 nm sample.
(a) fcc clusters, (b and c) decahedra, (d-f) multidomain particles.

D. Zanchet et al J. Phys. Chem. B **2000,** *104,* 11013-11018

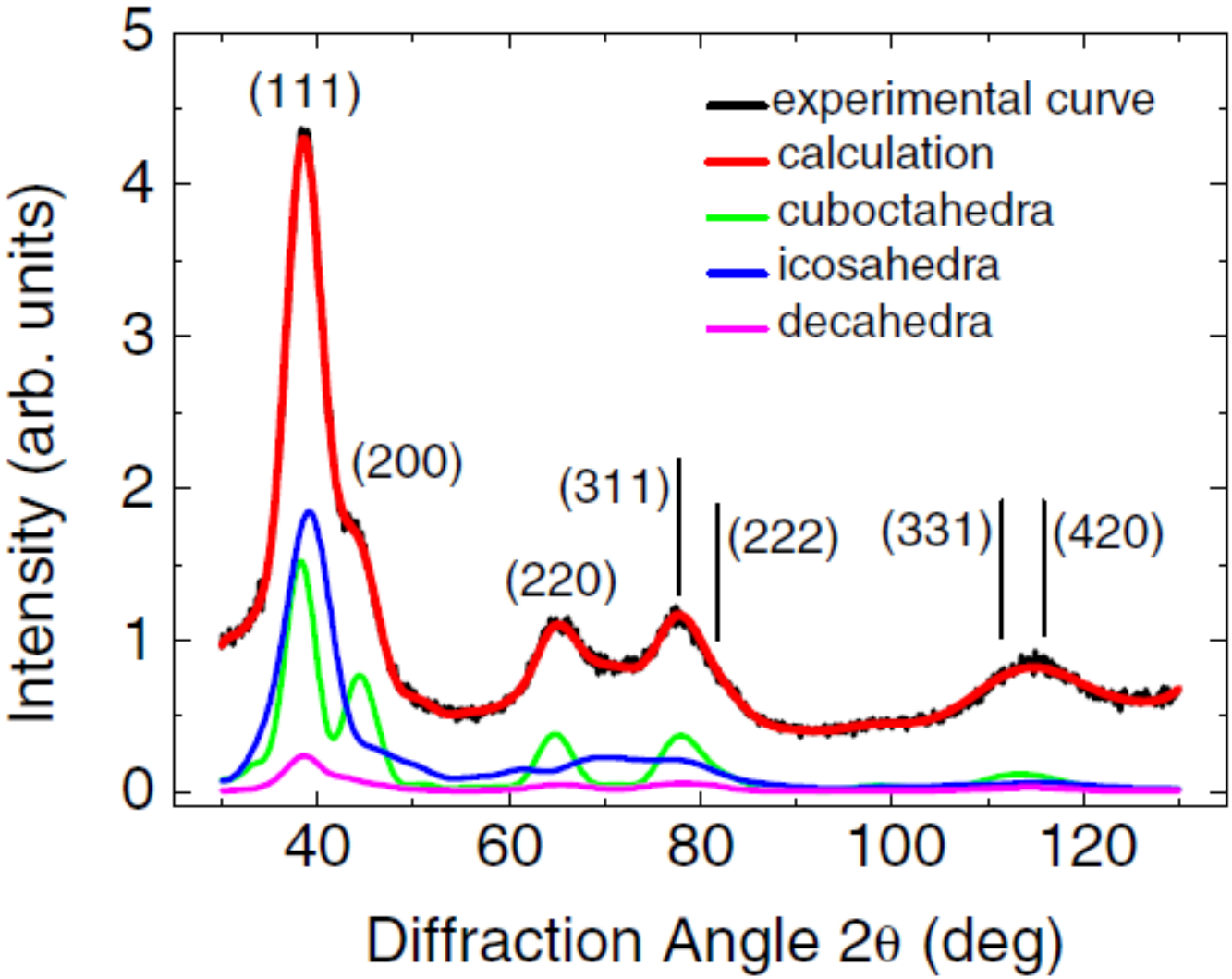
(111)
(200)
(220)
(311)
(222)
(331)
(420)
experimental curve
calculation
cuboctahedra
icosahedra
decahedra
Intensity (arb. units)
Diffraction Angle 2θ (deg)
0
1
2
3
4
5
40
60
80
100
120

LOG NORMAL DISTRIBUTION

Size

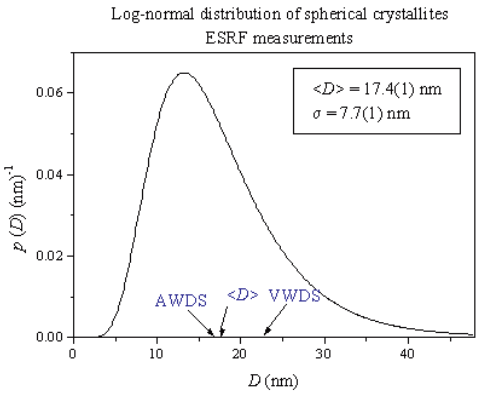

fcc clusters –
- cuboctahedra

decahedra

icosahedra

A VARIABLE-WIDTH STEP FUNCTION

(UNIFORM STRAIN)

Strain

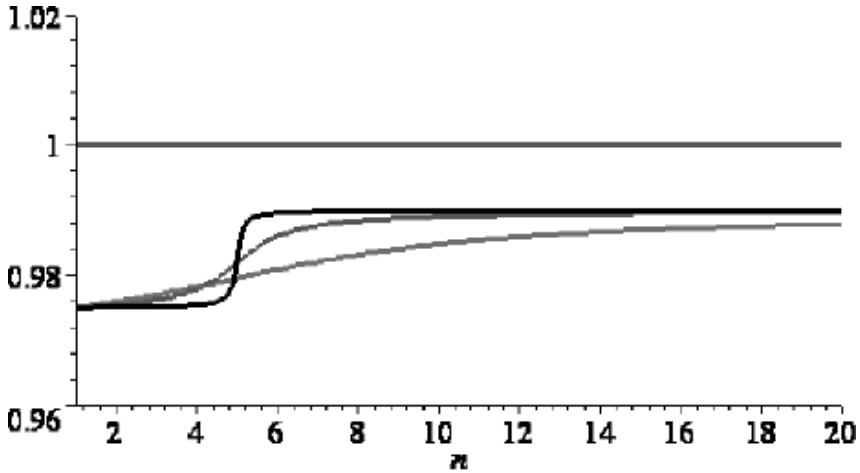

F. Vitale, R. Vitaliano, C. Battocchio, I. Fratoddi, C. Giannini, E. Piscopiello, A. Guagliardi, A. Cervellino, G. Polzonetti, M.V. Russo, L. Tapfer
Nanoscale Res Lett, **3**, 461 - 467 (2008) .

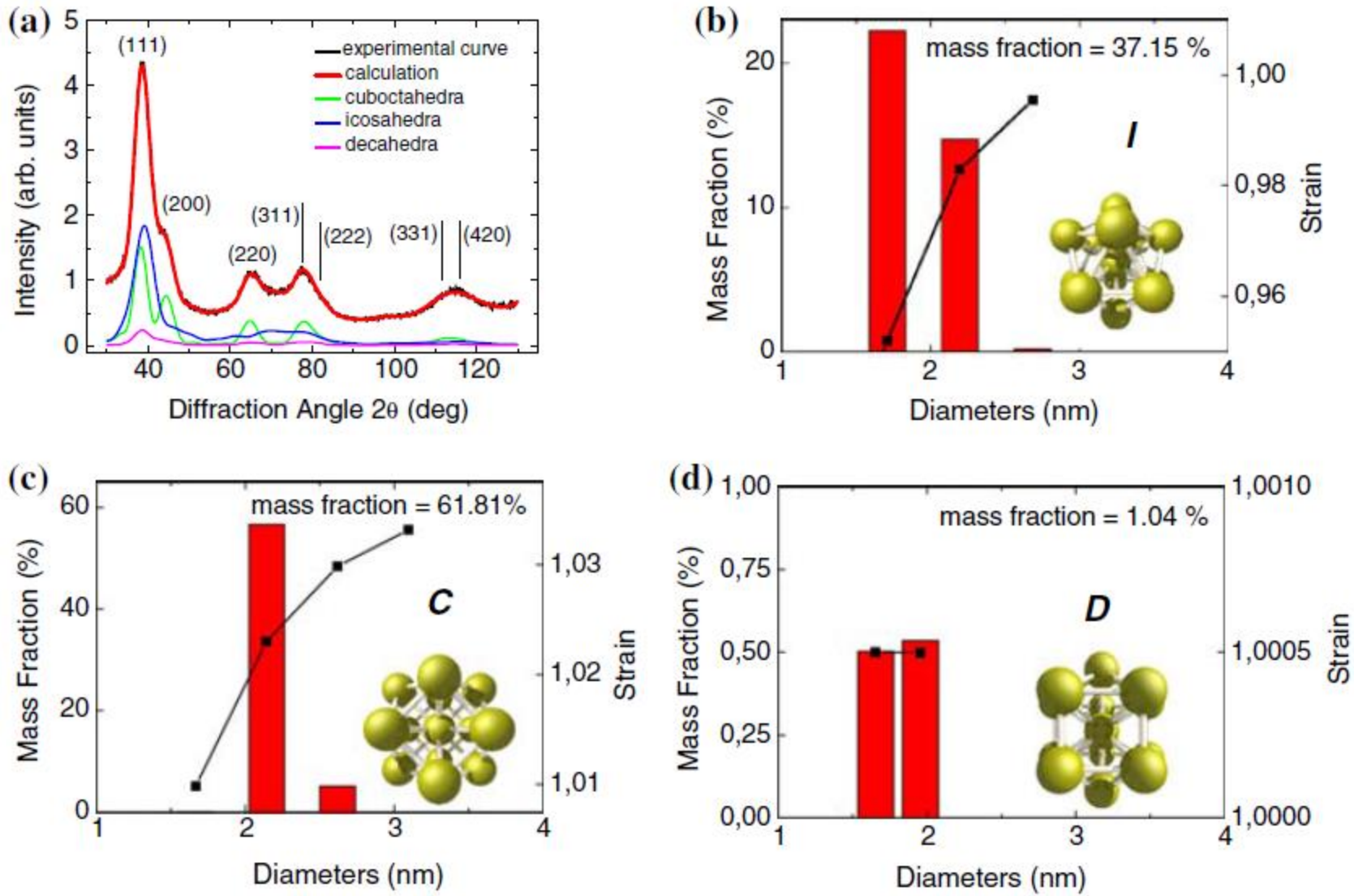

CNR Istituto di Cristallografia

Dipartimento Scienze Chimiche e Tecnologie dei Materiali

What is the effect of defects?

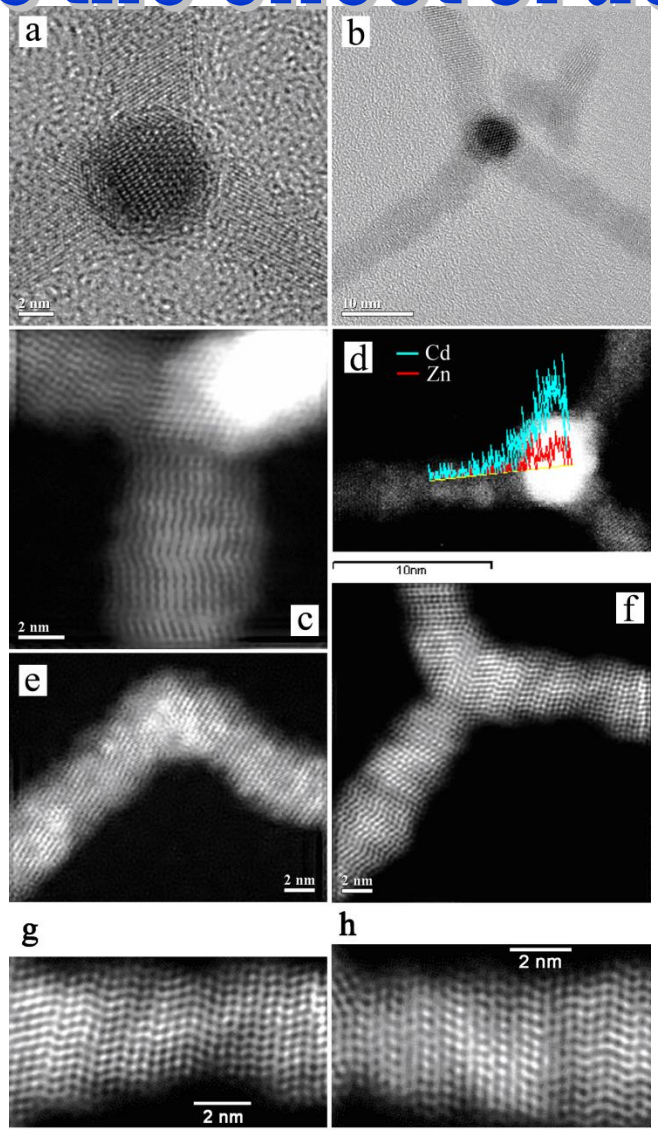

TetraPODS

JACS
JOURNAL OF THE AMERICAN CHEMICAL SOCIETY

Article

Tetrapod-Shaped Colloidal Nanocrystals of II#VI Semiconductors Prepared by Seeded Growth

Angela Fiore, Rosanna Mastria, Maria Grazia Lupo, Guglielmo Lanzani, Cinzia Giannini, Elvio Carlino, Giovanni Morello, Milena De Giorgi, Yanqin Li, Roberto Cingolani, and Liberato Manna

J. Am. Chem. Soc., **2009**, 131 (6), 2274-2282• DOI: 10.1021/ja807874e • Publication Date (Web): 26 January 2009

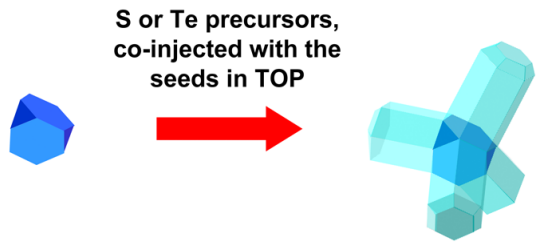

Cubic Sphalerite seed (CdSe, CdTe, ZnTe)

Sphalerite core (CdSe, CdTe, ZnTe) / Wurtzite arms (CdS, CdTe) Tetrapod

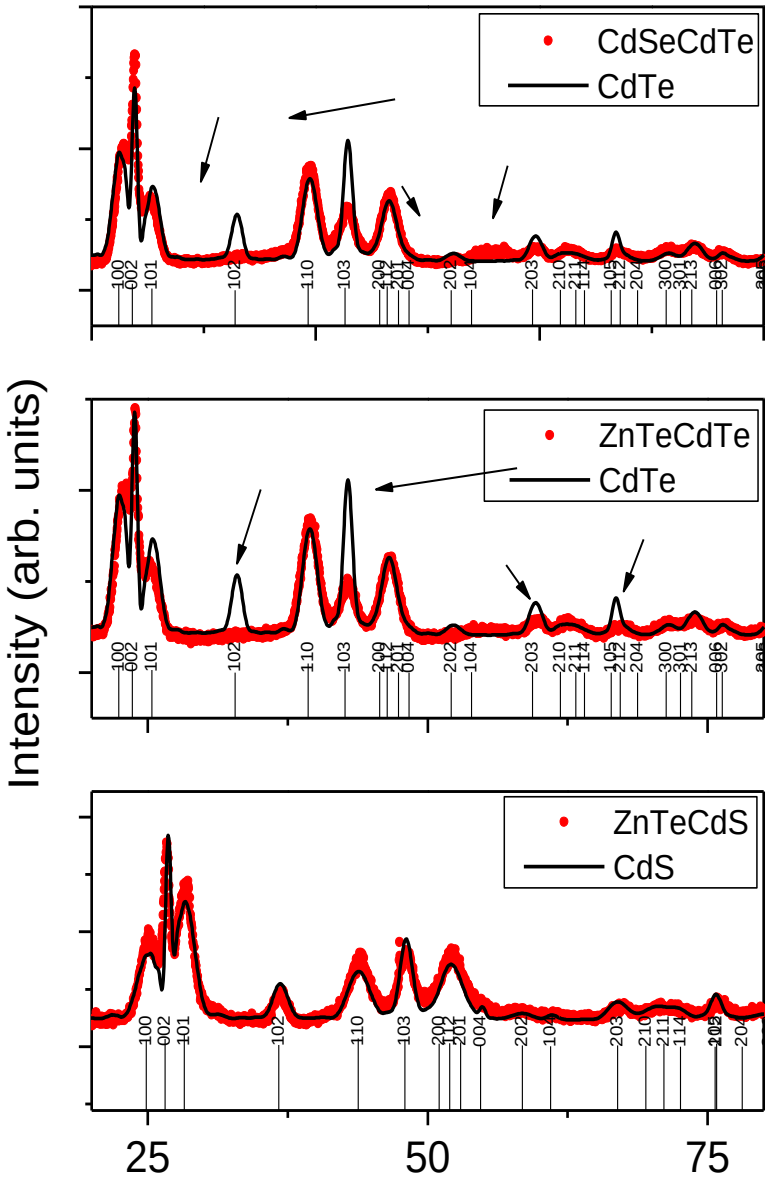

TetraPODS

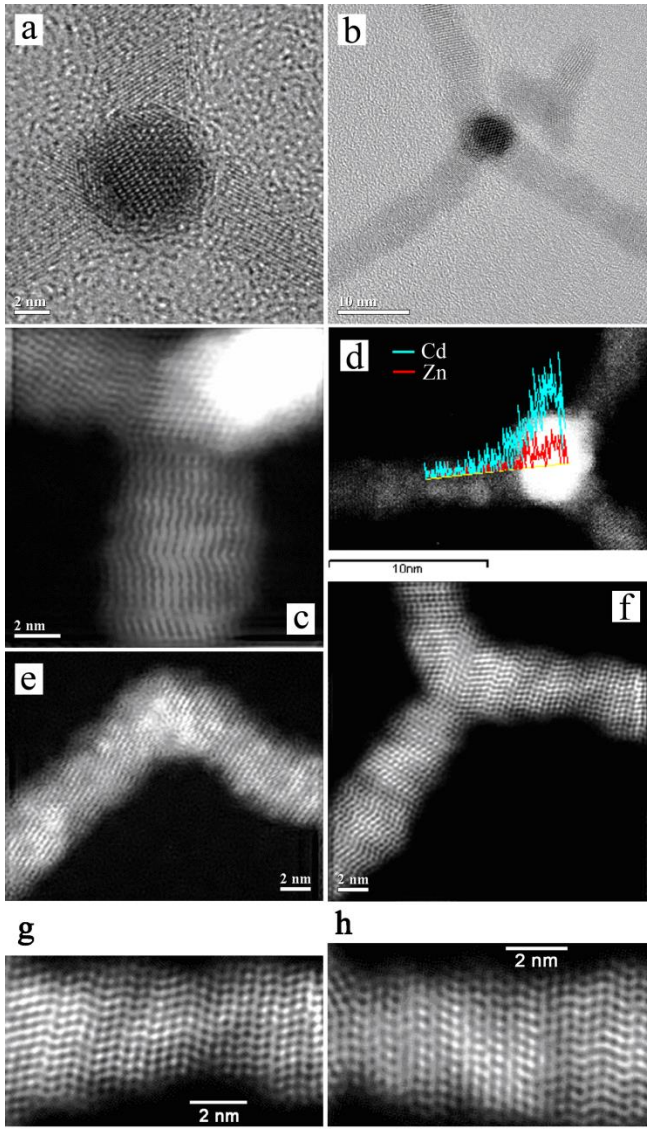

JACS
JOURNAL OF THE AMERICAN CHEMICAL SOCIETY
Article

Tetrapod-Shaped Colloidal Nanocrystals of II#VI Semiconductors Prepared by Seeded Growth

Angela Fiore, Rosanna Mastria, Maria Grazia Lupo, Guglielmo Lanzani, Cinzia Giannini, Elvio Carlino, Giovanni Morello, Milena De Giorgi, Yanqin Li, Roberto Cingolani, and Liberato Manna

J. Am. Chem. Soc., **2009**, 131 (6), 2274-2282• DOI: 10.1021/ja807874e • Publication Date (Web): 26 January 2009

STACKING FAULTED WURTZITE

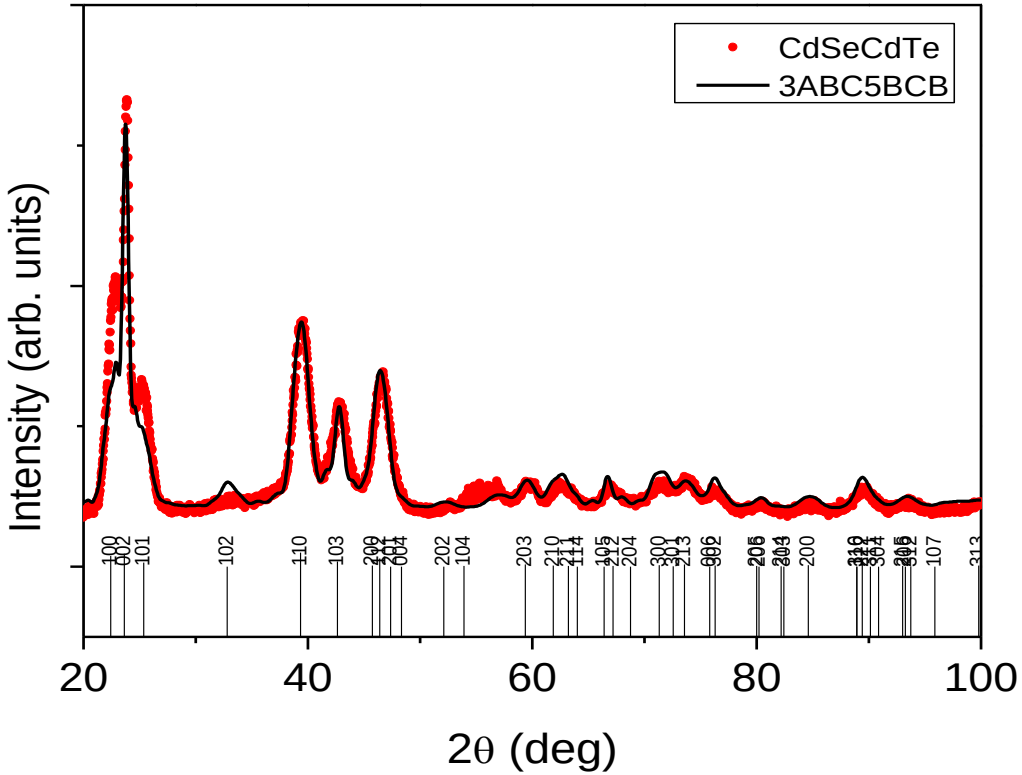

HRTEM image of a ZnTe/CdTe tetrapod. It is remarkable to note the changes of the lattice fringes contrast along the arms of the tetrapod, which indicates the presence of regions with either different orientations, or structure, or composition

Multi Length scales – Bragg law

$$q = \frac{4\pi}{\lambda}\sin(\theta) = \frac{2\pi}{d}$$

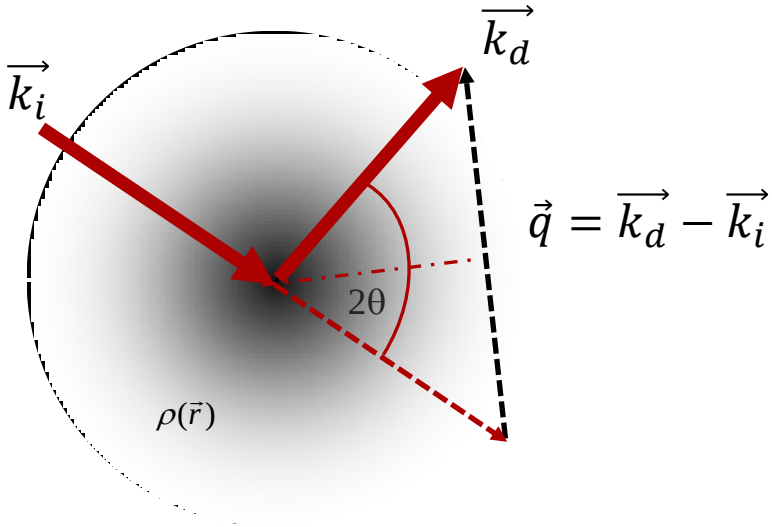

Technique	d (nm)	q (nm^{-1})	q ($Å^{-1}$)	θ(deg) for λ=1.5405Å
~~uSAXS/uSAXD~~	~~1000~~	~~0.0063~~	~~0.00063~~	~~0.0044~~
SAXS/SAXD	100	0.063	0.0063	0.044
SAXS/SAXD	10	0.63	0.063	0.44
WAXS/WAXD	1	6.3	0.63	4.4
WAXS/WAXD	0.1	63	6.3	50.6

THE XMI-Lab FACILITY

XMI-L@b: An X-ray synchrotron class rotating anode microsource for the structural micro imaging of nanomaterials and engineered biotissues

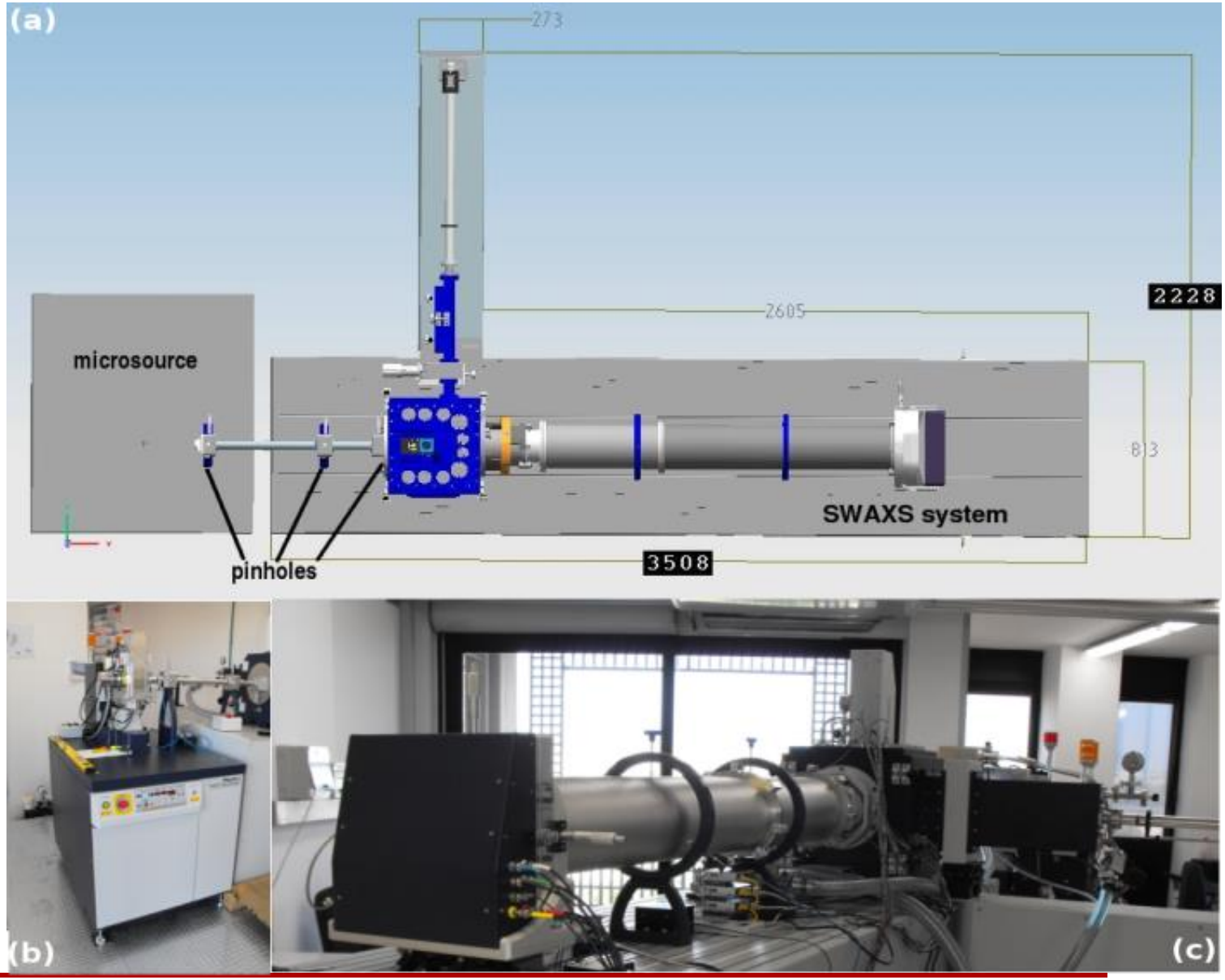

THE XMI-Lab FACILITY

Micro-Source: **Rigaku FRE+ Superbright**

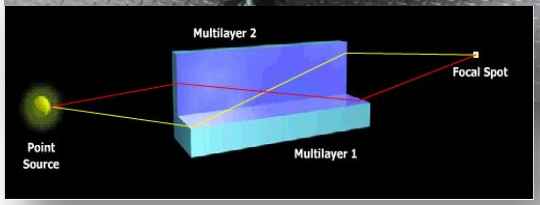

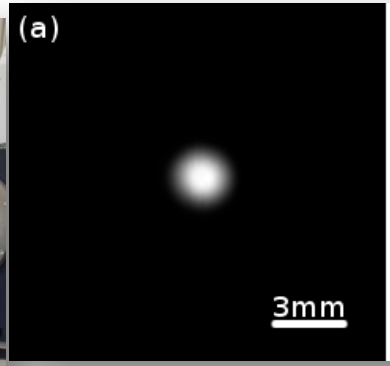

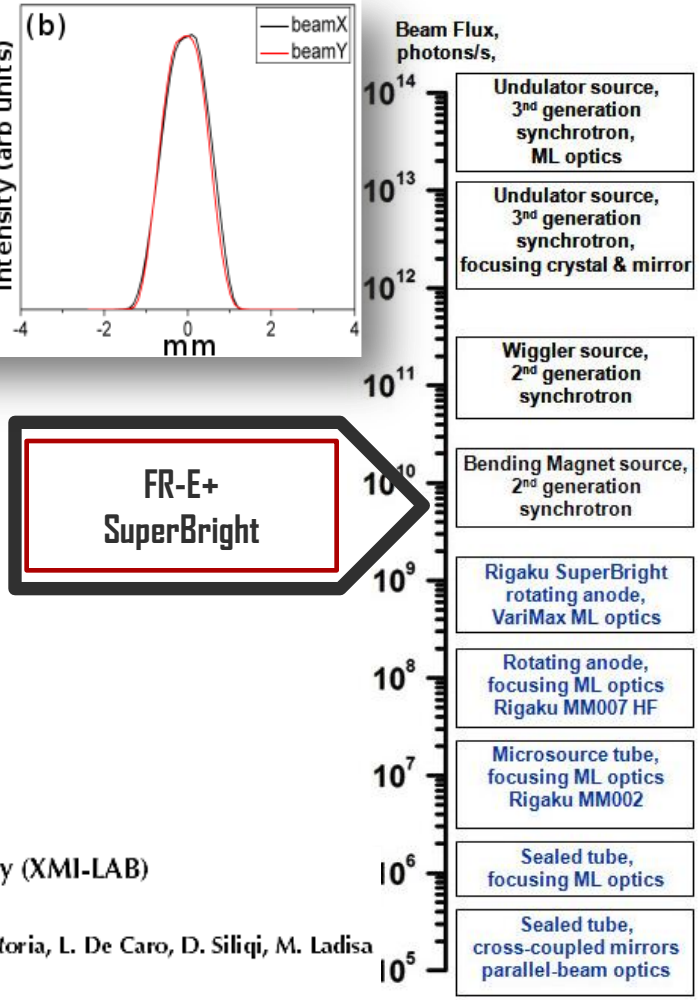

X-ray microimaging laboratory (XMI-LAB)

D. Altamura, R. Lassandro, F. A. Vittoria, L. De Caro, D. Siliqi, M. Ladisa and C. Giannini

J. Appl. Cryst. (2012). 45, 869–873

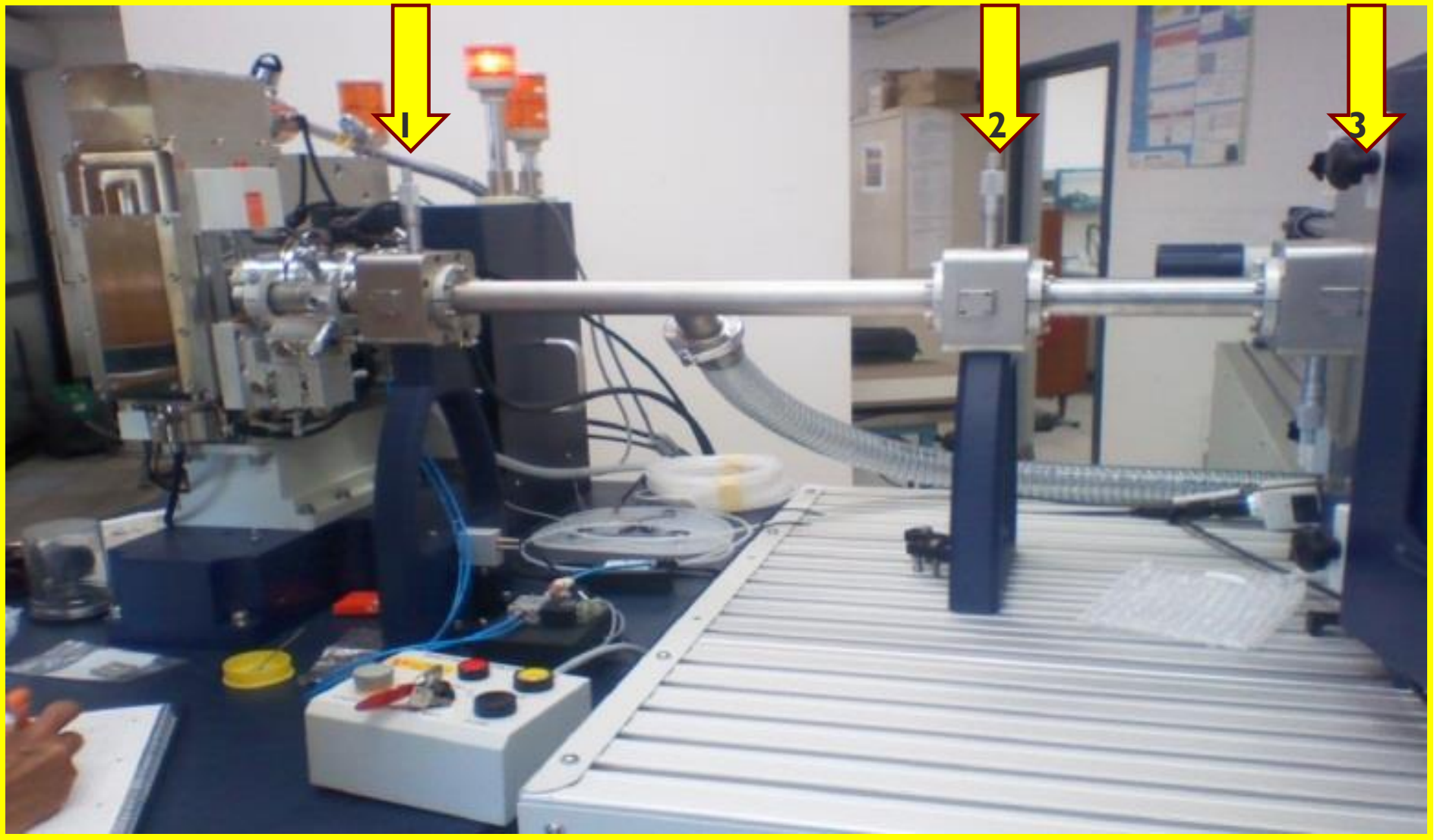
1
2
3

THREE PINHOLES CAMERA - RIGAKU SMAX3000

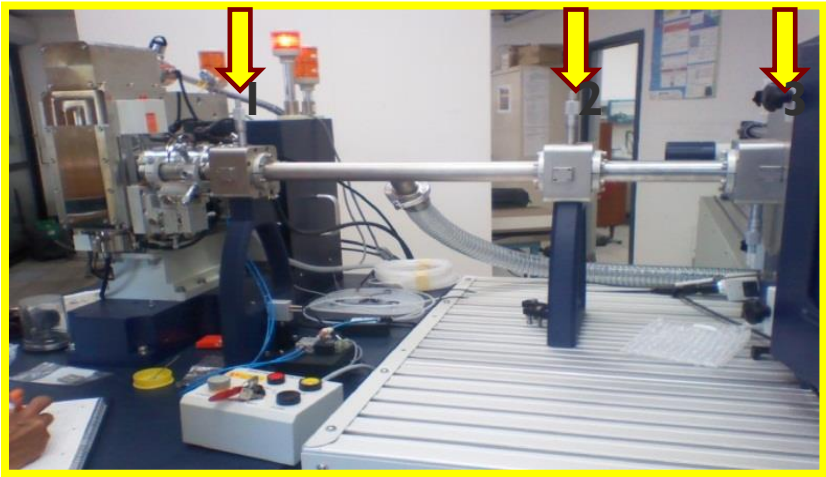

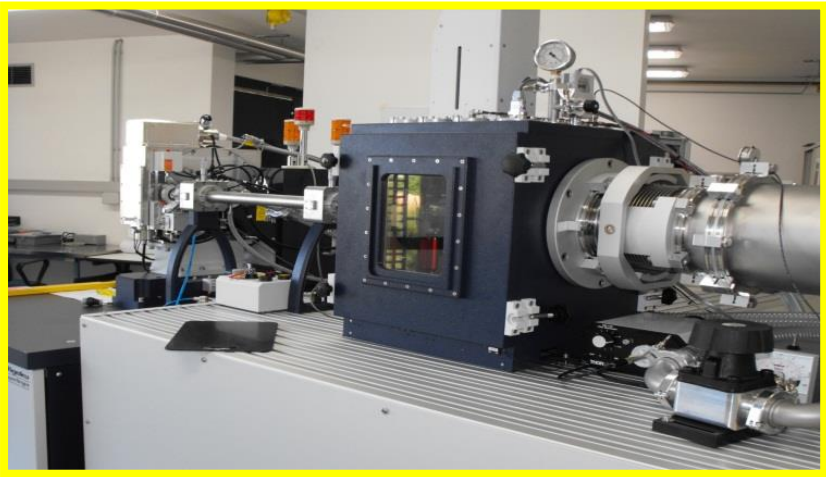

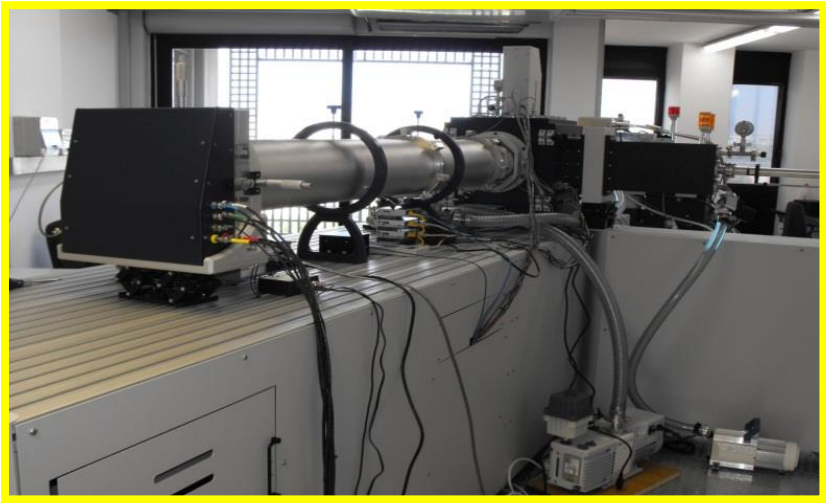

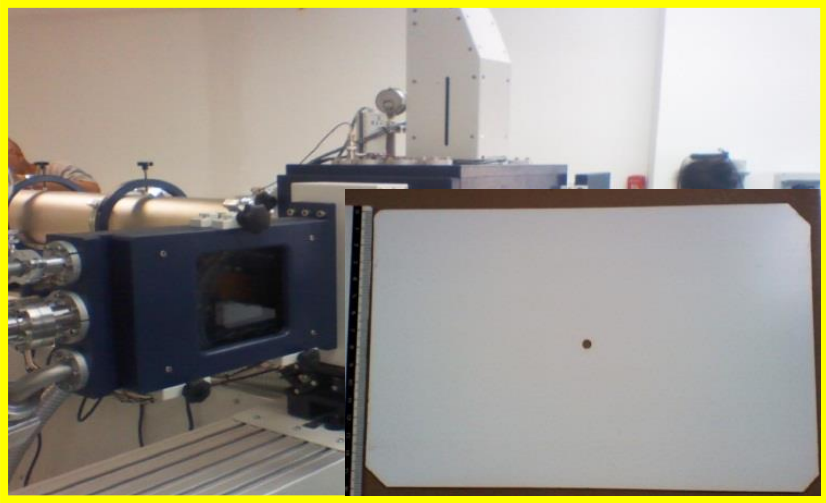

SAXS: Triton™20 detector, a 20cm diameter multi-wire gas-filled proportional counter

WAXS: RAXIA Image Plate with off line reader

X-ray microimaging laboratory (XMI-LAB)

D. Altamura, R. Lassandro, F. A. Vittoria, L. De Caro, D. Siliqi, M. Ladisa and C. Giannini

J. Appl. Cryst. (2012). 45, 869–873

ICCI
CNR Istituto di Cristallografia

DSCTM
Dipartimento Scienze Chimiche e Tecnologie dei Materiali

TYPE OF SPECIMENS

- liquids
- Biopsies / tissues

SAXS/WAXS

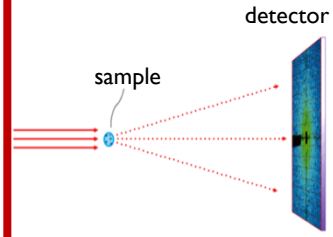

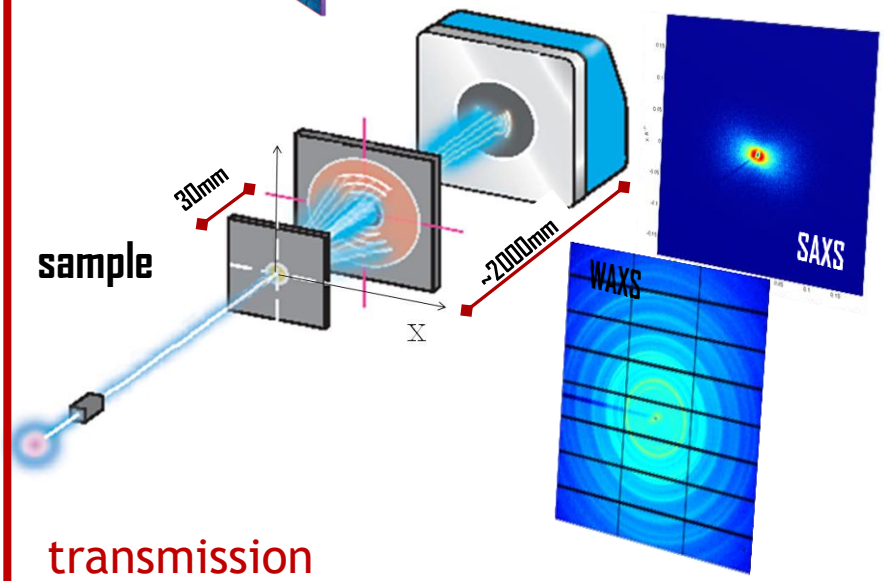

transmission

GISAXS/GIWAXS

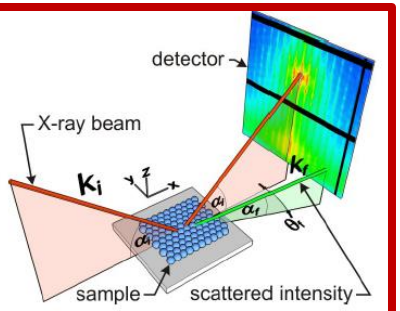

- Planar devices
- Nanostructured surfaces

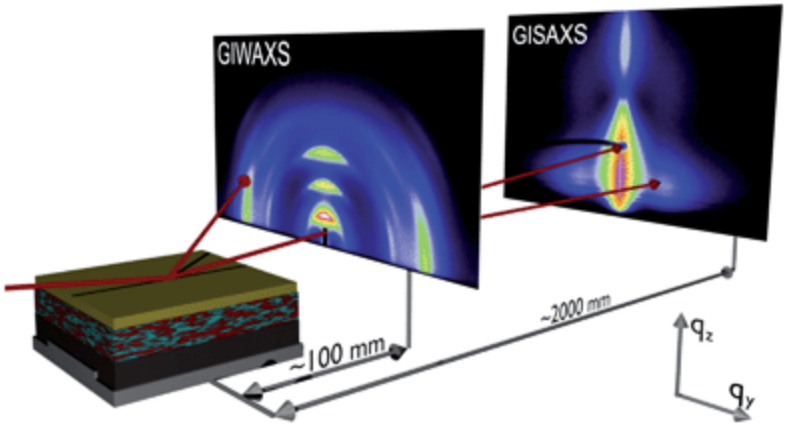

reflection

Morphological and Structural Characterization at the nano and atomic scale

NANOPARTICLES IN SOLUTIONS

SAXS/WAXS - nanometric lenght scale

- liquids
- tissues

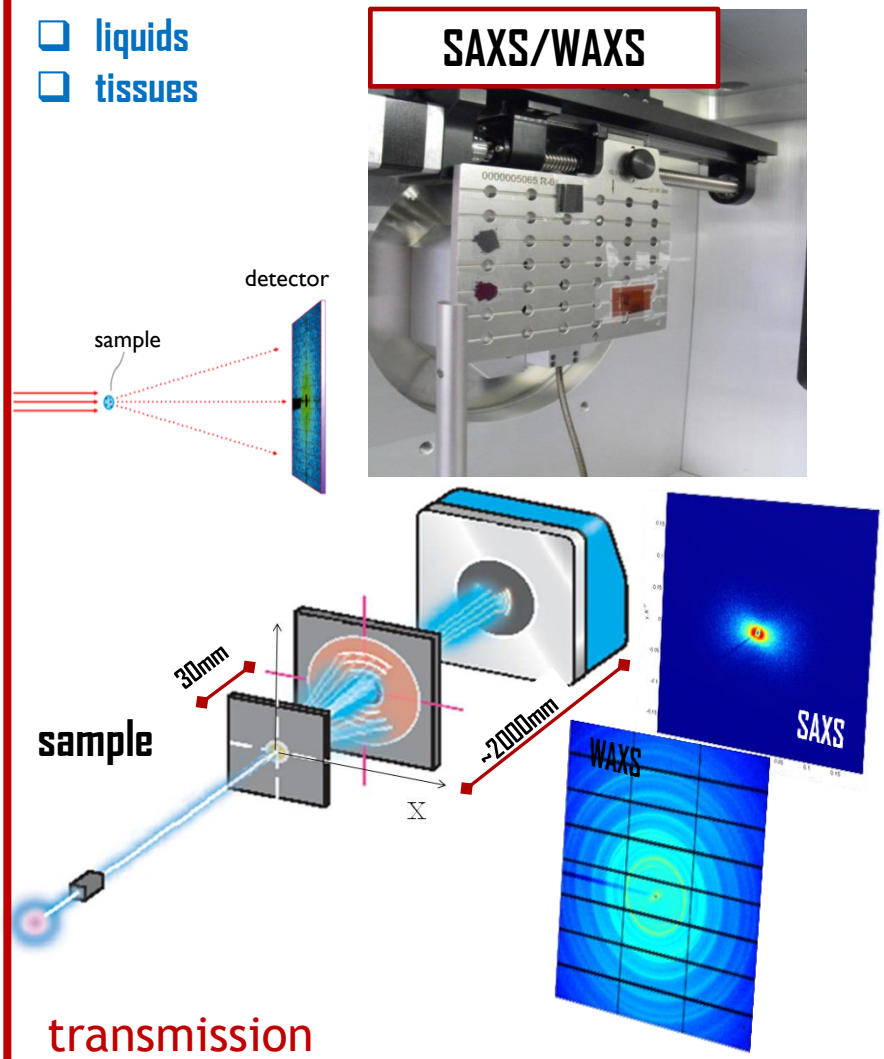

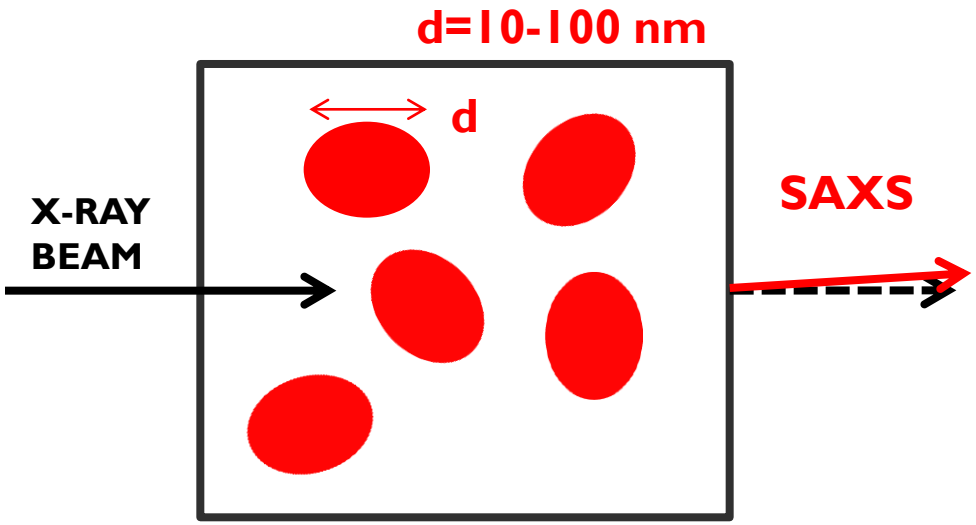

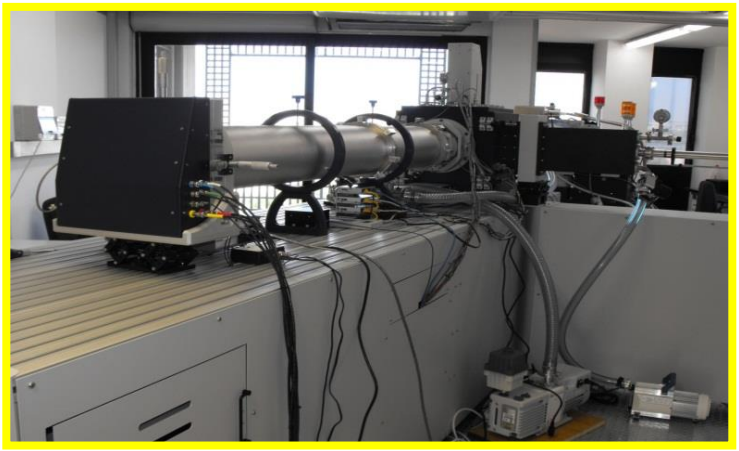

SAXS/WAXS: sample in solution

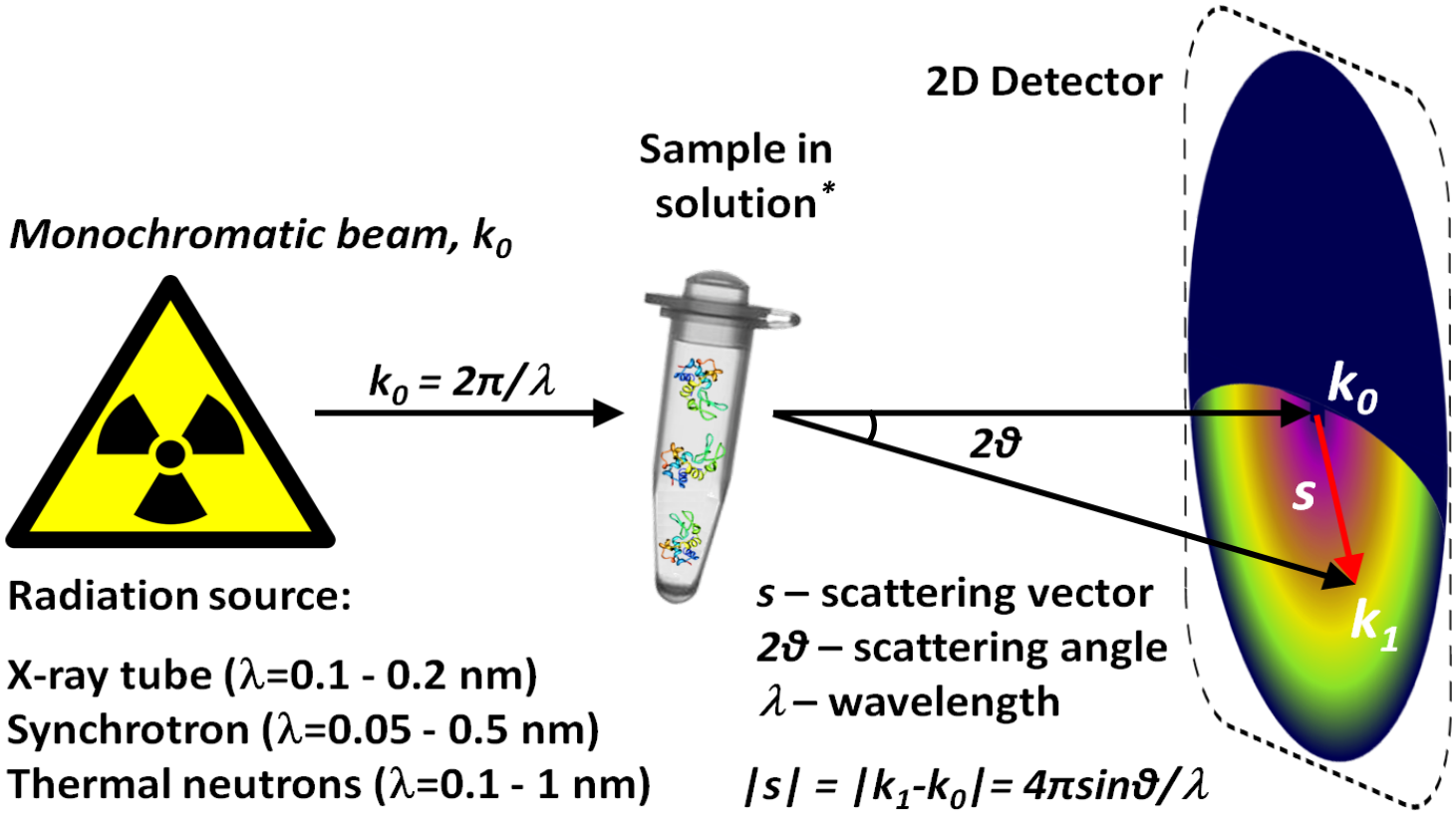

Radiation source:

X-ray tube (λ=0.1 - 0.2 nm)
Synchrotron (λ=0.05 - 0.5 nm)
Thermal neutrons (λ=0.1 - 1 nm)

s – scattering vector
2ϑ – scattering angle
λ – wavelength

$|s| = |k_1 - k_0| = 4\pi \sin\vartheta/\lambda$

SAXS: shape info

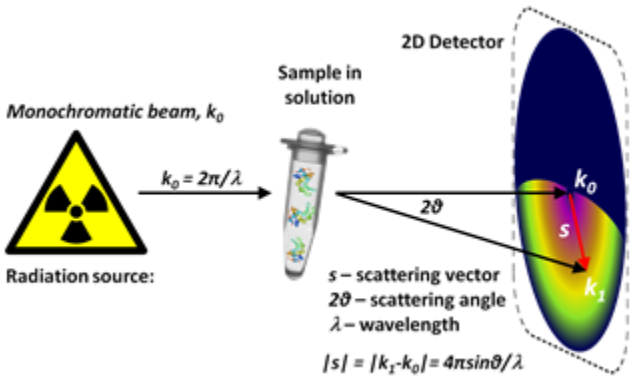

radially averaged

normalized:
sample concentration
incoming beam
exposure time

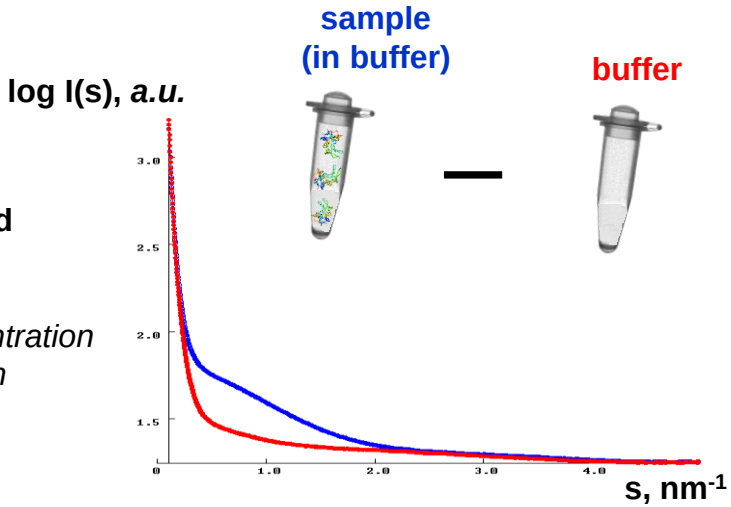

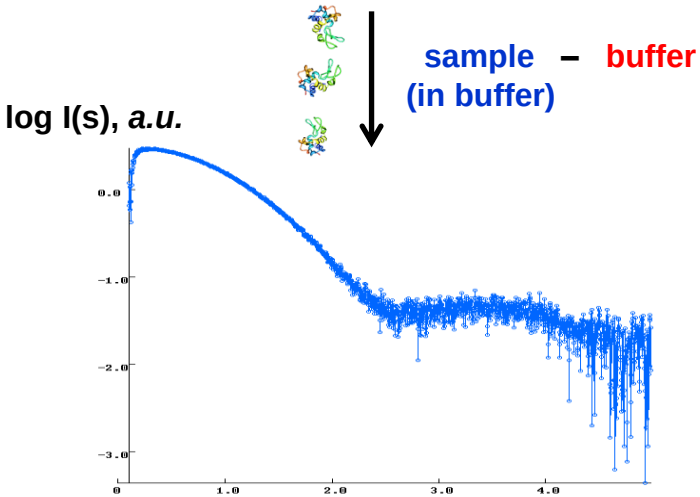

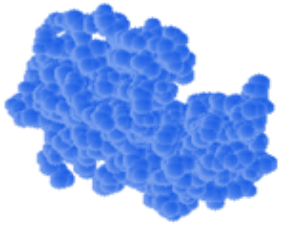

Shape

$$I(s) = 4\pi \int_0^D p(r) \frac{\sin sr}{sr} dr$$

for *monodisperse* systems the scattering is proportional to that of a single particle averaged over all orientations

SAXS: size/shape info

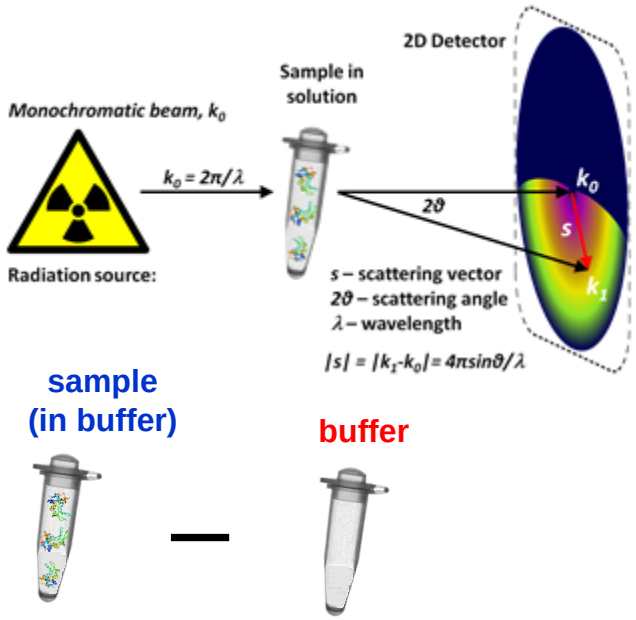

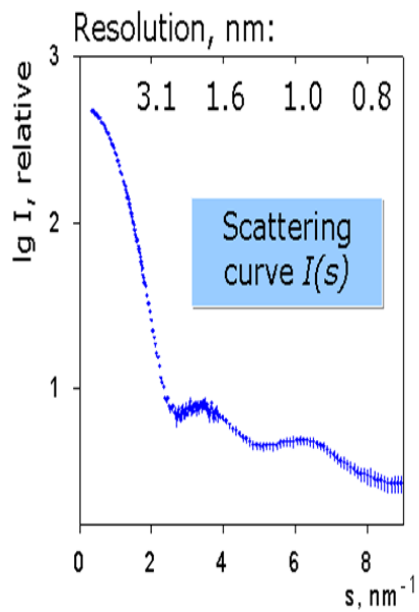

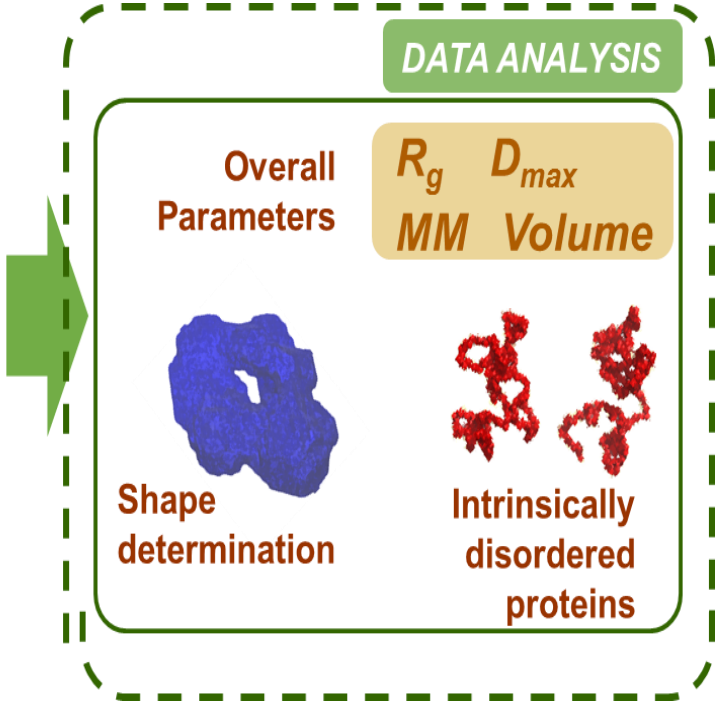

- Molecular weight*
- Molecular volume*
- Radius of gyration (Rg)
- Distance distribution function p(r)
- Various derived parameters such as longest cord from p (r)
- * requires absolute (or calibrated) intensity information

SPHERE

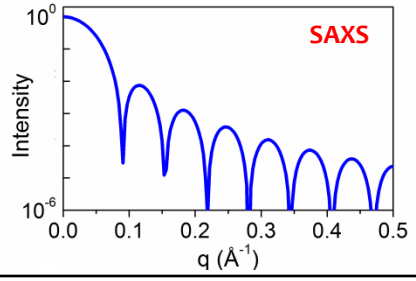

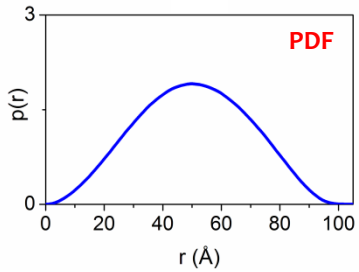

$$R_g{}^2 = \frac{3}{5}R^2$$

HOLLOW SPHERE

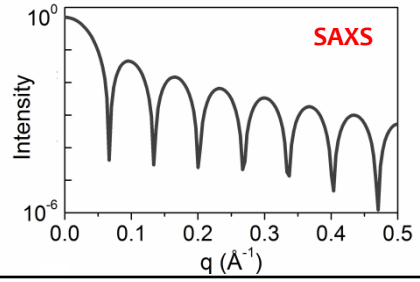

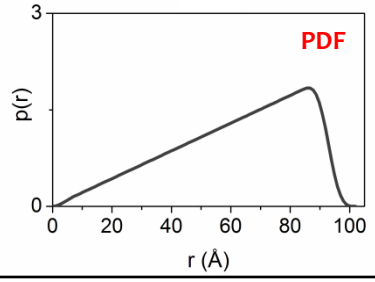

$$R_g{}^2 = \frac{3}{5}\frac{R_2{}^5 - R_1{}^5}{R_2{}^3 - R_1{}^3}$$

CYLINDER

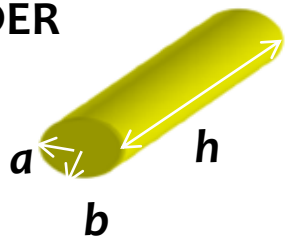

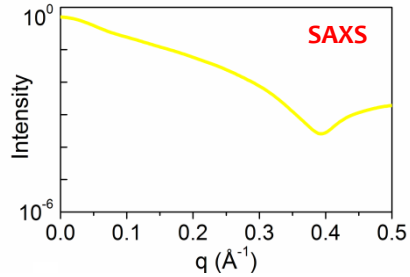

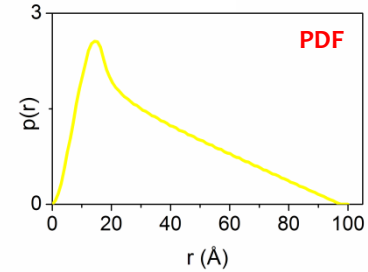

$$R_g{}^2 = \frac{a^2+b^2}{4} + \frac{h^2}{12}$$

FLAT DISK

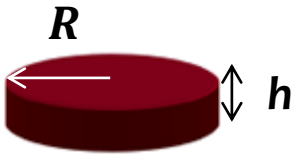

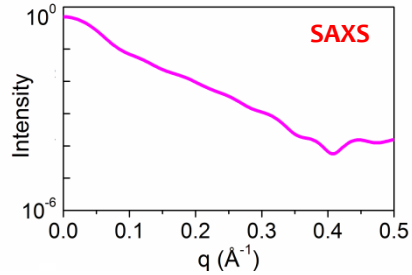

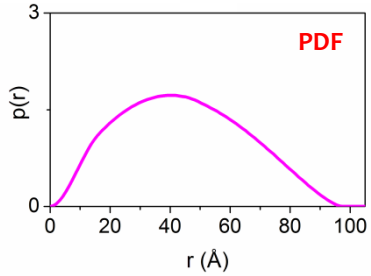

$$R_g{}^2 = \frac{R^2}{2} + \frac{h^2}{12}$$

DUMBELLS

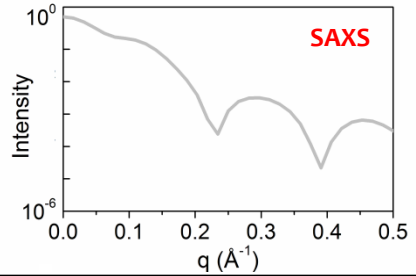

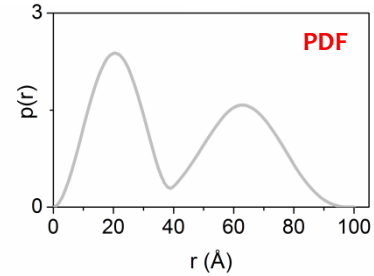

$$R_g{}^2 = \frac{\int_0^{d_{max}} P(r) r^2 dr}{\int_0^{d_{max}} P(r)\, dr}$$

SCIENTIFIC REPORTS

APOFERRITINE

OPEN

SUBJECT AREAS:
X-RAYS
CHARACTERIZATION AND ANALYTICAL TECHNIQUES

An Optimized Table-Top Small-Angle X-ray Scattering Set-up for the Nanoscale Structural Analysis of Soft Matter

T. Sibillano[1], L. De Caro[1], D. Altamura[1], D. Siliqi[1], M. Ramella[2], F. Boccafoschi[2], G. Ciasca[3], G. Campi[4], L. Tirinato[5,6], E. Di Fabrizio[5,6] & C. Giannini[1]

SAXS studies on apoferritin protein in aqueous solution

Apoferritin: a globular nanosized cage-shaped protein composed by 24 subunits forming a stable and soluble hollow sphere.

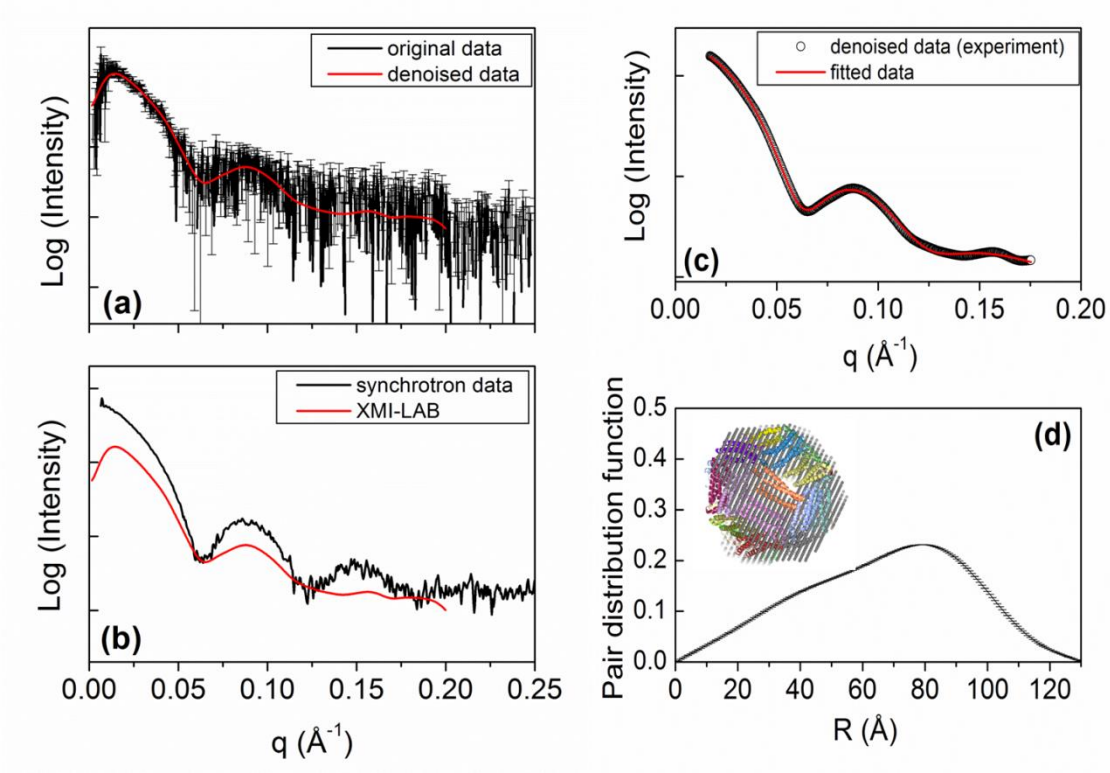

Hollow Sphere

Gyration Radius R_g = 5.1 ± 0.2nm

SCIENTIFIC REPORTS

APOFERRITINE

OPEN

SUBJECT AREAS:
X-RAYS
CHARACTERIZATION AND ANALYTICAL TECHNIQUES

An Optimized Table-Top Small-Angle X-ray Scattering Set-up for the Nanoscale Structural Analysis of Soft Matter

T. Sibillano[1], L. De Caro[1], D. Altamura[1], D. Siliqi[1], M. Ramella[2], F. Boccafoschi[2], G. Ciasca[3], G. Campi[4], L. Tirinato[5,6], E. Di Fabrizio[5,6] & C. Giannini[1]

SAXS studies on apoferritin protein in aqueous solution

It is in perfect agreement to what expected for an external and internal radii R2=6 nm and R1=4 nm of the apoferritin molecule (Rg=5.16 nm)

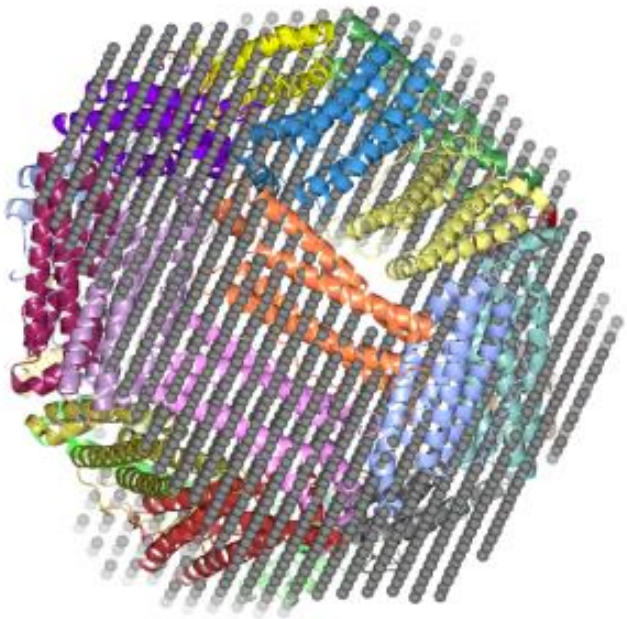

$$R_g^{\,2} = \frac{3}{5}\frac{R_2^{\,5} - R_1^{\,5}}{R_2^{\,3} - R_1^{\,3}}$$

SAXS is the ONLY technique which can extract the shape/size of an hollow sphere in a solution

PASSIVE/ACTIVE Nanomaterials: chemistry & morphology

γ-Fe_2O_3 spheres

CdSe nanorods

CdTe tetrapods

Ag nanocubes

PbSe stars

PbSe nanowires

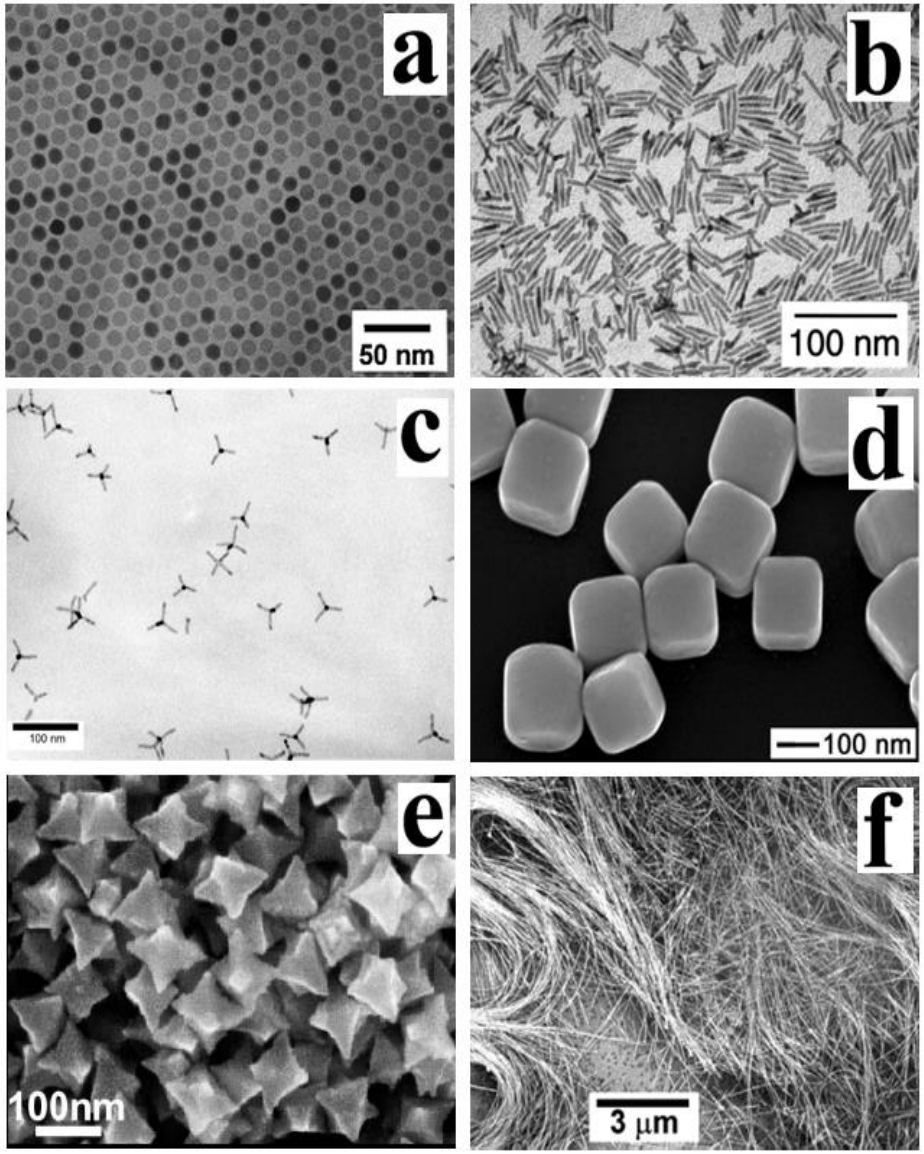

SAXS/WAXS - atomic lenght scale

- liquids
- tissues

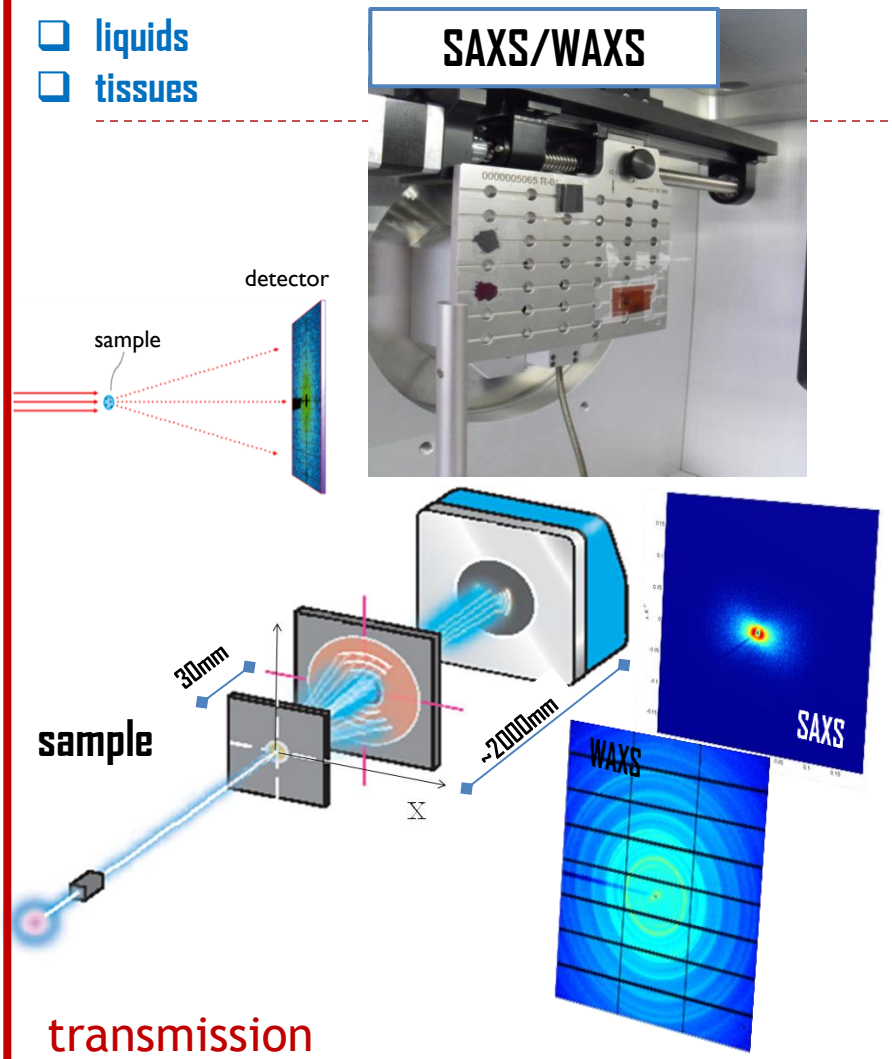

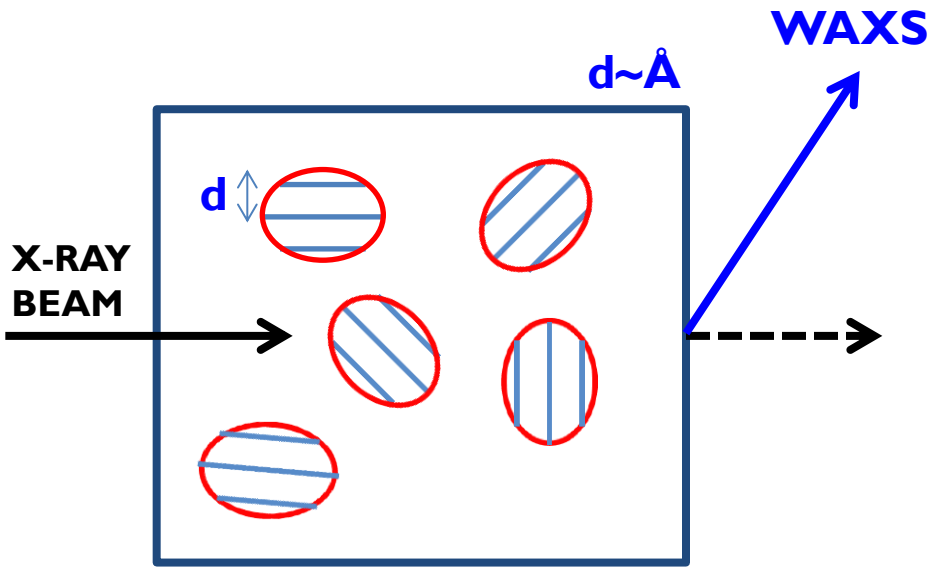

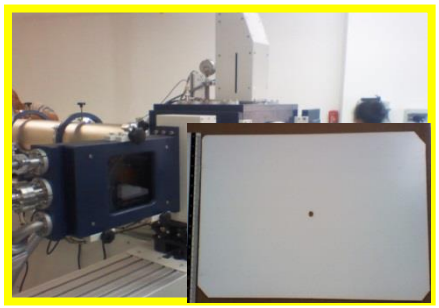

1.08 Quantum Dots: Synthesis and Characterization

D Dorfs, R Krahne, A Falqui, and L Manna, Istituto Italiano di Tecnologia, Genoa, Italy
C Giannini, CNR-Istituto di Cristallografia (IC), Bari, Italy
D Zanchet, Laboratório Nacional de Luz Síncrotron, Campinas-SP, Brazil

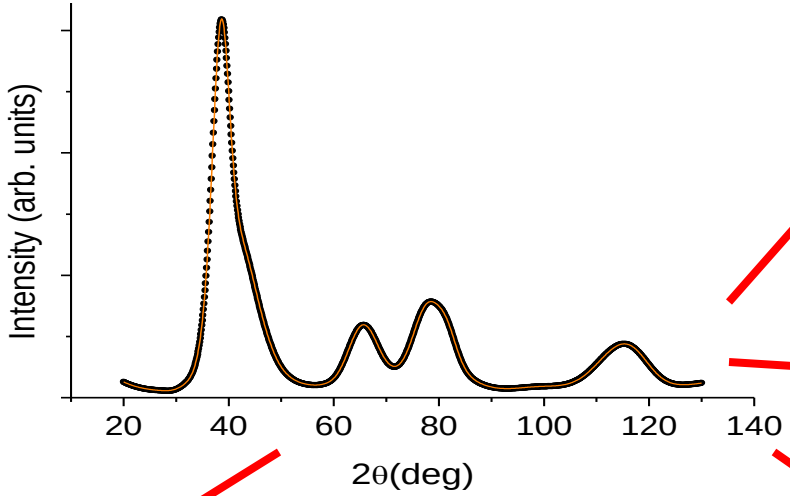

(a)

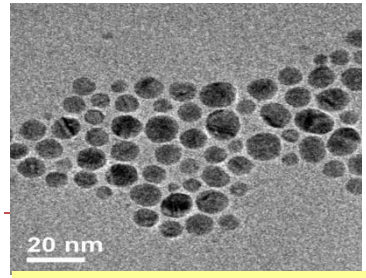

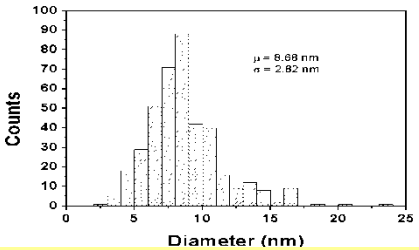

Size

(b)

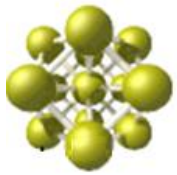

Structure(s)

(c)

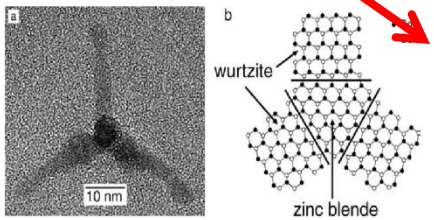

Shape

(e)

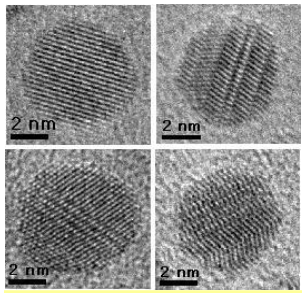

Defects

(d)

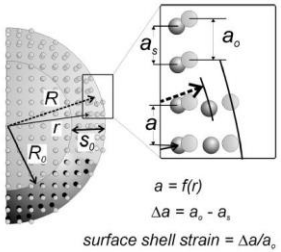

Surface/Strain

SAXS/WAXS: Ag nanoparticles in water

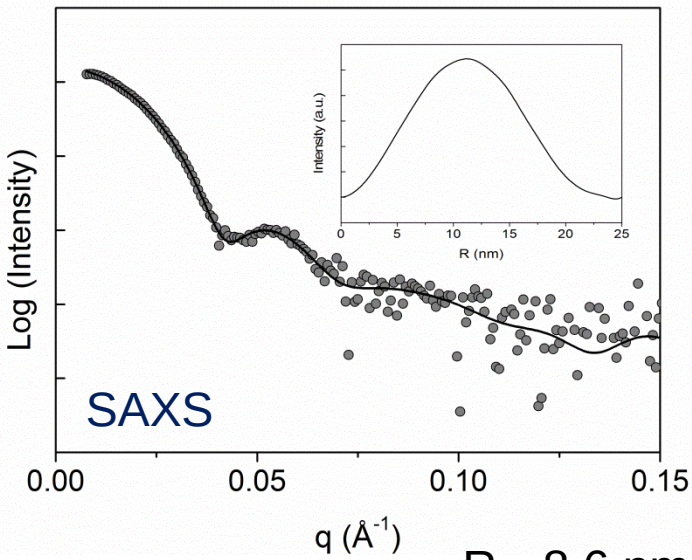

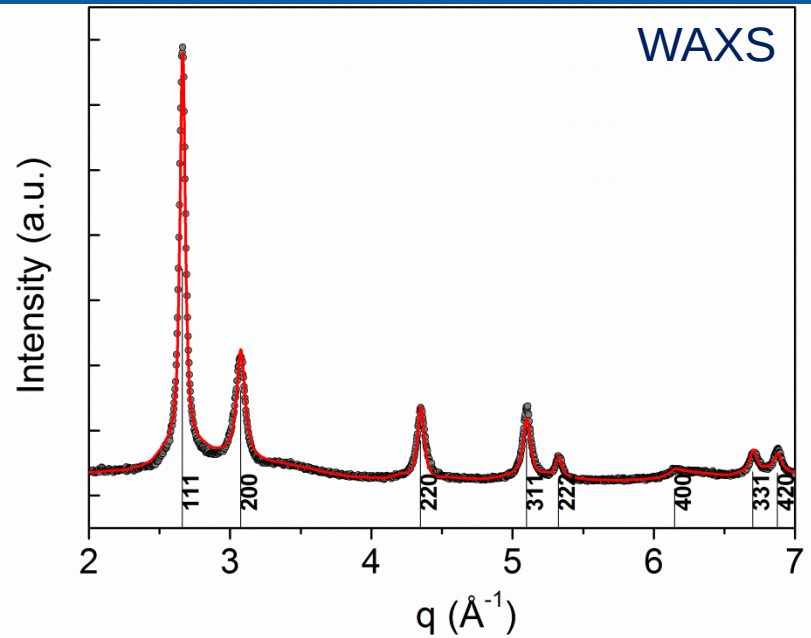

R_g=8.6 nm

$D = 2*\sqrt{5/3}R_g \sim 22\pm1$ nm

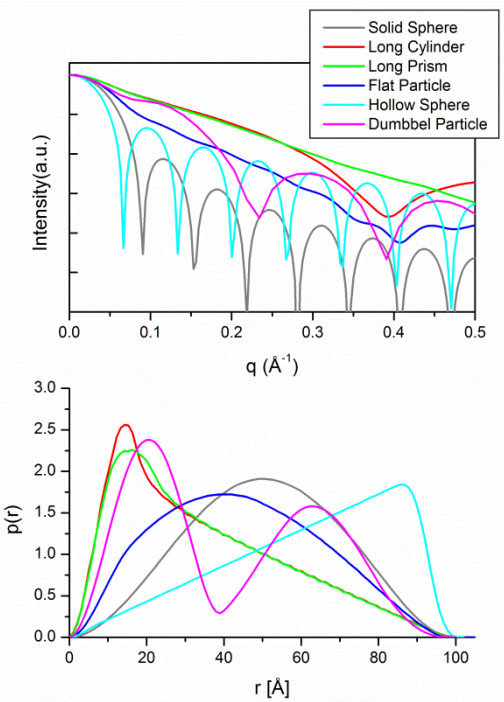

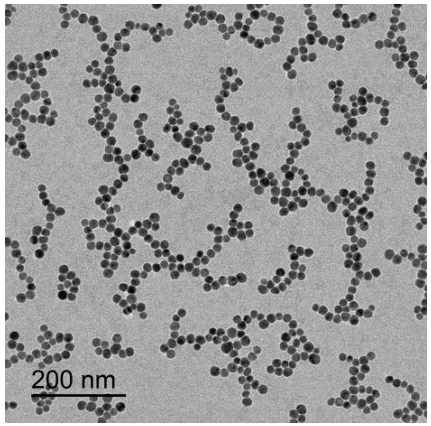

TEM

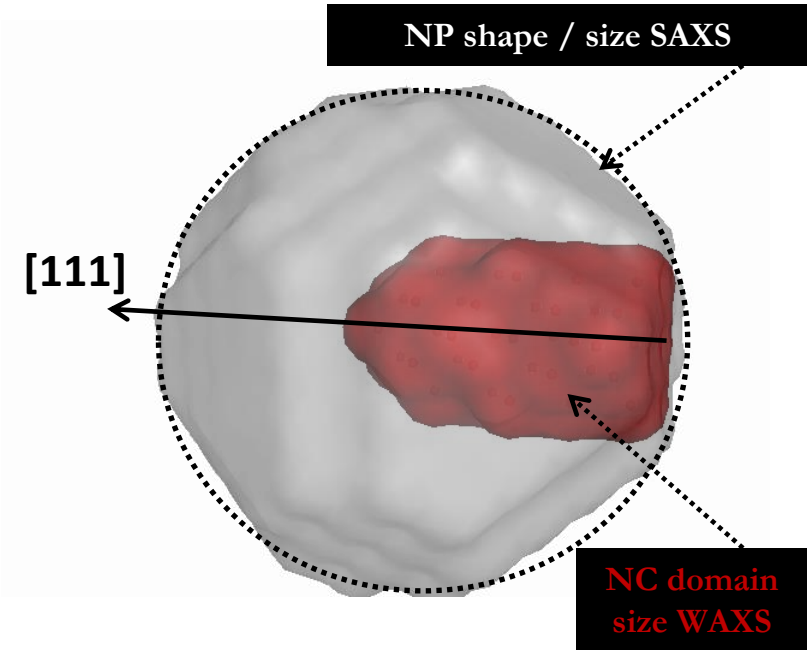

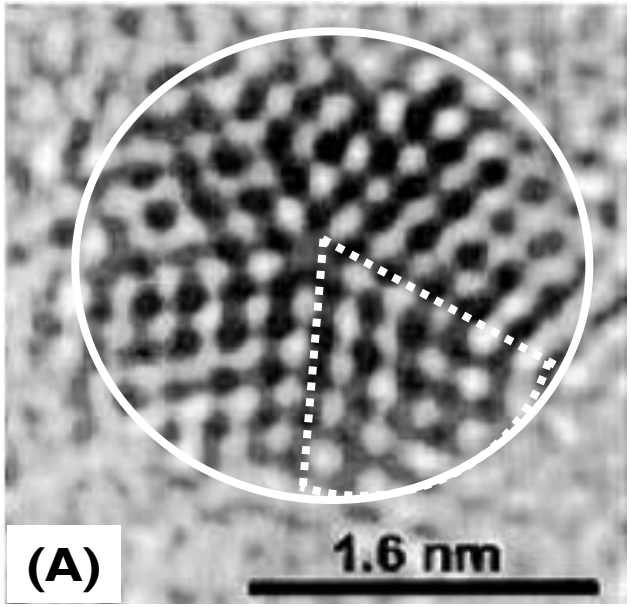
(A)
1.6 nm

(C)

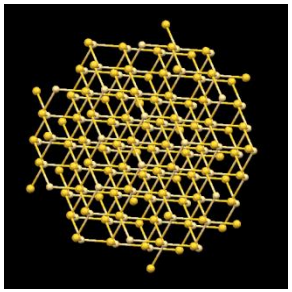

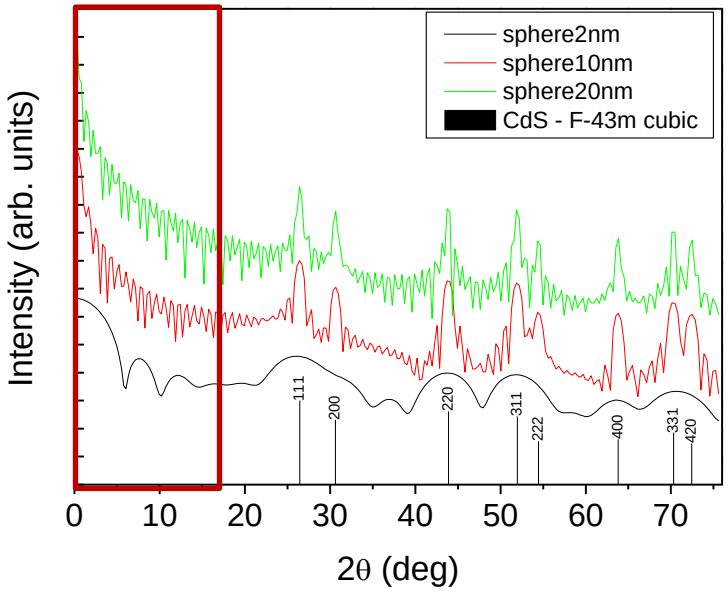
sphere2nm
sphere10nm
sphere20nm
CdS - F-43m cubic
Intensity (arb. units)
111
200
220
311
222
400
331
420
0
10
20
30
40
50
60
70
2θ (deg)

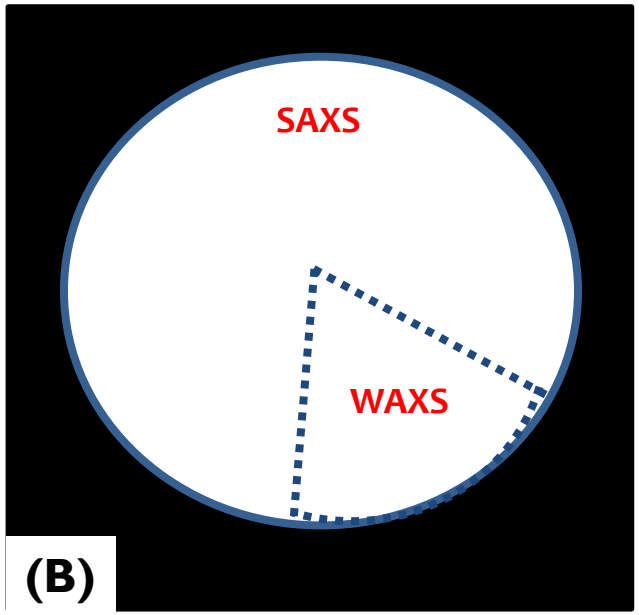
SAXS
WAXS
(B)

(D)

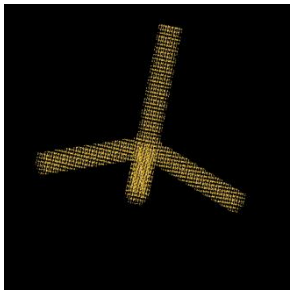

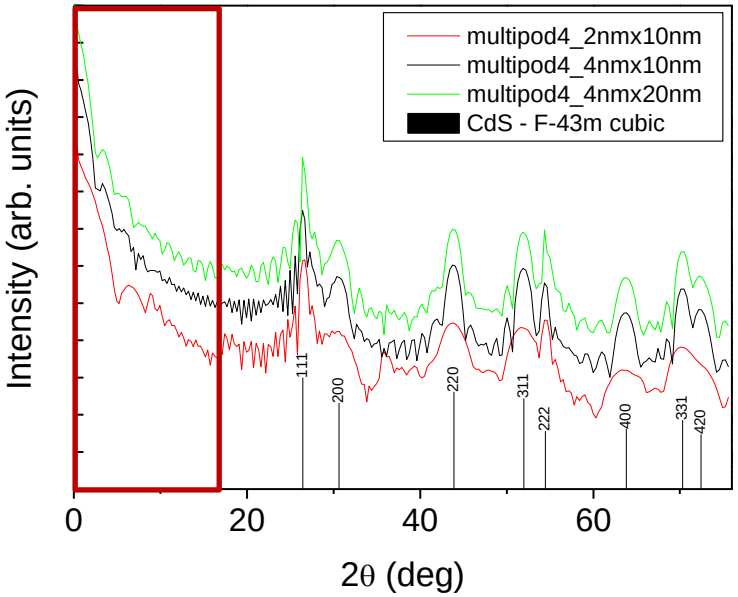
multipod4_2nmx10nm
multipod4_4nmx10nm
multipod4_4nmx20nm
CdS - F-43m cubic
Intensity (arb. units)
111
200
220
311
222
400
331
420
0
20
40
60
2θ (deg)

Debye Function: atomistic approach

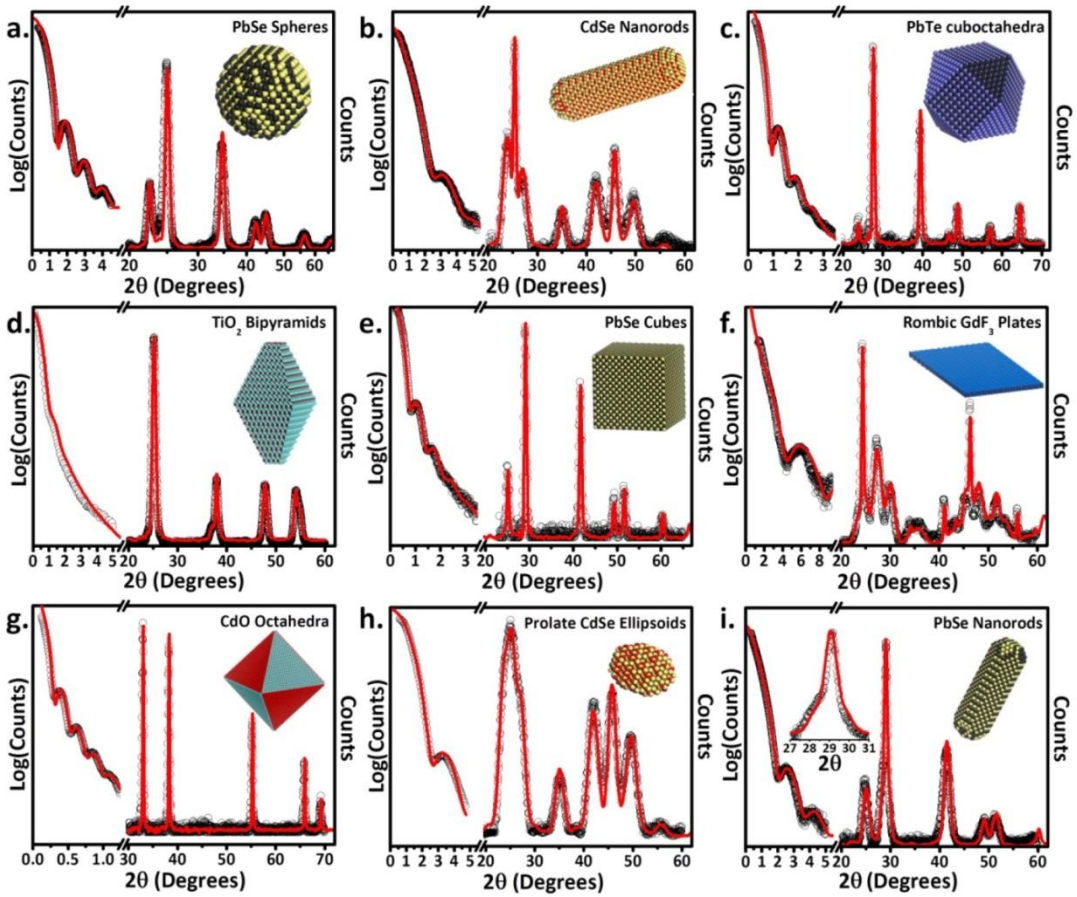

CHEMISTRY OF MATERIALS

Article

Characterization of Shape and Monodispersity of Anisotropic Nanocrystals through Atomistic X-ray Scattering Simulation

Thomas R. Gordon†, Benjamin T. Diroll†, Taejong Paik†, Vicky V. T. Doan-Nguyen‡, E. Ashley Gaulding‡, and Christopher B. Murray*†‡
†Department of Chemistry and ‡Department of Materials Science and Engineering, University of Pennsylvania Philadelphia, Pennsylvania 19104, United States

Chem. Mater., **2016**, *27* (7), pp 2502–2506
DOI: 10.1021/cm5047676
Publication Date (Web): March 19, 2015

*E-mail: cbmurray@sas.upenn.edu.

DF approach holds for SMALL and WIDE angle scattering data, for crystalline, partially crystalline and amorphous samples, does not need any crystallographic rule

Hybrid NANOMATERIALS: organic/inorganic

Colloidal nanocrystals and nanoparticles share the **same size regime** of biologically relevant systems and components

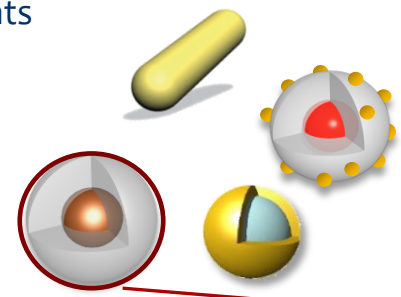

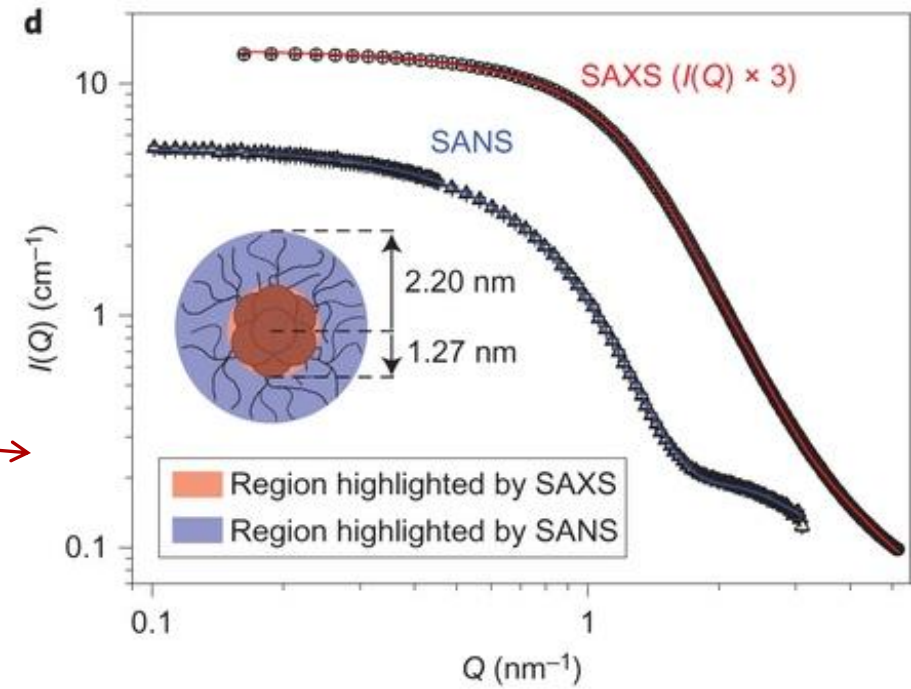

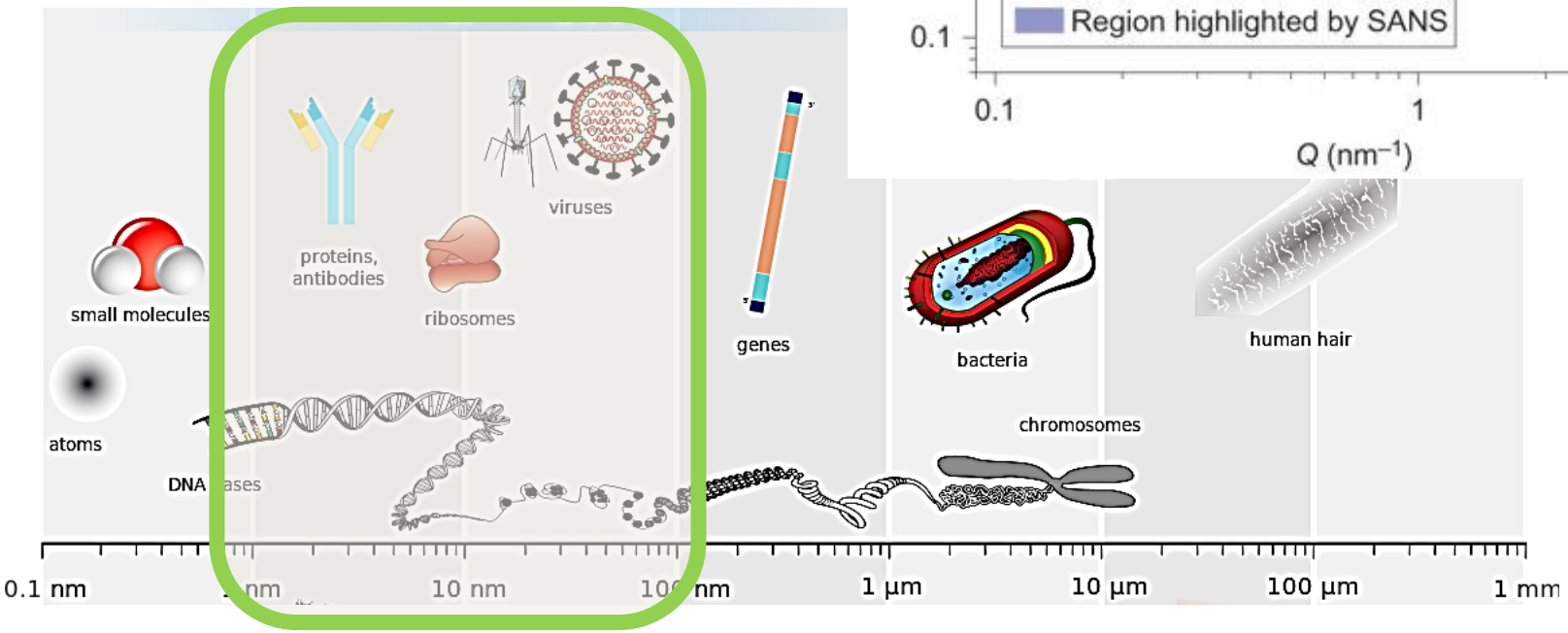

WAXS: fibers in solution

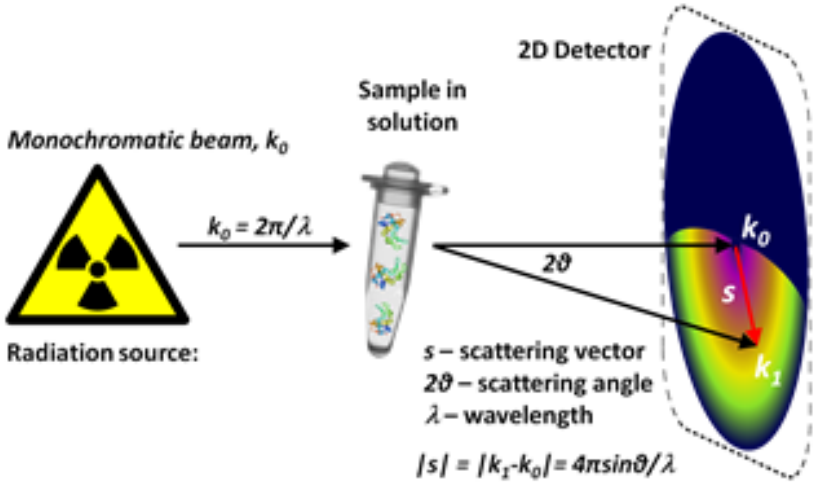

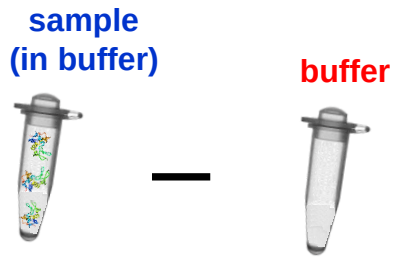

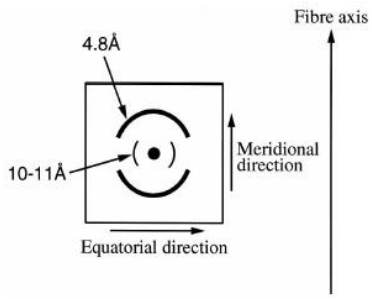

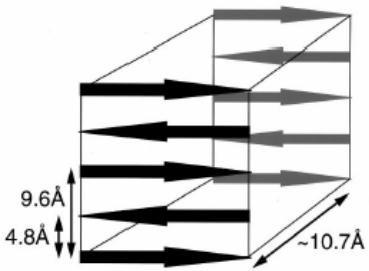

Fiber information

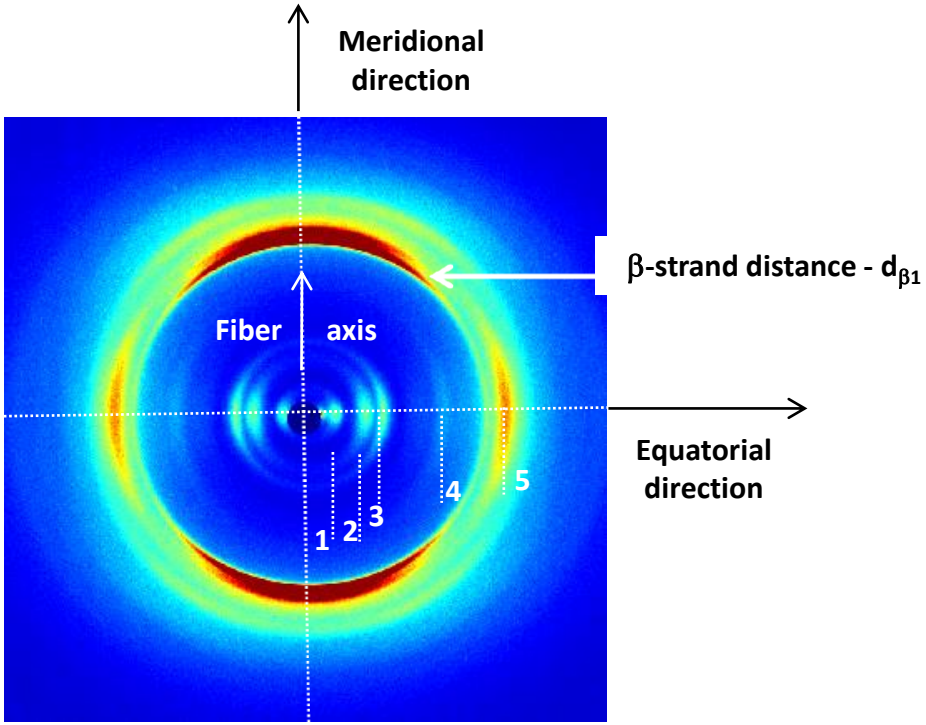

PEGylated tetra-phenylalanine (dried and in solution) fibers for MRI

In collaboration with Dr. Antonella Accardo University of Naples - Italy

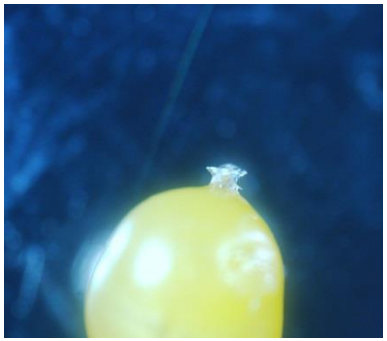

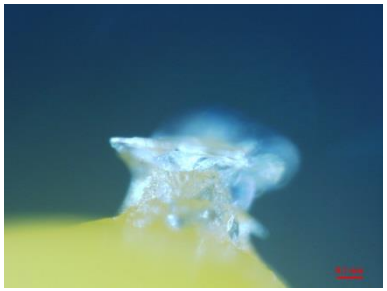

WAXS analysis on water soluble fibers of PEGylated tetra-phenylalanine (F4), chemically modified at the N-terminus with the DOTA chelating agent, showed:

- the typical cross-β fibre diffraction of amyloid-like fibrils, both on the dried fibrils and on the fibrils in solution

- the additional DOTA produces fibers with a higher order degree (atomic & nano).

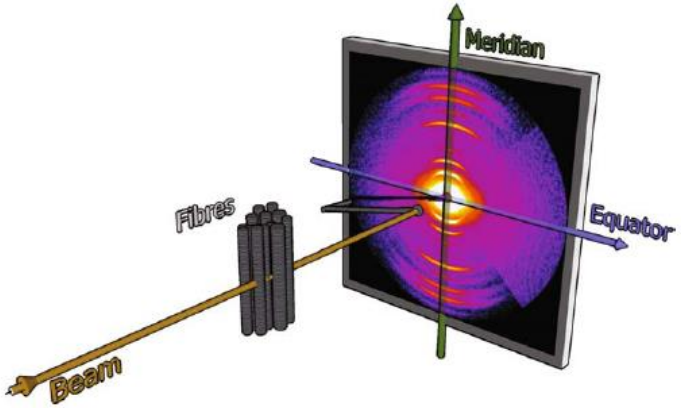

SCIENTIFIC REPORTS

Self-assembly of PEGylated tetra-phenylalanine derivatives: structural insights from solution and solid state studies

Carlo Diaferia, Flavia Anna Mercurio, Cinzia Giannini, Teresa Sibillano, Giancarlo Morelli, Marilisa Leone & Antonella Accardo

Scientific Reports **6**, Article number: 26638 (2016)
doi:10.1038/srep26638
Download Citation

Received: 02 February 2016
Accepted: 04 May 2016
Published online: 25 May 2016

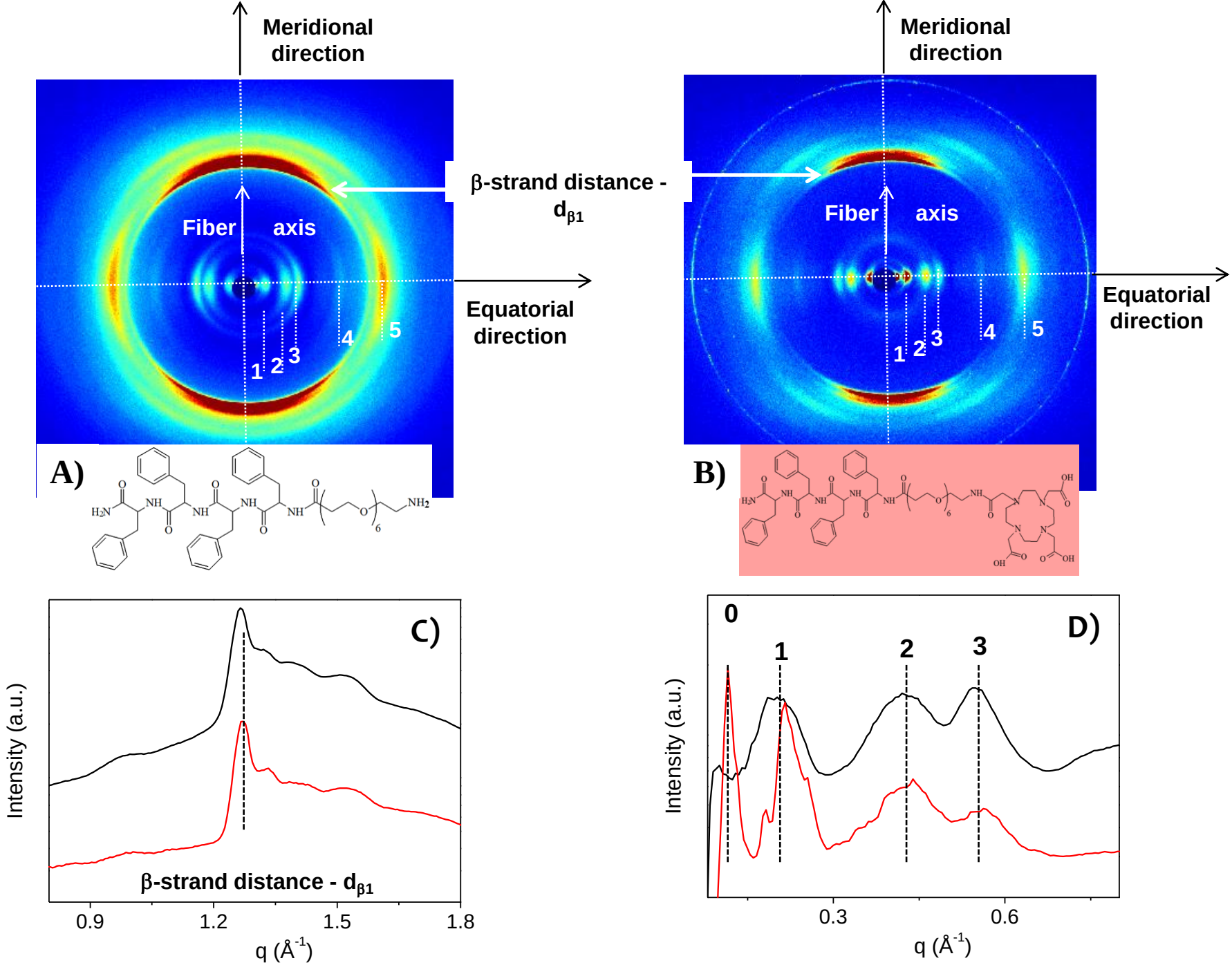
Meridional direction
Fiber axis
β-strand distance - $d_{\beta 1}$
Equatorial direction
1
2
3
4
5
A)
B)
C)
D)
Intensity (a.u.)
β-strand distance - $d_{\beta 1}$
0.9
1.2
1.5
1.8
q (Å^{-1})
0
0.3
0.6

PEGylated tetra-phenylalanine (dried and in solution) fibers for MRI

In collaboration with Dr. Antonella Accardo University of Naples - Italy

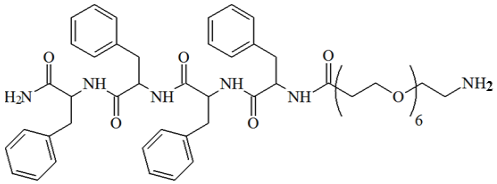

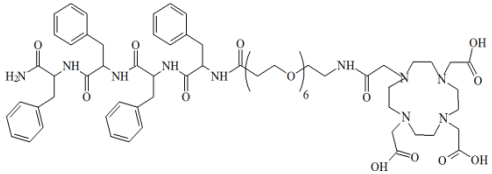

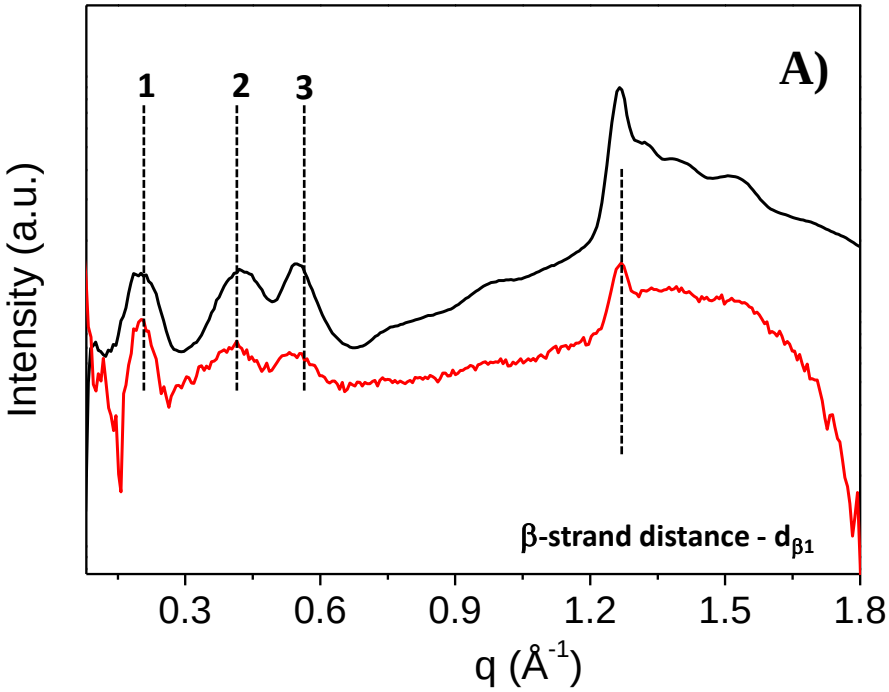

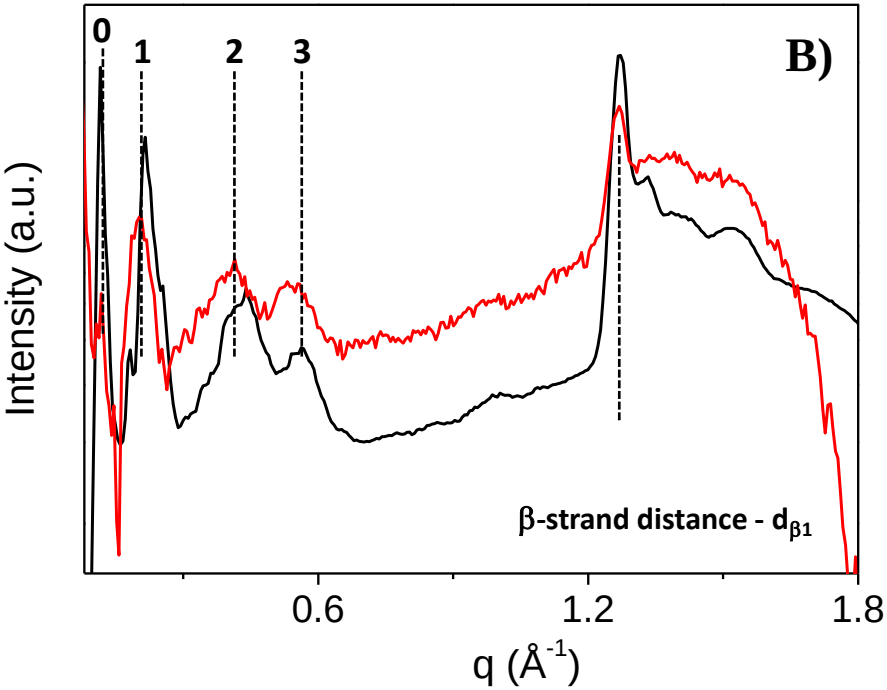

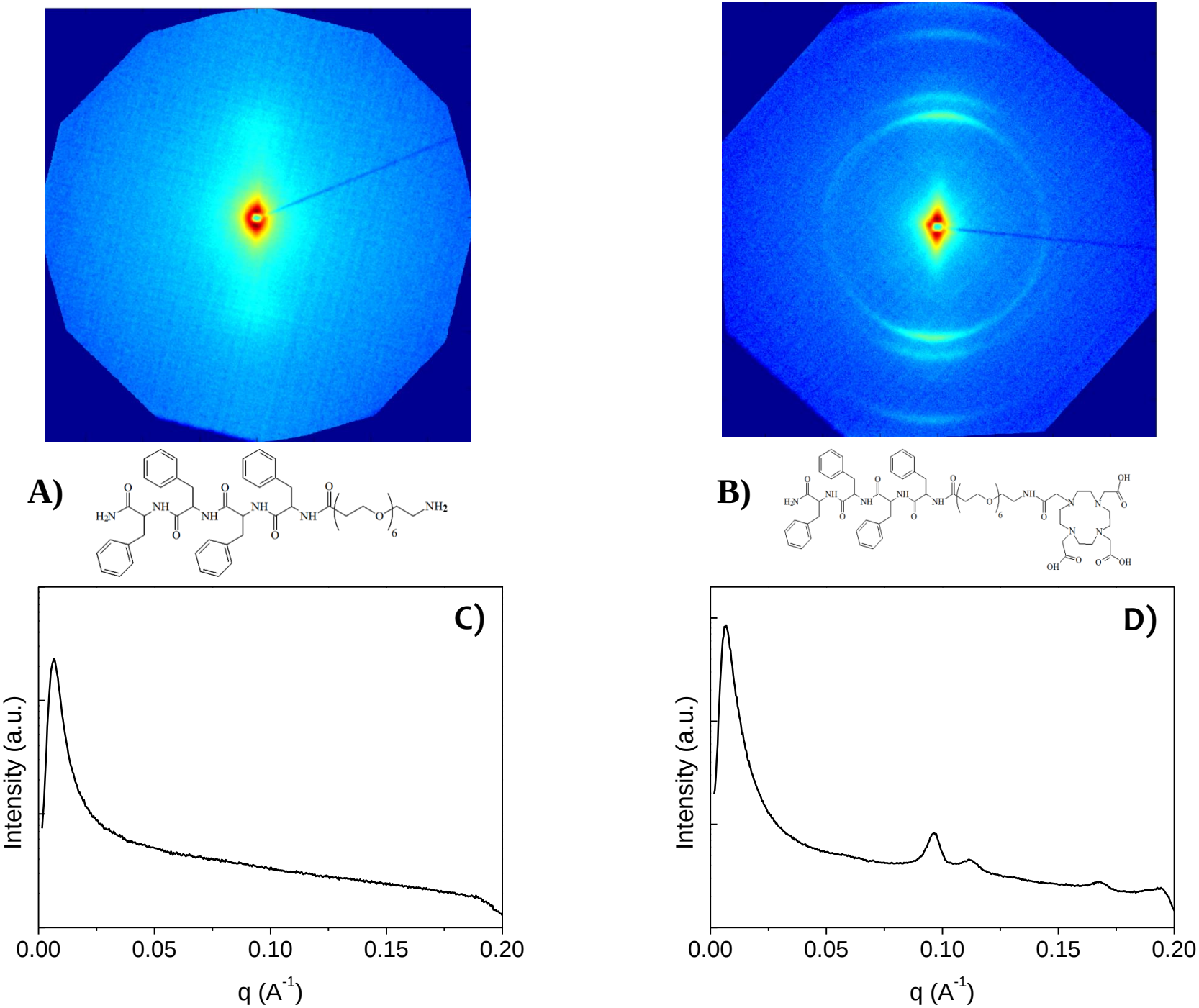
A)
B)
C)
D)
Intensity (a.u.)
q (A-1)
0.00
0.05
0.10
0.15
0.20

PEGylated tetra-phenylalanine (dried and in solution) fibers for MRI

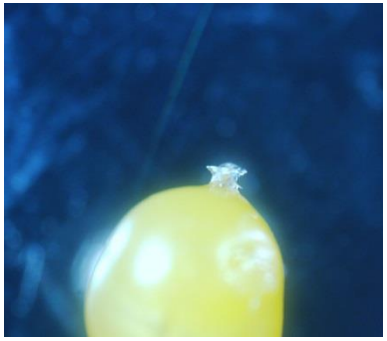

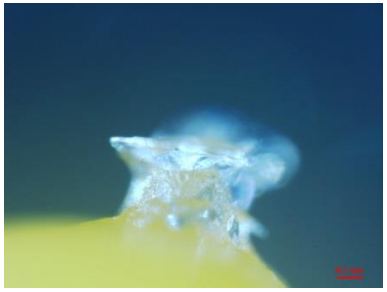

WAXS analysis on water soluble fibers of PEGylated tetra-phenylalanine (F4), chemically modified at the N-terminus with the DOTA chelating agent, showed:

- the typical cross-β fibre diffraction of amyloid-like fibrils, both on the dried fibrils and on the fibrils in solution

- the additional DOTA produces fibers with a higher order degree.

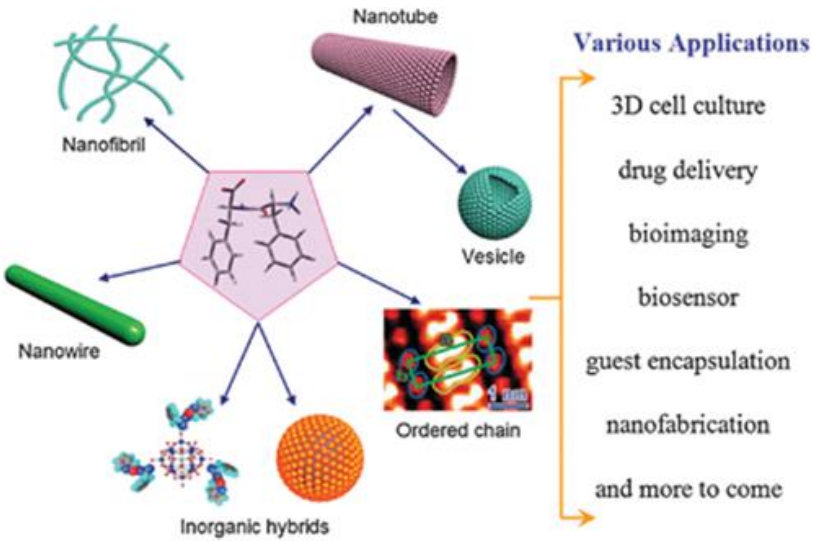

Chem. Soc. Rev., 2010, 39, 1877–1890

SCIENTIFIC REPORTS

Self-assembly of PEGylated tetra-phenylalanine derivatives: structural insights from solution and solid state studies

Carlo Diaferia, Flavia Anna Mercurio, Cinzia Giannini, Teresa Sibillano, Giancarlo Morelli, Marilisa Leone & Antonella Accardo

Scientific Reports **6**, Article number: 26638 (2016)
doi:10.1038/srep26638
Download Citation

Received: 02 February 2016
Accepted: 04 May 2016
Published online: 25 May 2016

PEGylated hexa-phenylalanine photoluminescent nanofibers

In collaboration with Dr. Antonella Accardo University of Naples - Italy

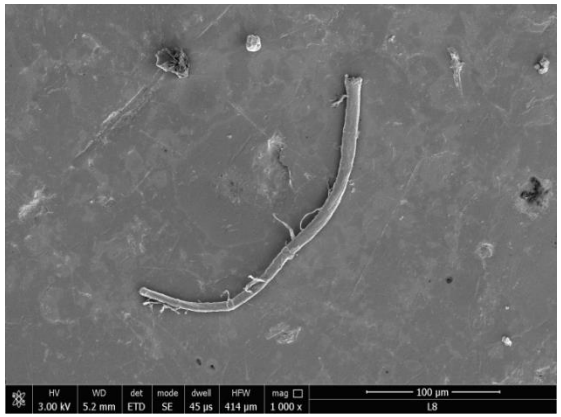

Aromatic peptide self-assembles in water in stable and well-ordered nanofibers with optoelectronic properties. A variety of techniques such as fluorescence, FTIR, CD, DLS, SEM, SAXS and WAXS allowed us to correlate the photoluminescence (PL) properties of the self-assembled nanofibers with the structural organization of the peptide building block at the micro- and nano-scale.

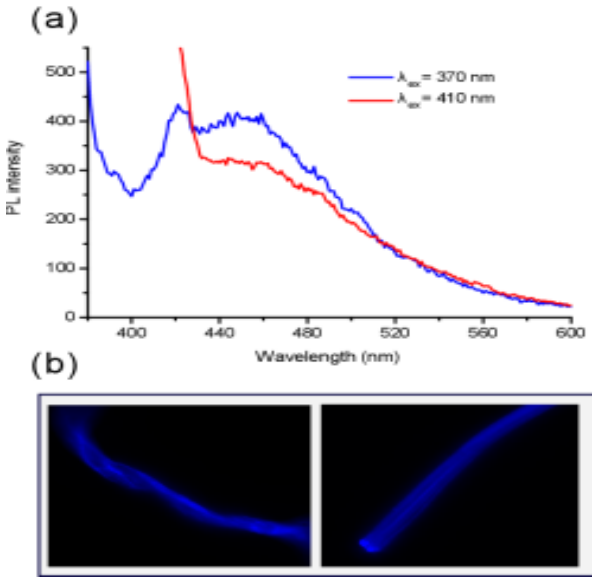

PL of PEG_8-F6 nanofibers at 10 mg/mL. (a) Blue PL emission spectra for sample in solution upon excitation at ~370 nm (blue line) and at ~410 nm (red line).

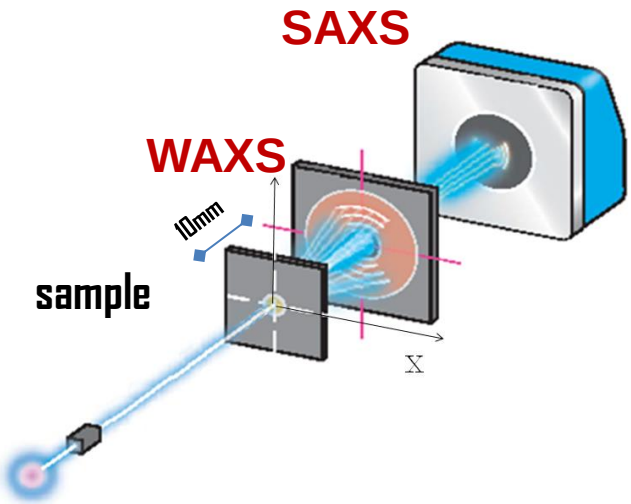

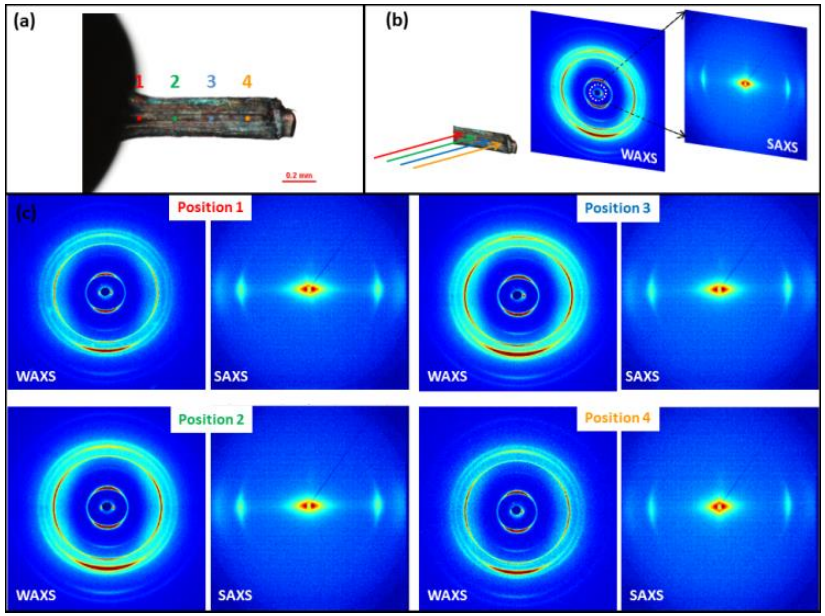

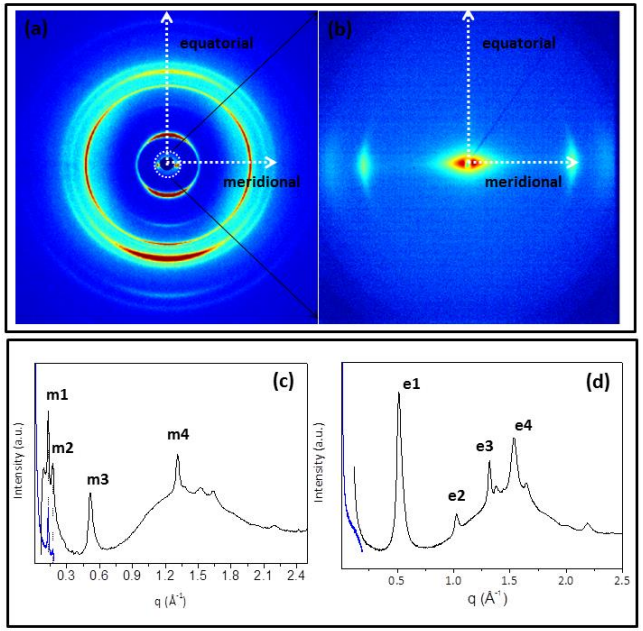

Meridional reflections		
Label	q (Å^{-1})	d (Å)
m1	0.132	48.0
m2	0.171	37.0
m3	0.514	12.2
m4 (β strand)	1.32	4.8
Equatorial reflections		
e1	0.514	12.2
e2	1.026	6.1
e3 (β strand)	1.319	4.8
e4	1.536	4.1

“cross-β” diffraction pattern of amyloid-like fibers, with a diffraction peak **of 4.8 Å along the meridian**, representing the inter-chain distance between the hydrogen-bonded strands, and a diffraction peak of **12.5 Å along the equatorial direction, distinctive of the stacking of β-sheets perpendicularly to the fiber axis**.

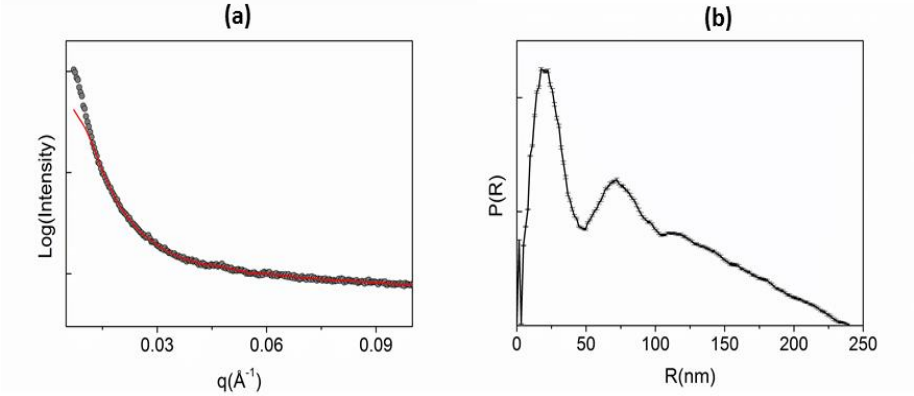

(a) equatorial SAXS (dotted curve) and best fit (full line); (b) pair distribution function extracted from (a). The gyration radius, determined by this analysis, is Rg=69±1nm.

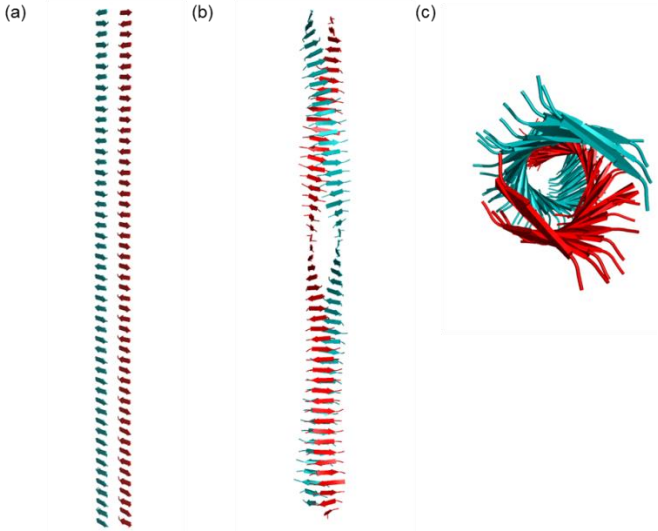

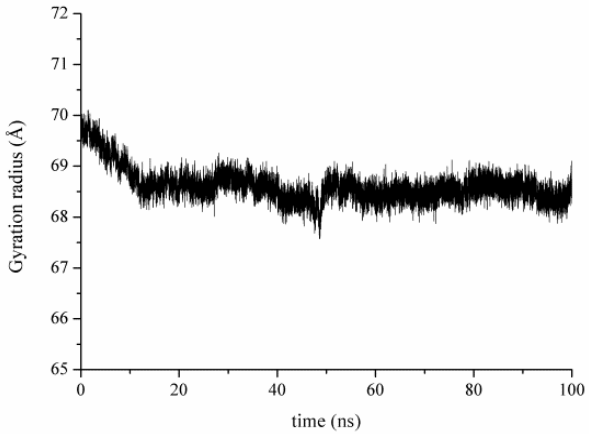

The starting model undergoes major transition during the simulation. The system adopts a novel structural state in the equilibrated region of the trajectory (20-100 ns). This transition is also coupled with a significant variation of the assembly gyration radius . At the steady state Rg=69±1 nm

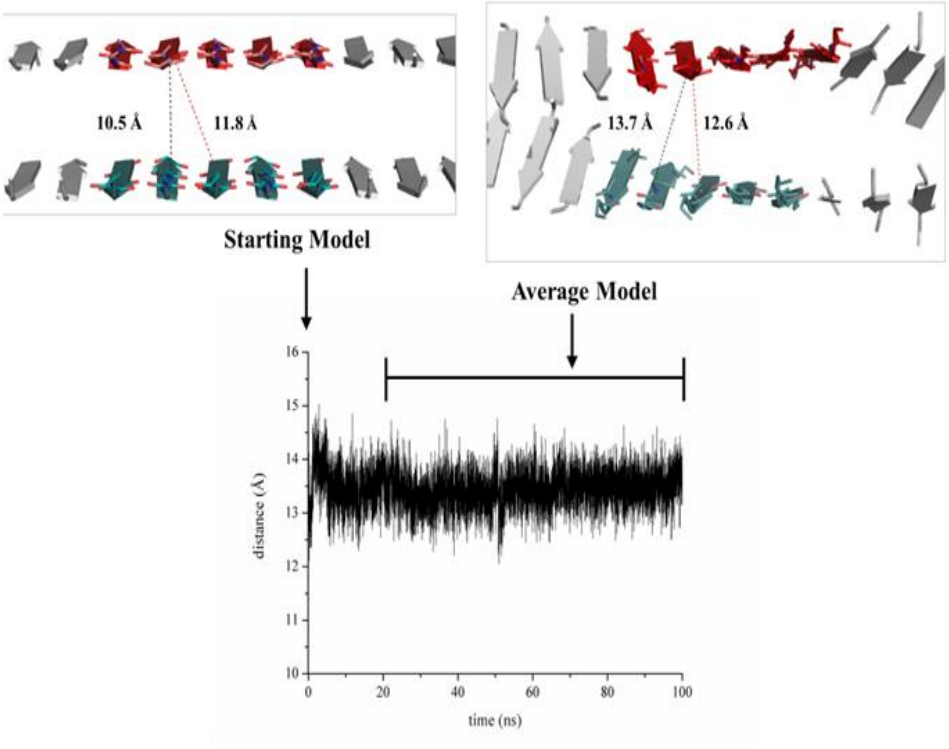

The inter-sheet separation ≡ WAXS data of a strong equatorial reflection at ~ 12.5 Å.

CHEMISTRY
A European Journal
ChemPubSoc Europe
Explore this journal >

Full Paper

Hierarchical Analysis of Self-Assembled PEGylated Hexaphenylalanine Photoluminescent Nanostructures

Dr. Carlo Diaferia, Dr. Teresa Sibillano, Dr. Nicole Balasco, Dr. Cinzia Giannini, Dr. Valentina Roviello, Dr. Luigi Vitagliano, Prof. Giancarlo Morelli, Dr. Antonella Accardo

First published: 5 October 2016 Full publication history

NANOCRYSTALS ASSEMBLED ON TOP OF SURFACES

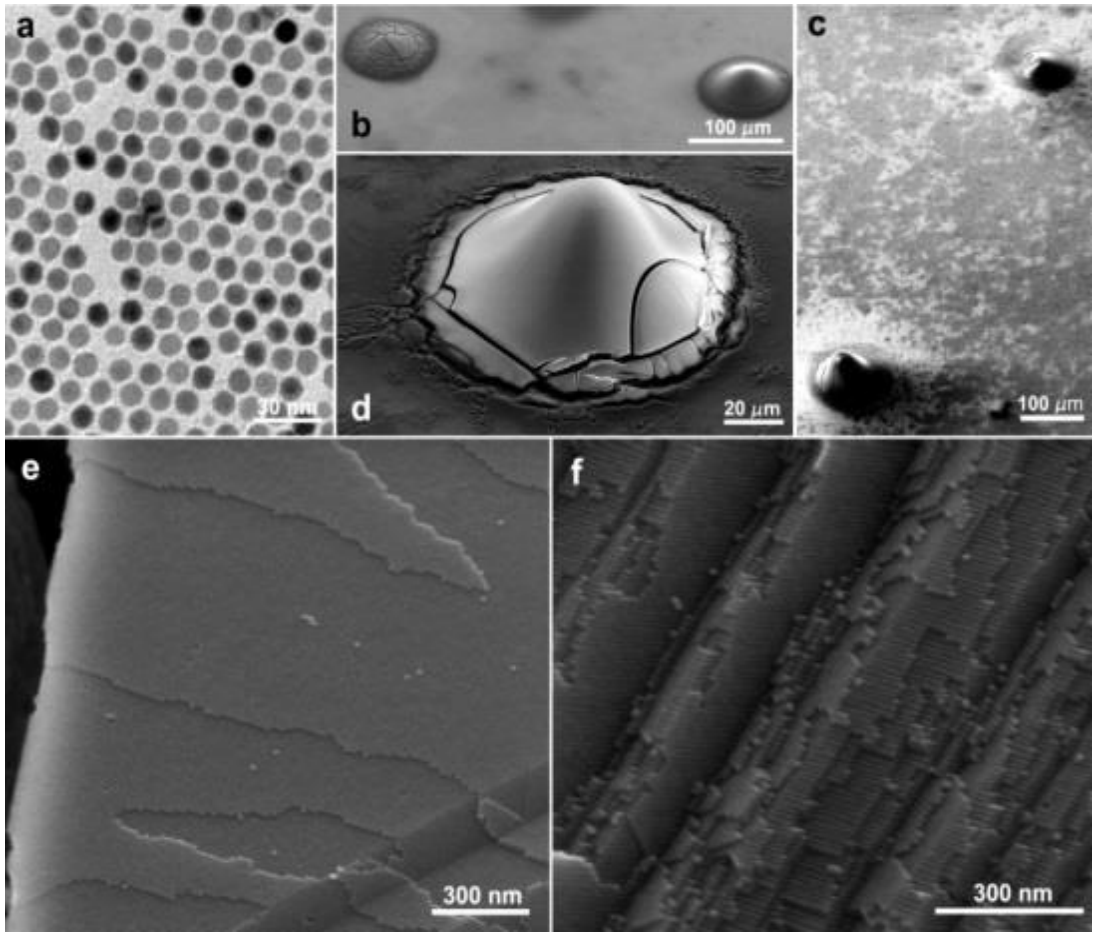

SAXS-WAXS or GISAXS-GIWAXS

- liquids
- tissues

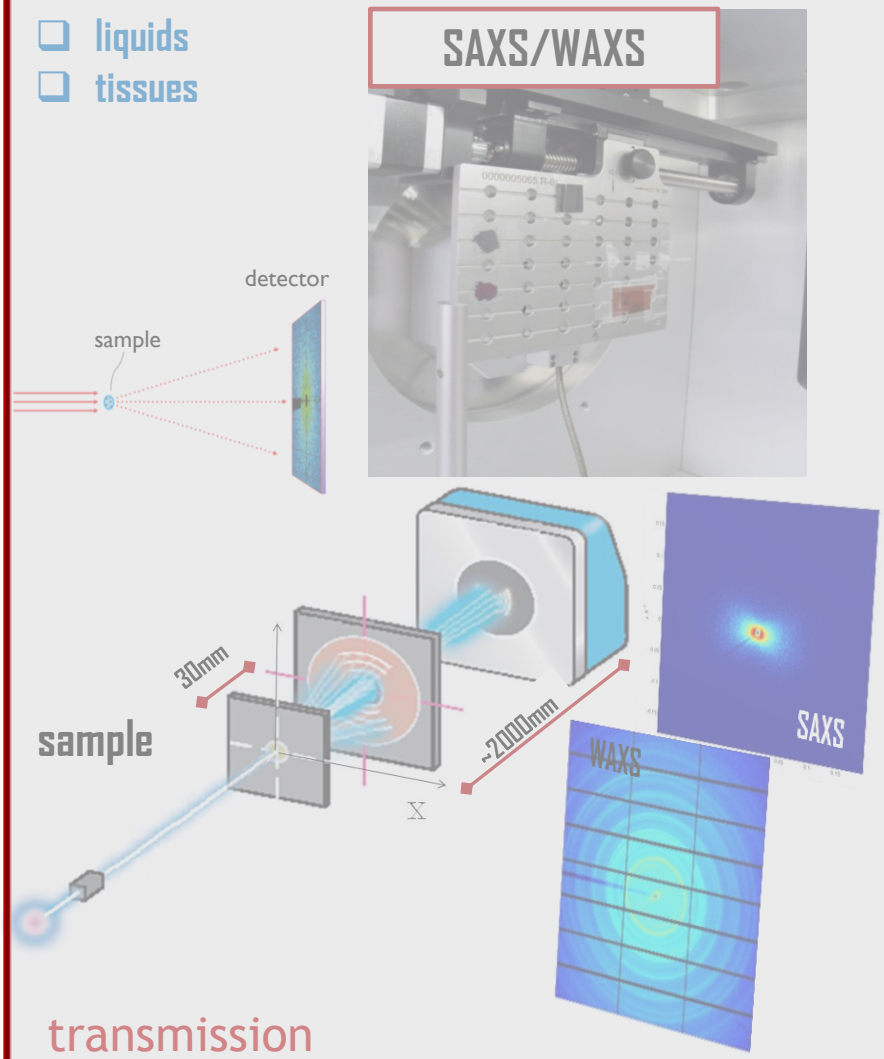

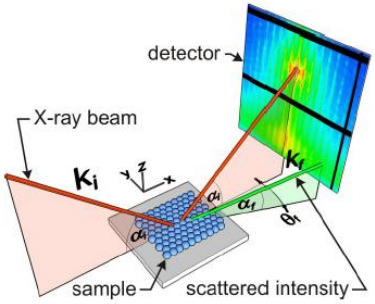

- Planar devices
- Nanostructured surfaces

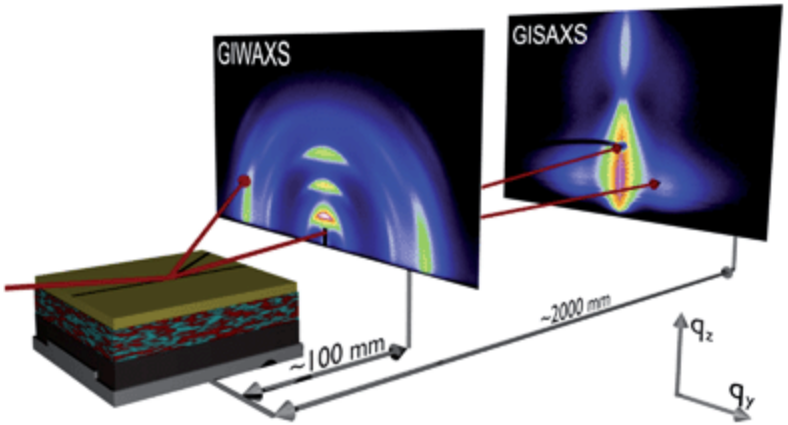

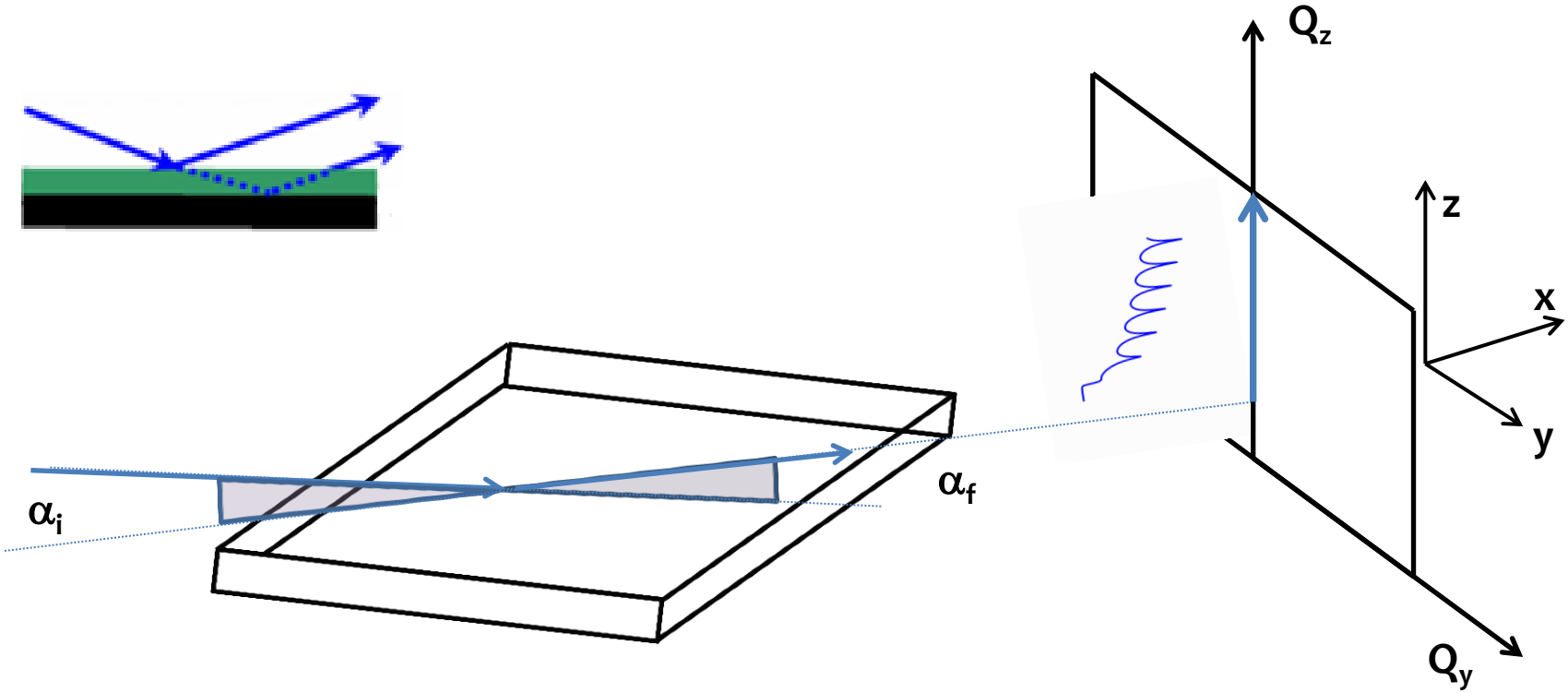
Q_z
z
x
y
Q_y
α_i
α_f

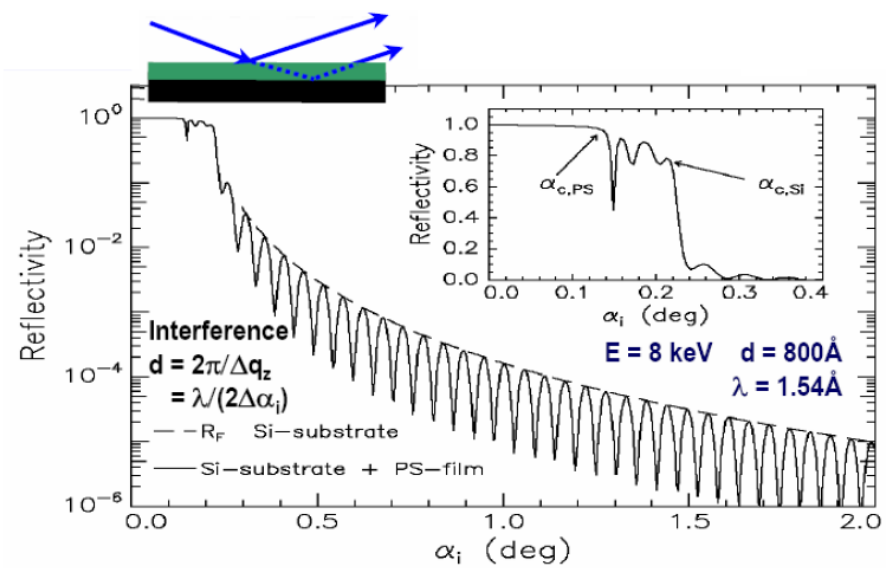
Reflectivity
α_i (deg)
Interference
$d = 2\pi/\Delta q_z$
$= \lambda/(2\Delta\alpha_i)$
R_F Si–substrate
Si–substrate + PS–film
E = 8 keV d = 800Å
λ = 1.54Å
$\alpha_{c,PS}$
$\alpha_{c,Si}$

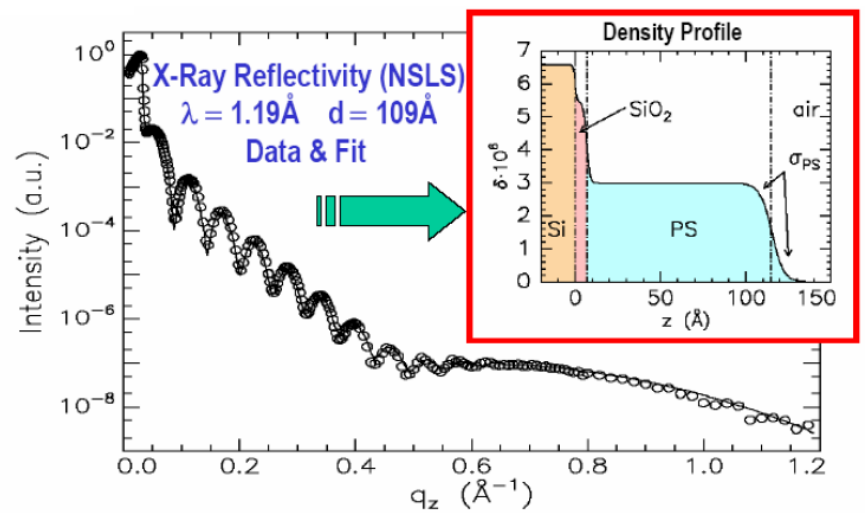
X-Ray Reflectivity (NSLS)
λ = 1.19Å d = 109Å
Data & Fit
Intensity (a.u.)
q_z (Å^{-1})
Density Profile
SiO_2
air
σ_{PS}
Si
PS
$\delta \cdot 10^6$
z (Å)

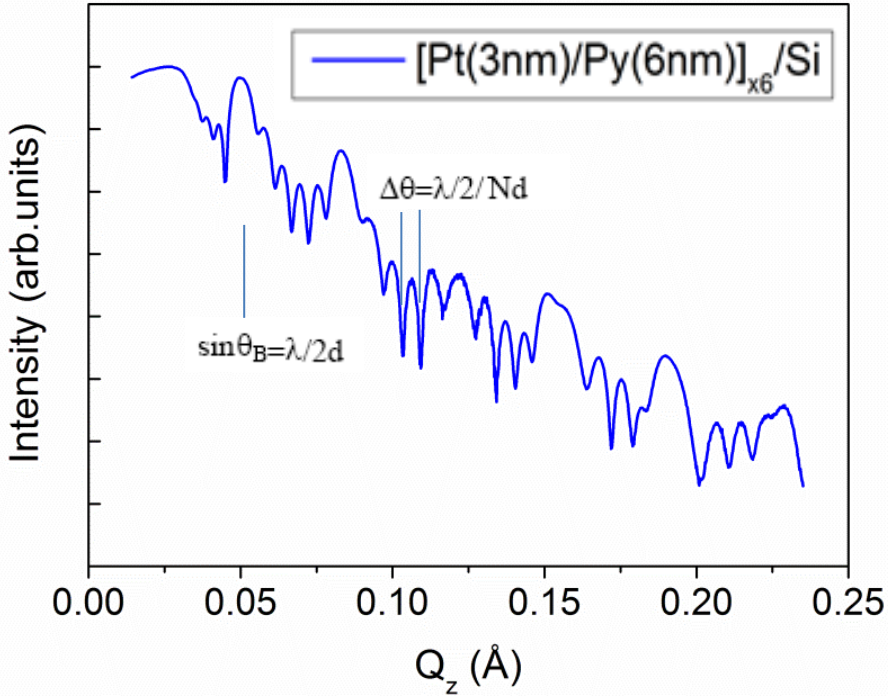

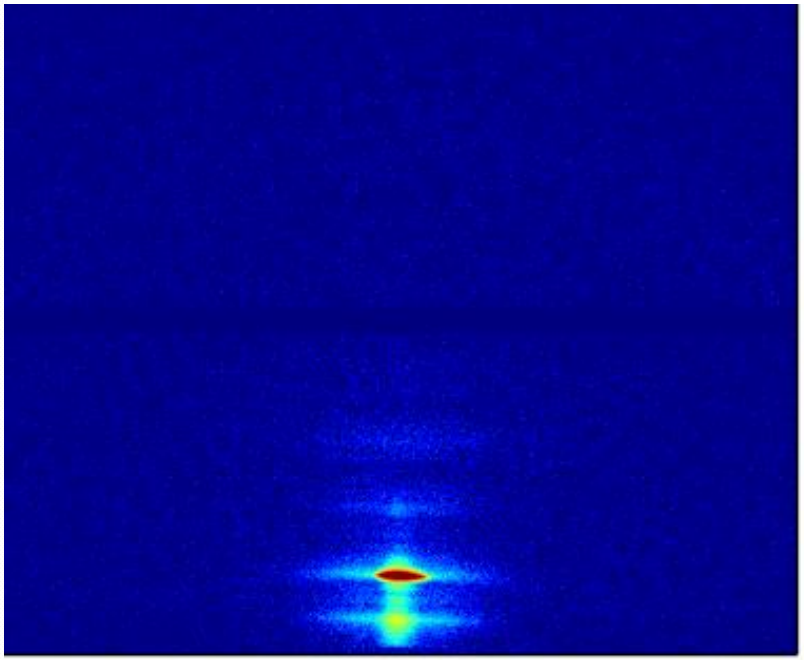

d=A+B;
A=3nm; B=6nm
N=6

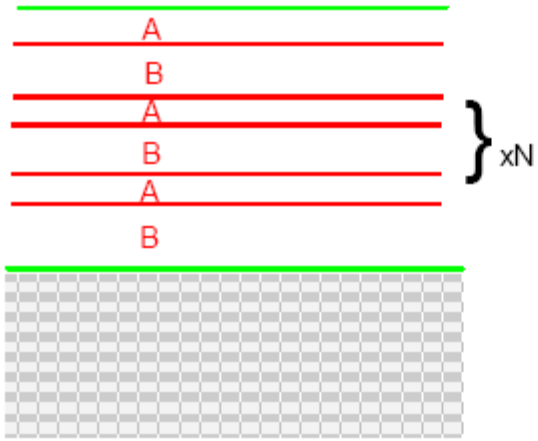

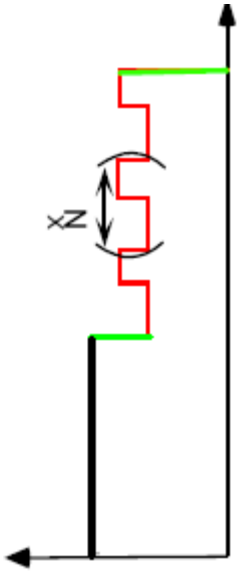

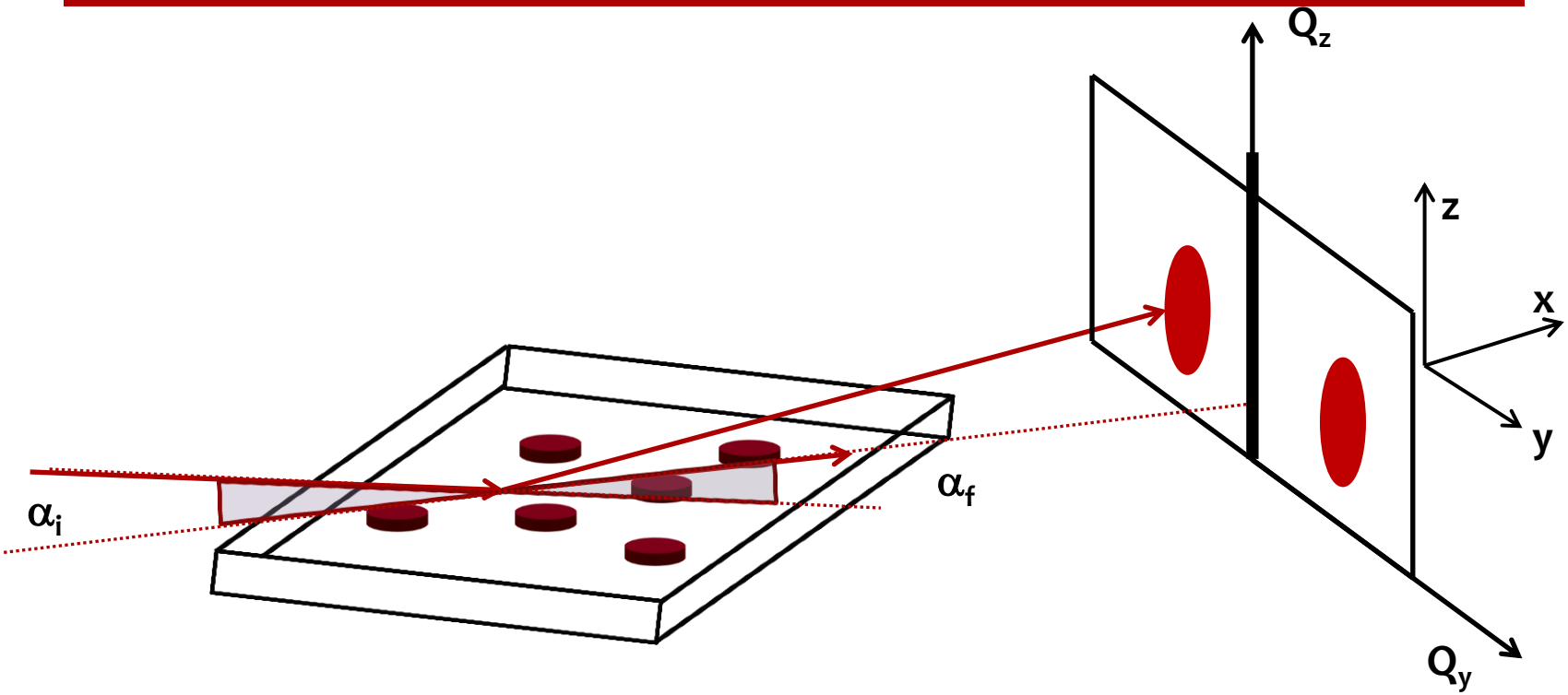
Q_z
z
x
y
α_i
α_f
Q_y

GISAXS-GIWAXS

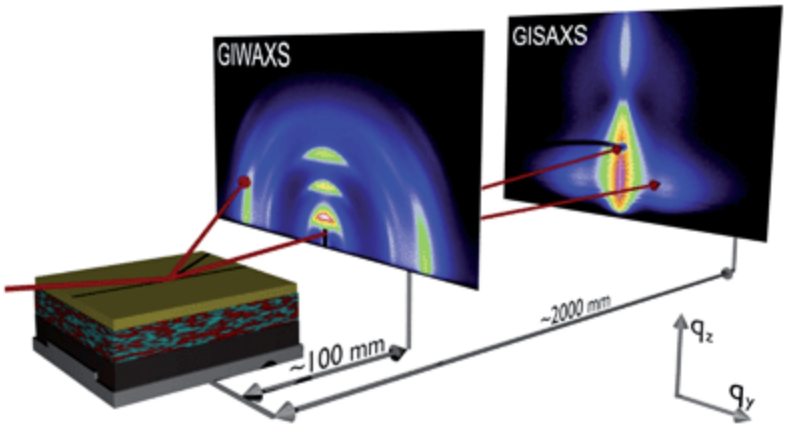

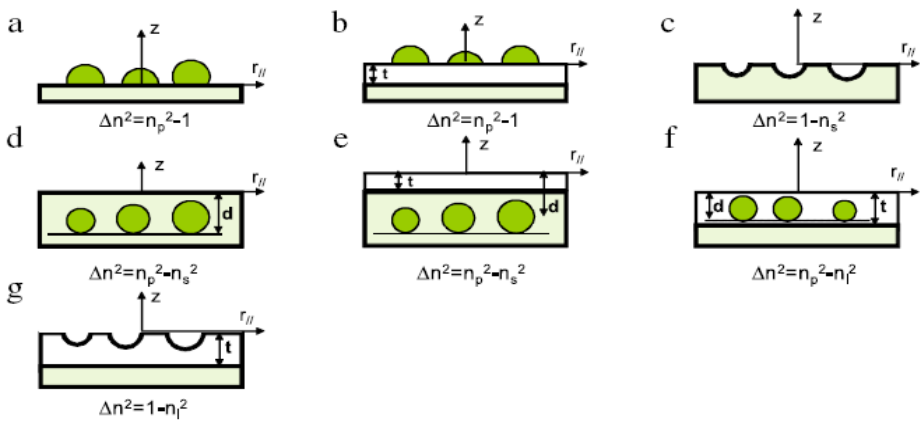

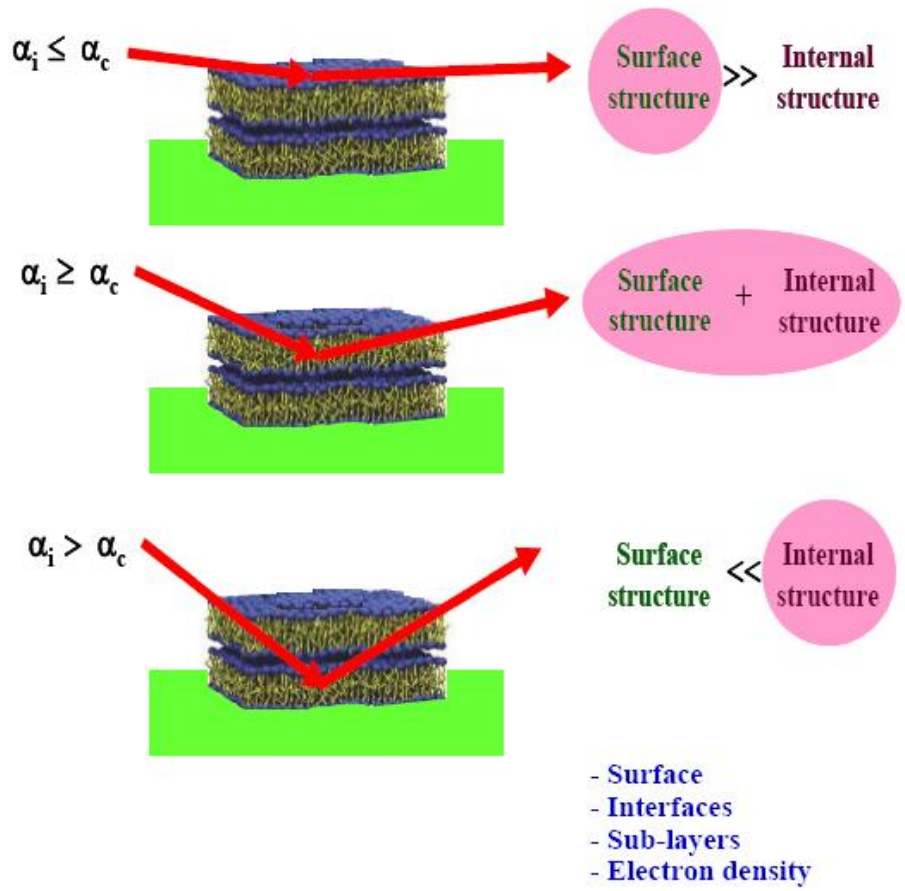

SPHERE

$R = 5\ nm$

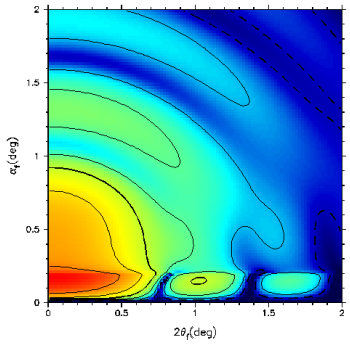

FORM FACTOR

HOLLOW SPHERE

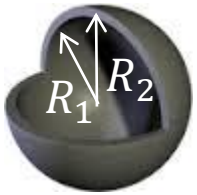

$R_2 - R_1 = 1\ nm$

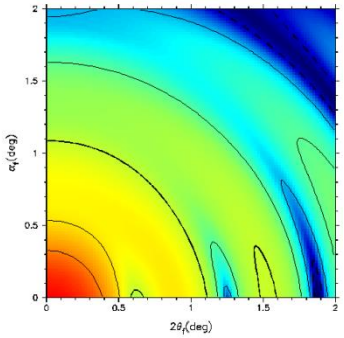

FORM FACTOR

CYLINDER

$a = b = R = 5\ nm$

$h = 25\ nm$

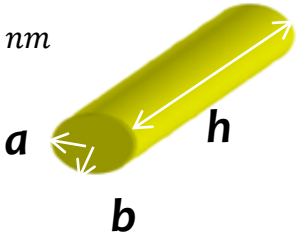

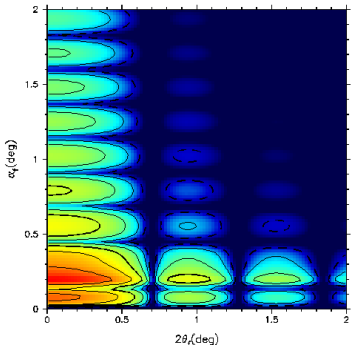

FORM FACTOR

FLAT DISK

$R = 12.5\ nm$

$h = 5\ nm$

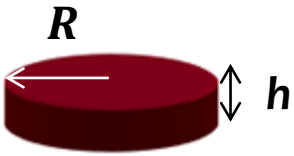

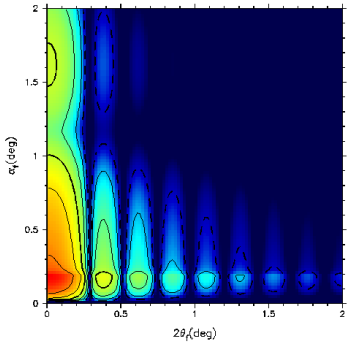

FORM FACTOR

SPHERE

$R = 5\ nm$

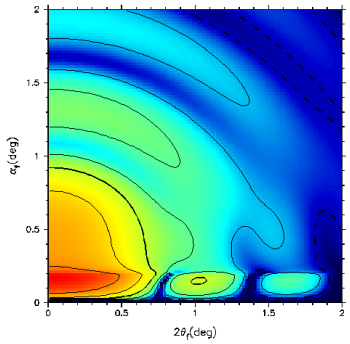

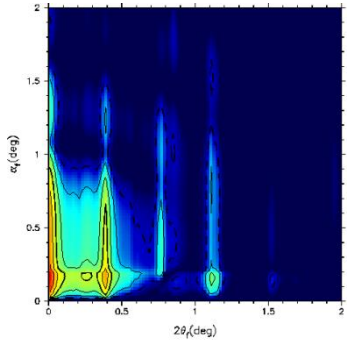

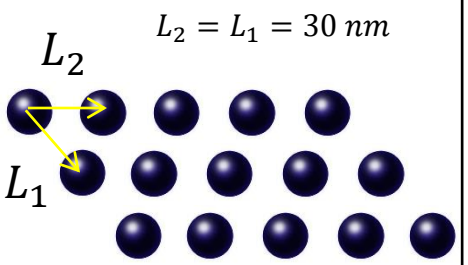

HOLLOW SPHERE

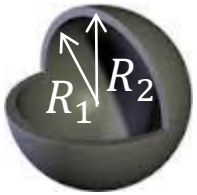

$R_2 - R_1 = 1\ nm$

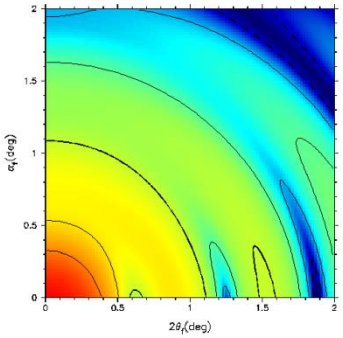

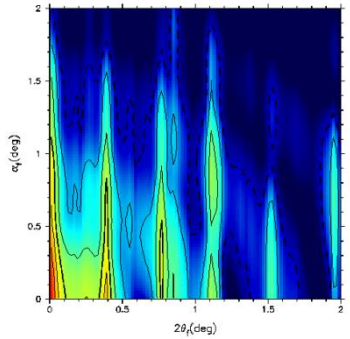

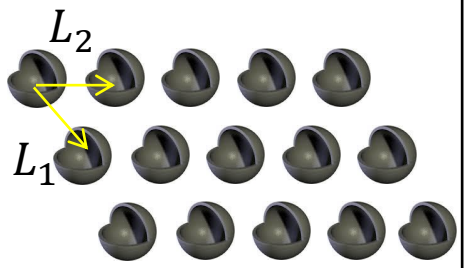

$L_2 = L_1 = 30\ nm$

CYLINDER

$a = b = R = 5\ nm$

$h = 25\ nm$

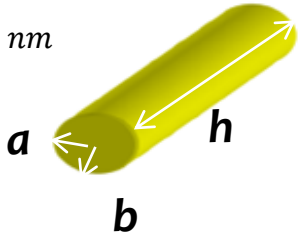

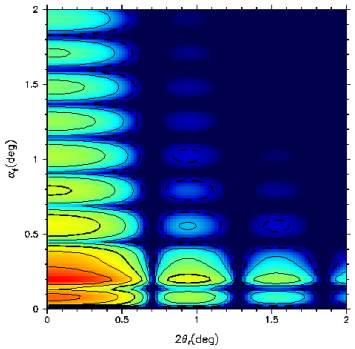

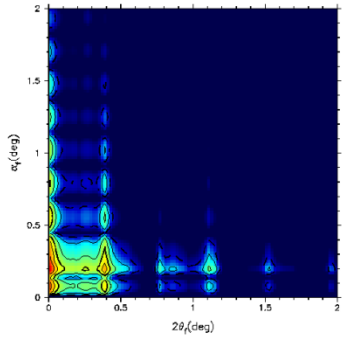

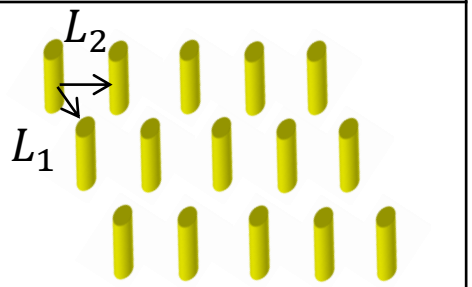

$L_2 = L_1 = 30\ nm$

FLAT DISK

$R = 12.5\ nm$

$h = 5\ nm$

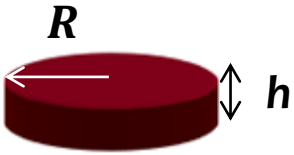

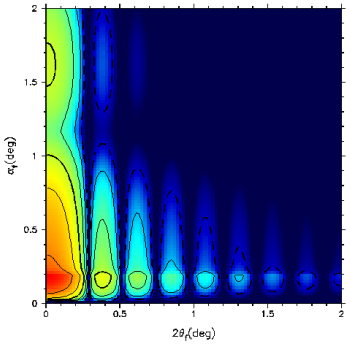

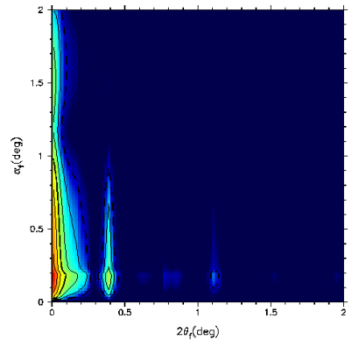

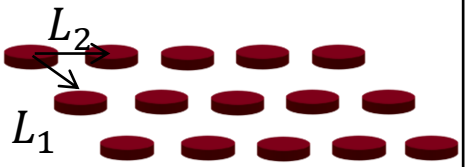

$L_2 = L_1 = 30\ nm$

GISAXS - 2D assemblies

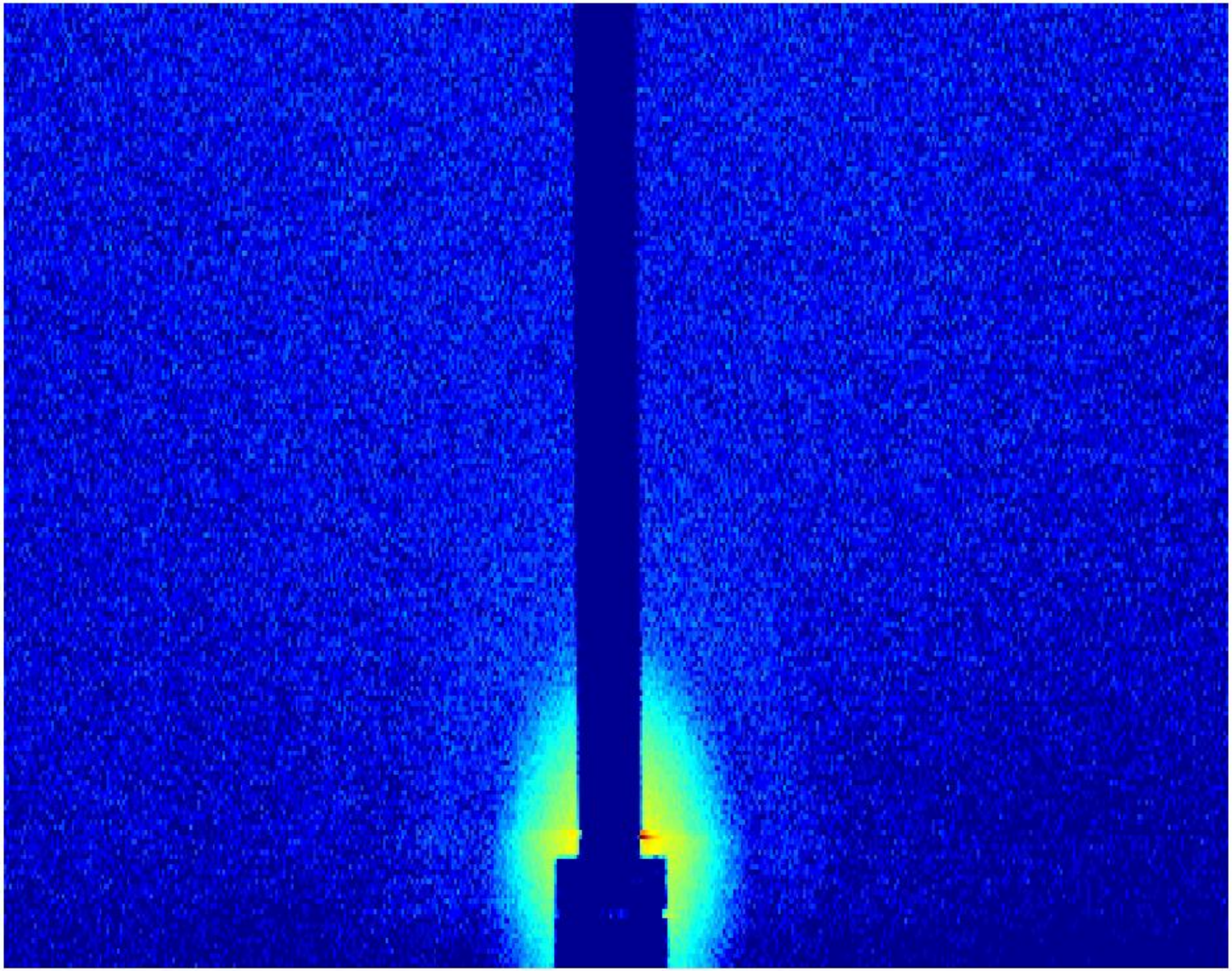

GISAXS - 3D assemblies

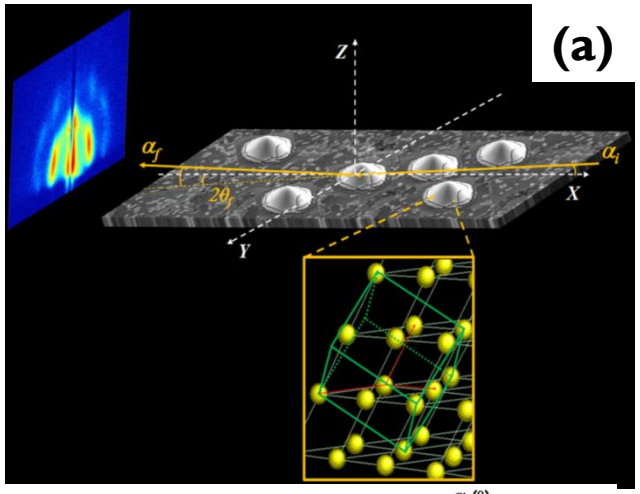

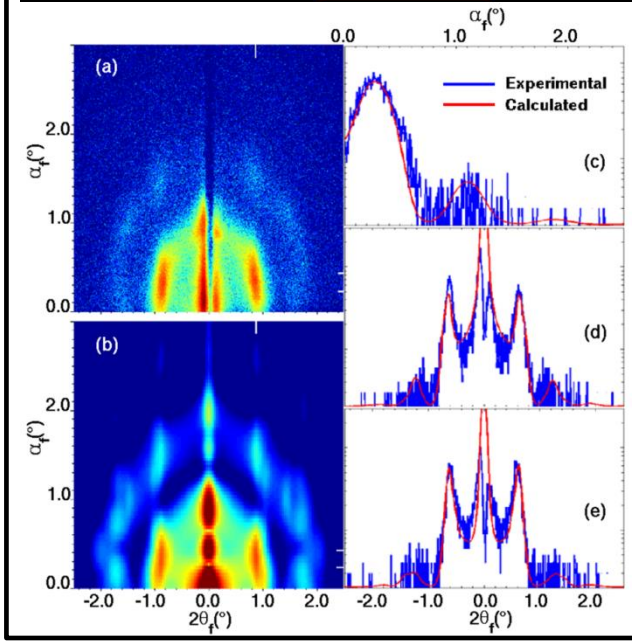

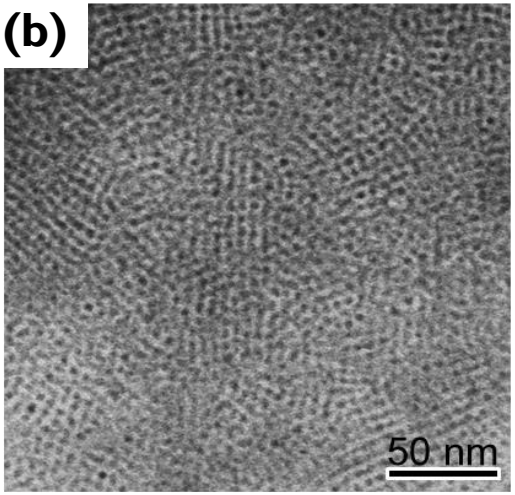

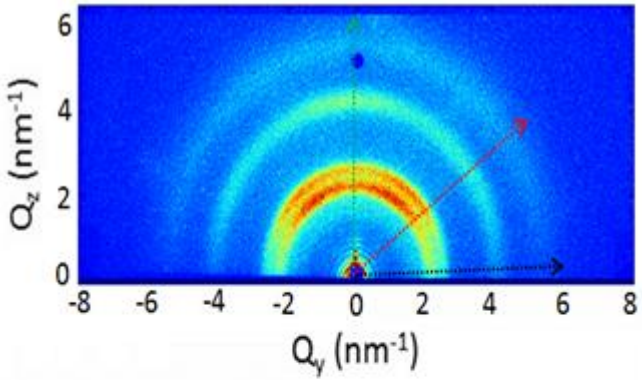

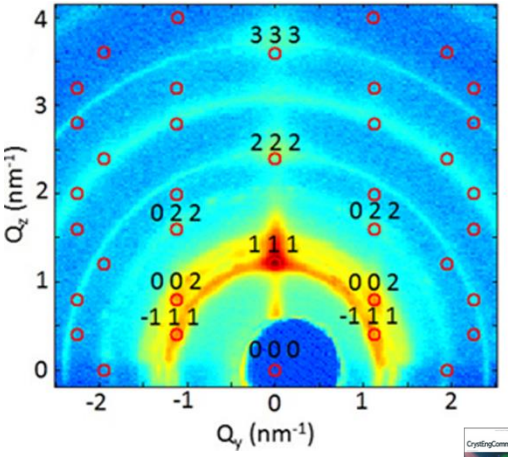

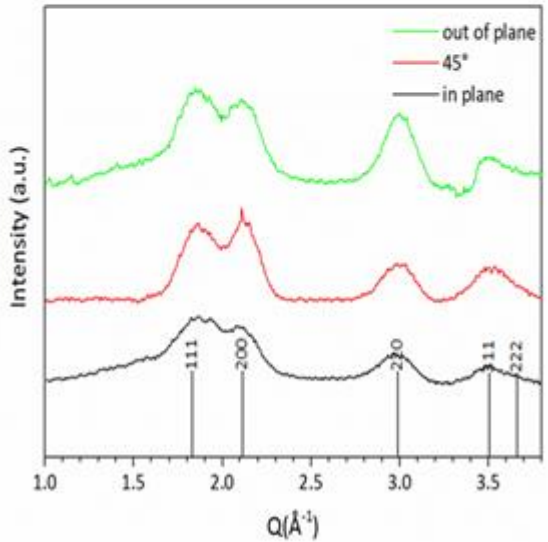

CrystEngComm

Design and understanding of solid-state and crystalline materials

Impact Factor 3.879 | 48 Issues per Year

Paper

GISAXS and GIWAXS study on self-assembling processes of nanoparticle based superlattices

Michela Corricelli, Davide Altamura, Maria Lucia Curri, Teresa Sibillano, Dritan Siliqi, Annamaria Mazzone, Nicoletta Depalo, Elisabetta Fanizza, daniela Zanchet, Cinzia Giannini and Marinella Striccoli

CrystEngComm, 2014, Accepted Manuscript

DOI: 10.1039/C4CE01291G

Received 25 Jun 2014, Accepted 13 Aug 2014

First published online 13 Aug 2014

CRYSTAL GROWTH & DESIGN

Article

pubs.acs.org/cryst

Exploiting GISAXS for the Study of a 3D Ordered Superlattice of Self-Assembled Colloidal Iron Oxide Nanocrystals

Davide Altamura,[1] Václav Holý,[2] Dritan Siliqi,[1] Indira Chaitanya Lekshmi,[3] Concetta Nobile,[4] Giuseppe Maruccio,[4,5] P. Davide Cozzoli,[4,5] Lixin Fan,[6] Fabia Gozzo,[6] and Cinzia Giannini[1,*]

[1]Institute of Crystallography (CNR-IC), V. Amendola 122/O, 70126-Bari, Italy
[2]Faculty of Mathematics and Physics, Charles University, Ke Karlovu 5, 121 16 Prague, Czech Republic
[3]National Nanotechnology Laboratory (NNL), CNR Istituto Nanoscienze , c/o Distretto Tecnologico, via per Arnesano km 5, 73100 Lecce, Italy
[4]Dipartimento di Matematica e Fisica "E. De Giorgi", Università del Salento, via per Arnesano, 73100 Lecce
[5]Rigaku Innovative Technologies (RIT), 1900 Taylor Road, Auburn Hills, Michigan 48326, United States
[6]Paul Scherrer Institut, Swiss Light Source, 5232 Villigen PSI, Switzerland

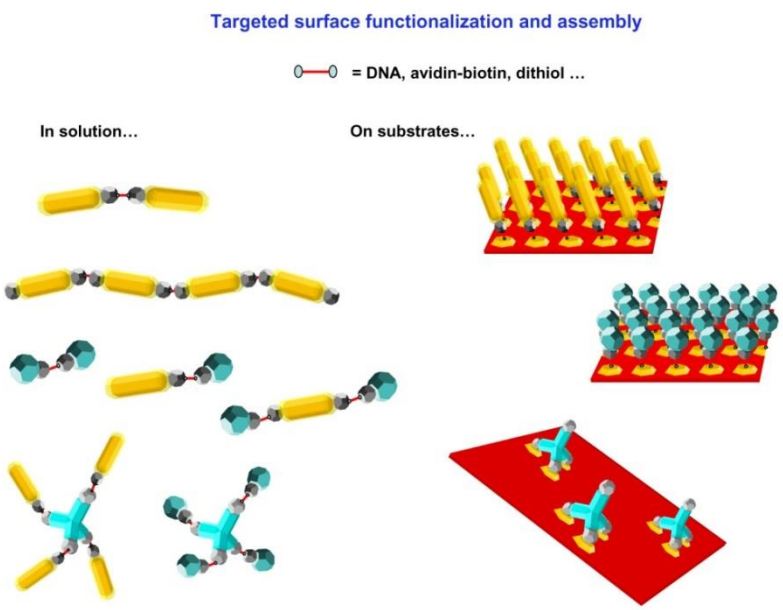

self-assembly

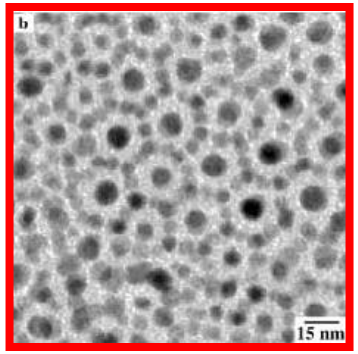

end-to-end assembly

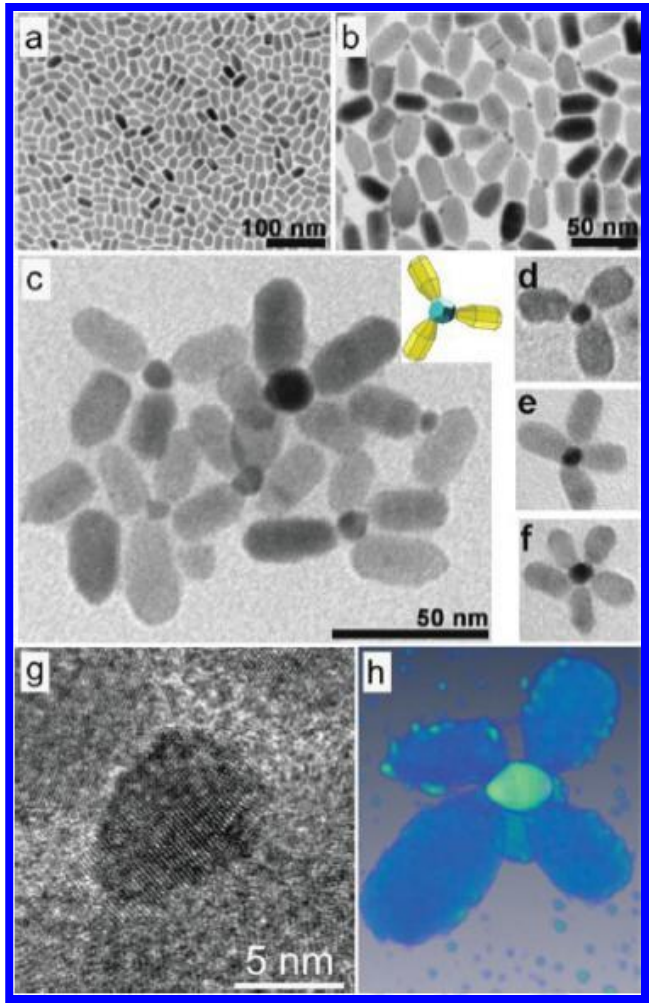

NANOCRYSTALS EMBEDDED IN POLYMERS

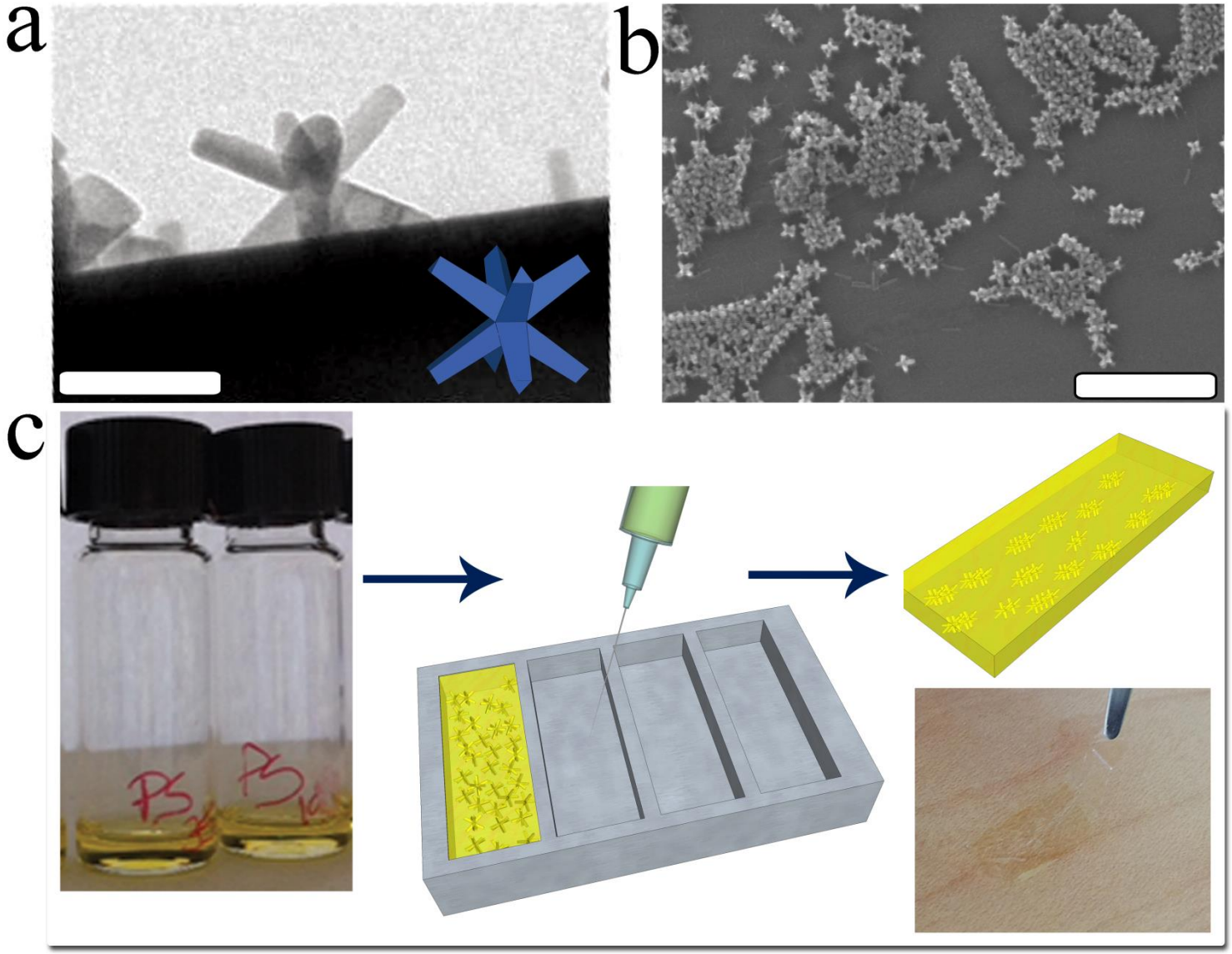

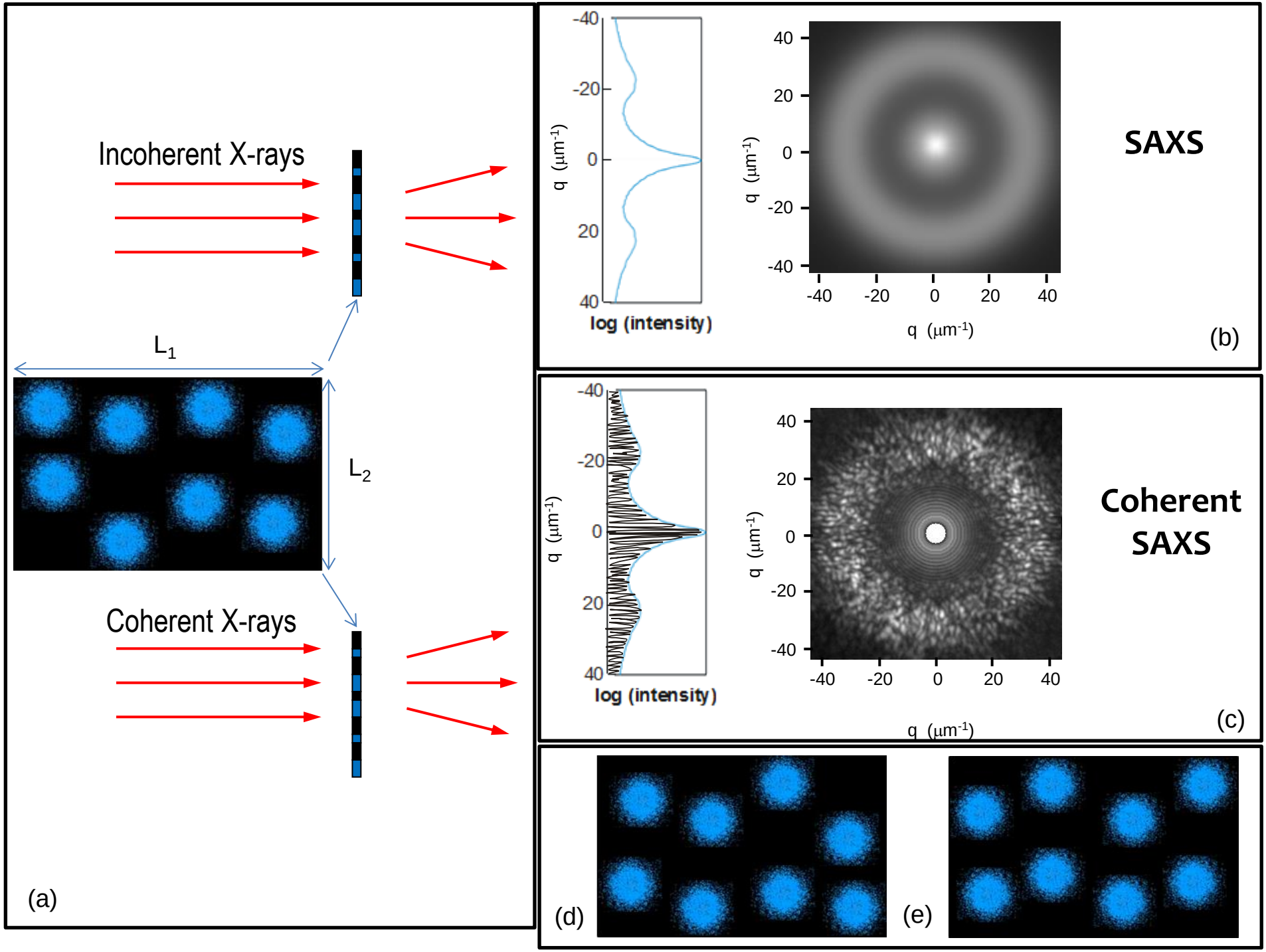
Incoherent X-rays
L1
L2
Coherent X-rays
(a)
-40
-20
0
20
40
q (μm-1)
log (intensity)
SAXS
(b)
Coherent SAXS
(c)
(d)
(e)

Ptychography on NanoCrystals in Polymers

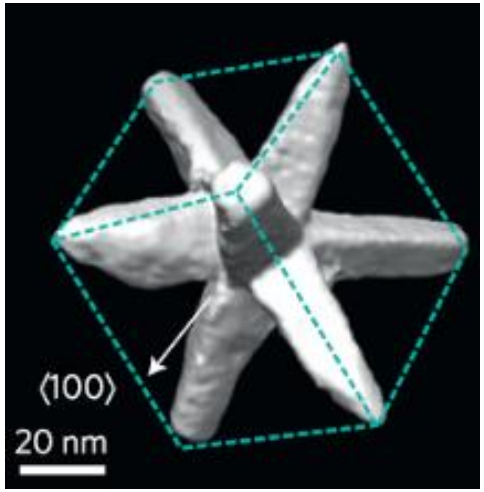

SCIENTIFIC REPORTS

OPEN

Ptychographic Imaging of Branched Colloidal Nanocrystals Embedded in Free-Standing Thick Polystyrene Films

Received: 13 January 2015
Accepted: 07 December 2015
Published: 18 January 2016

Liberato De Caro[1], Davide Altamura[1,*], Milena Arciniegas[2,*], Dritan Siliqi[1], Mee R. Kim[2,†], Teresa Sibillano[1], Liberato Manna[2] & Cinzia Giannini[1]

Object of the work:
investigate the dispersion of octapod-shaped NCs (made of a CdSe core and eight CdS arms) embedded in ~25 μm thick polystyrene (PS) free-standing films.
A reliable non-destructive high resolution imaging technique with the capability to penetrate μm-thick samples and with the necessary resolution to visualize nanometre-scale structures is needed. This stringent requirement rules out any electron-based microscopic technique, as they are not suited for the observation of μm thick films.

Ptychography on NanoCrystals in Polymers

Experiment of ptychography performed at the c-SAXS beamline in SLS-Villigen

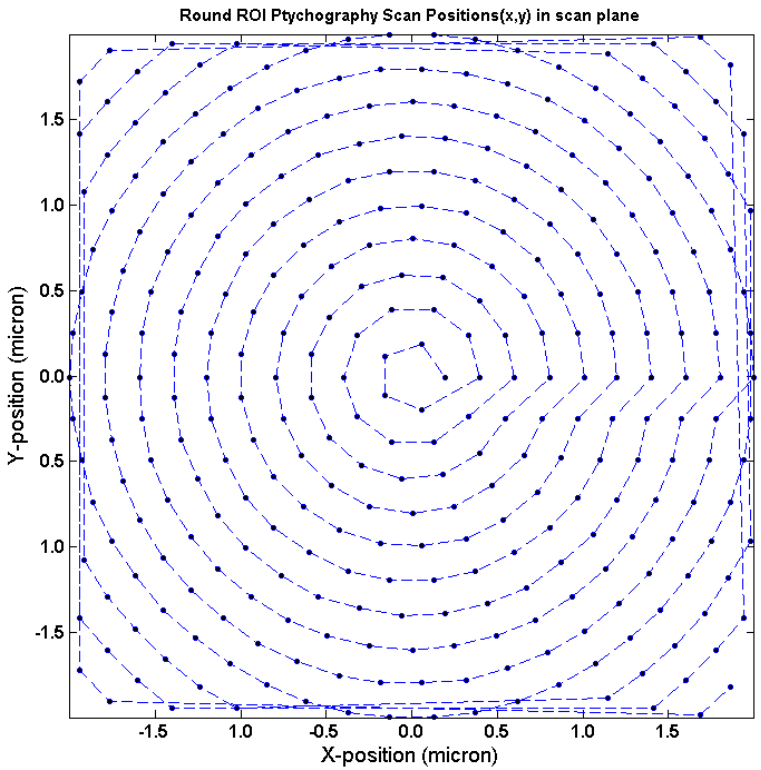

Energy= 6.2 keV (λ= 0.2 nm).
Au Fresnel zone plate (FZP):
diameter = 200 μm
outermost zone width = 50 nm
thickness of 500 nm
focal distance = 50 mm
depth of focus = 50 μm.
Pilatus 2M detector
$\Delta_{det\text{-}pixel}$ = 172 µm pixel size
Sample-detector z = 2.236 m
Optics-sample distance z_1= 270 µm
beam size d = 450 nm at the sample

total scanned area was 4×4 mm^2 with a total of 324 scanning points
0.2s exposure time at each scanning point
5 repeated scans of the sample area

Ptychography on NanoCrystals in Polymers

(a)

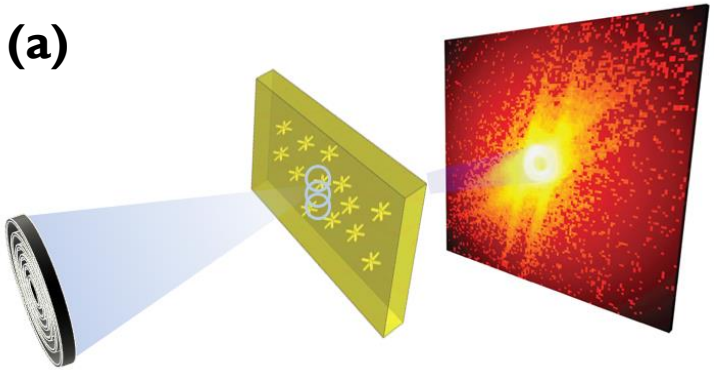

Sample	$\Delta\phi$	M_w	t_{PS} [µm]
OCT	0.044	---	0
PS 350	0.089	350	24±4
PS 350_thin	0.133	350	0.307±0.010
PS 190	0.164	190	24±4

(b)

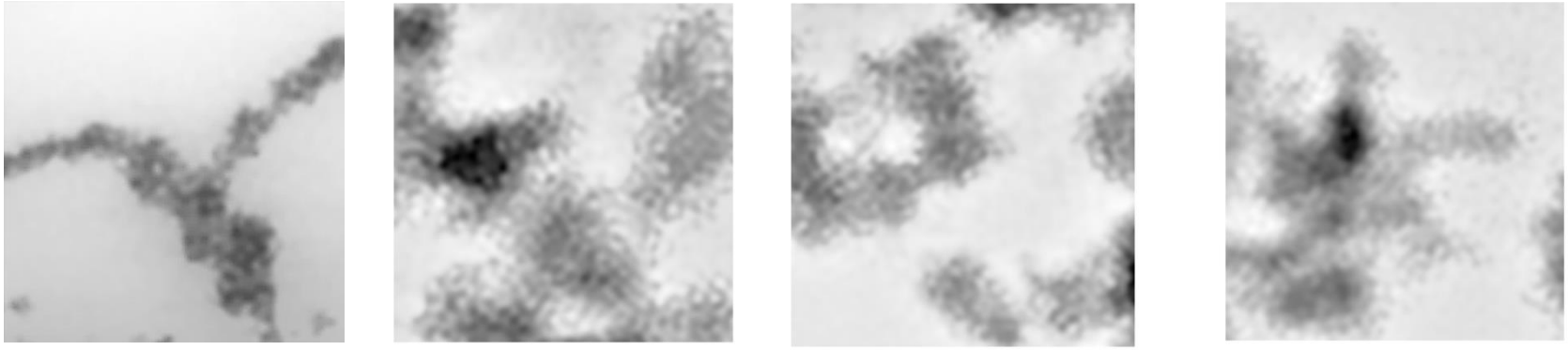

OCT PS 350 PS 350_thin PS 190

Increasing phase retardation

Ptychography on NanoCrystals in Polymers

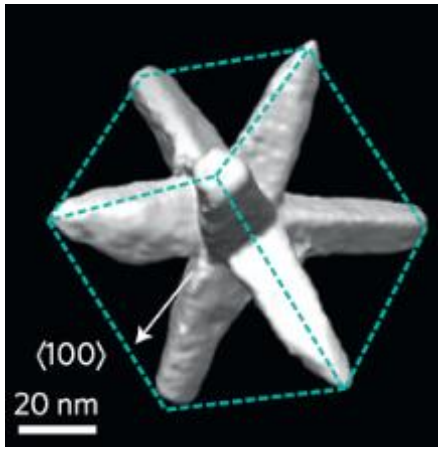

Result of the work:
we have imaged through ptychography the aggregation of **CdSe/CdS octapod-shaped nanocrystals in 25 μm thick free standing polystyrene polymers**. This X-ray-based microscopy technique allowed imaging, with a resolution of few tens of nanometers, the aggregation of the octapods in **interconnected architectures**.

SCIENTIFIC REPORTS

OPEN

Ptychographic Imaging of Branched Colloidal Nanocrystals Embedded in Free-Standing Thick Polystyrene Films

Received: 13 January 2015
Accepted: 07 December 2015
Published: 18 January 2016

Liberato De Caro[1], Davide Altamura[1,*], Milena Arciniegas[2,*], Dritan Siliqi[1], Mee R. Kim[2,†], Teresa Sibillano[1], Liberato Manna[2] & Cinzia Giannini[1]

Ptychographic data were shown on: i) PS350_thin and PS350 samples to explore the effect on the packing due to different polymer thickness for the same molecular weight; ii) PS350 and PS190 samples to explore the effect due to different molecular weights, for the same thickness of the polymer. **Data proved that both polymer molecular weight and thickness influence octapods packing.**

SINGLE NANOCRYSTAL

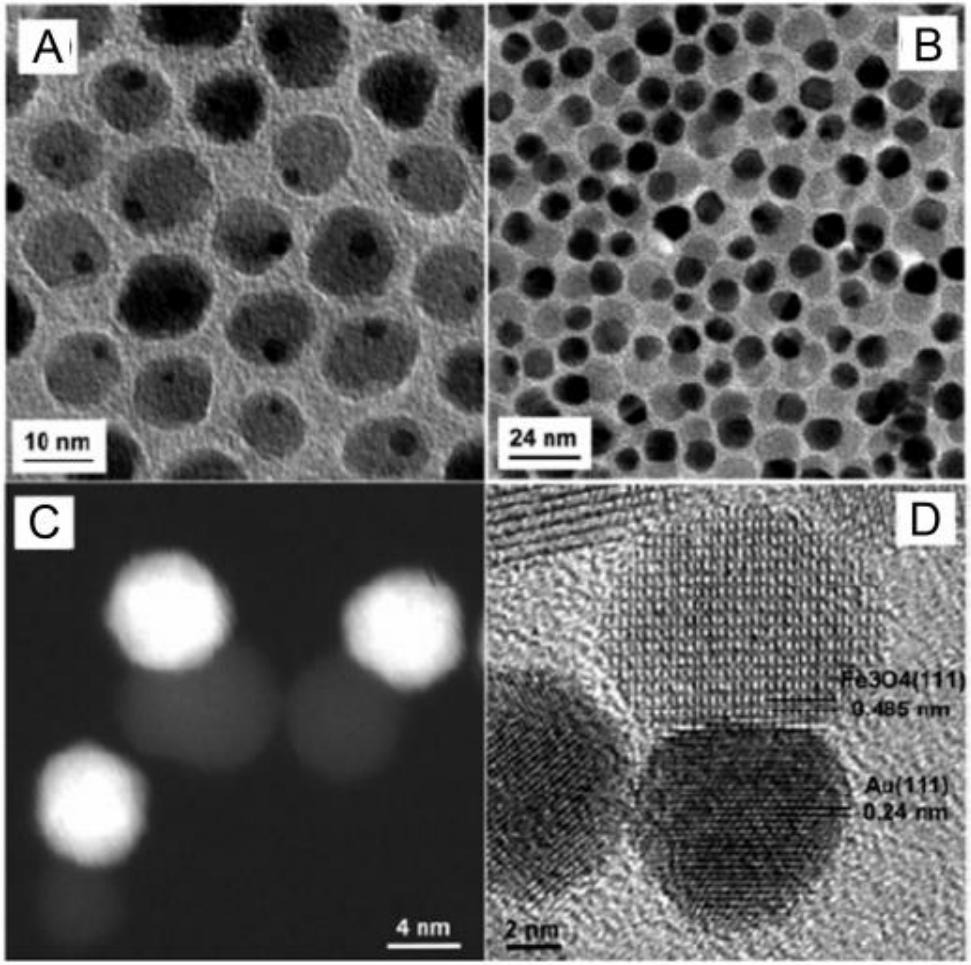

SINGLE NANOCRYSTAL

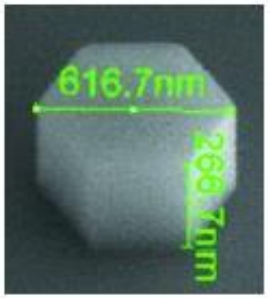

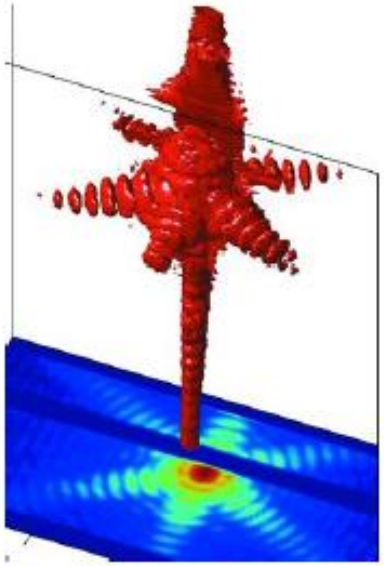

J. Synchrotron Rad. (2009). 16
Biermanns et al
GaAs Ø ~ 600nm

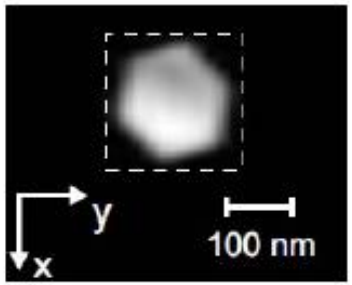

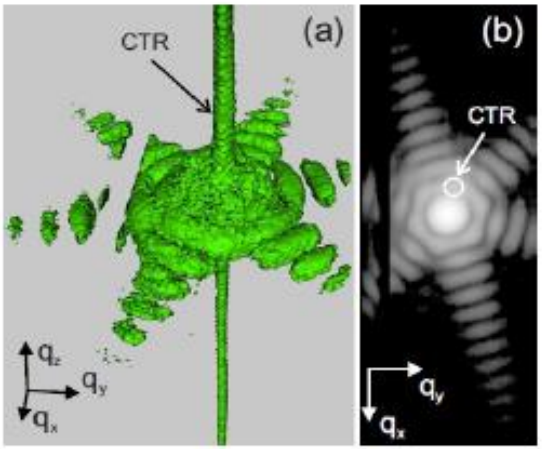

Phys. Rev. B 79, 125324 (2009)
Diaz et al
InAs Ø ~ 150 nm

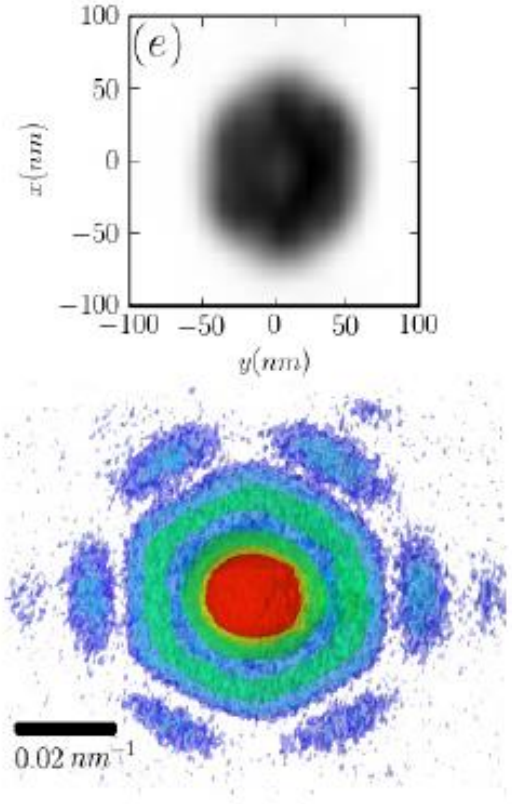

Phys. Rev. B 79, 195401 (2009)
Favre-Nicolin et al
Si Ø ~ 95 nm

Low resolution TEM

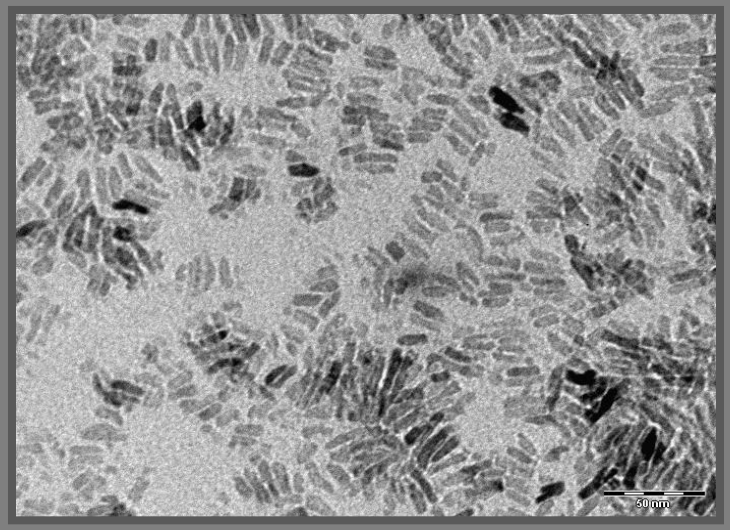

High resolution TEM

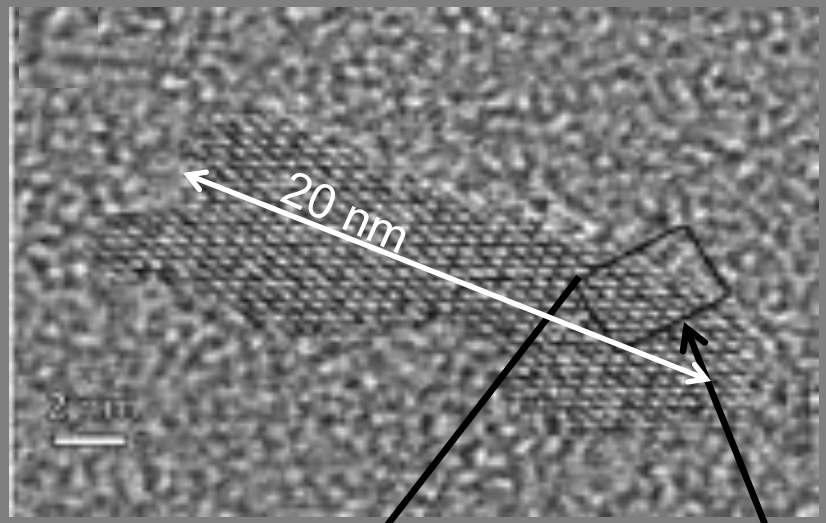

anatase nano rod

complete diffraction data

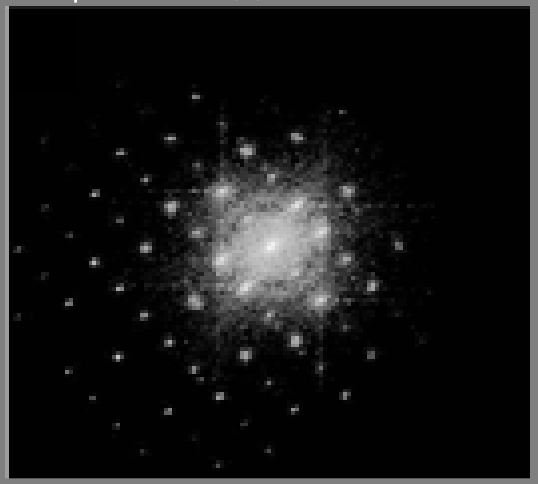

electron diffraction

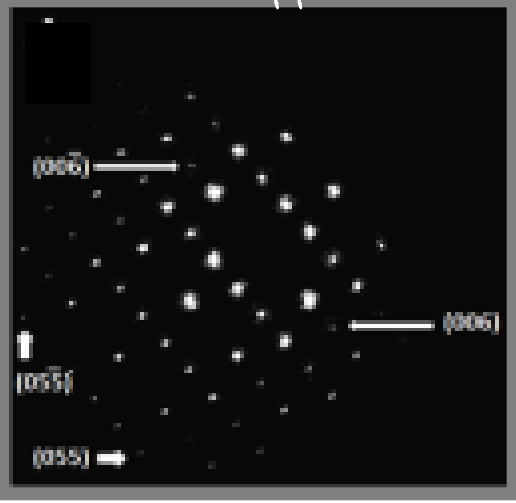

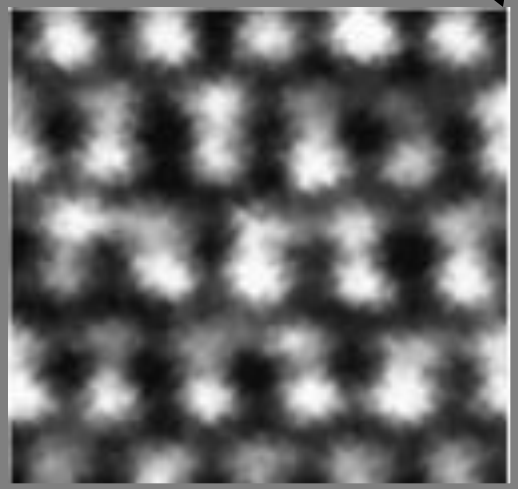

Transmission electron diffraction data

PHASE RETRIEVAL: GENERAL SCHEME

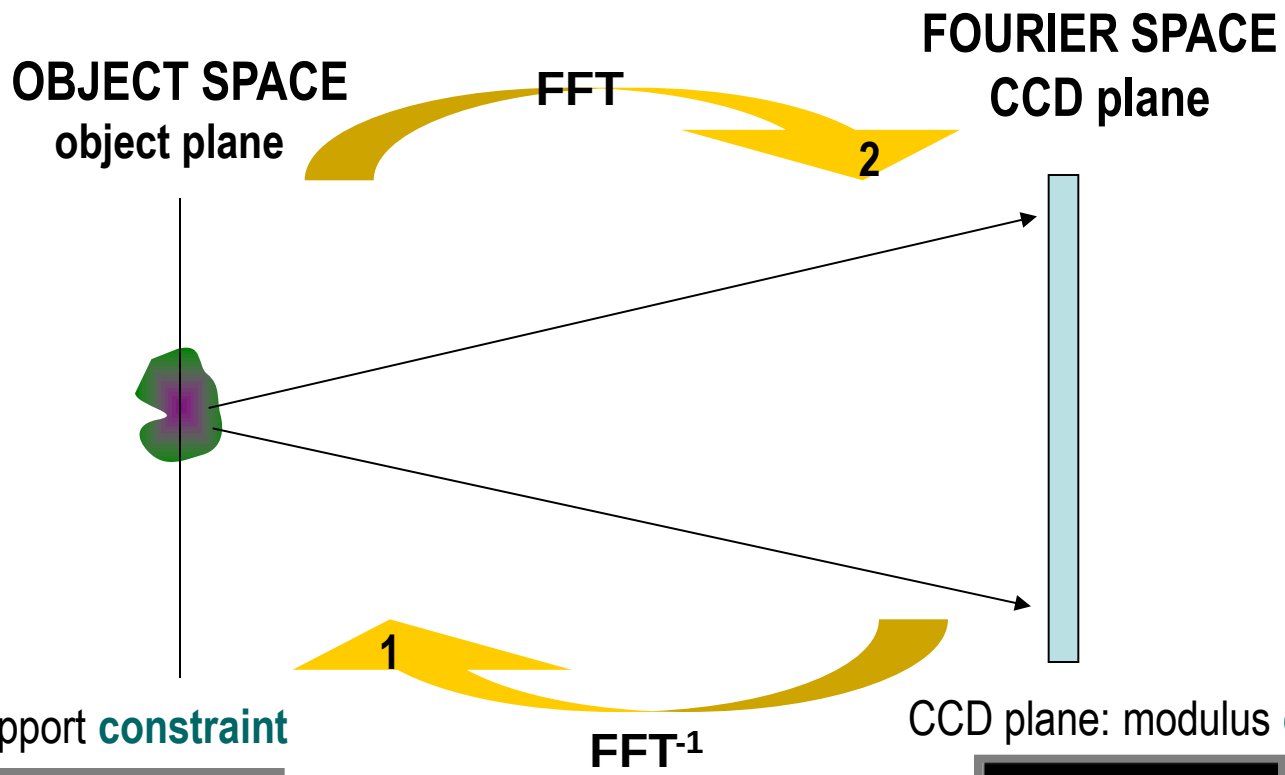

object space : support **constraint**

CCD plane: modulus **constraint**

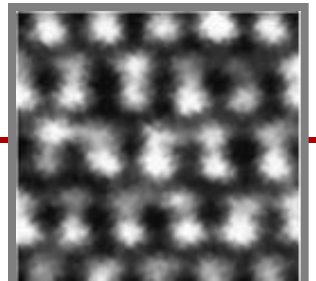

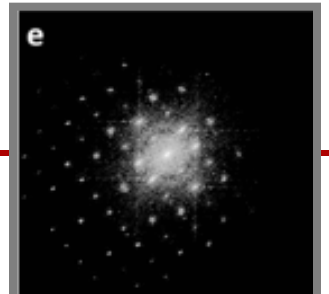

Coherent Di

ARTICLES
PUBLISHED ONLINE: 4 APRIL 2010 | DOI: 10.1038/NNANO.2010.55
nature nanotechnology

TiO_2 anatase nanocrystals
Resolution = 0.7 Å

Electron diffractive imaging of oxygen atoms in nanocrystals at sub-ångström resolution

Liberato De Caro[1], Elvio Carlino[2], Gianvito Caputo[3,4], Pantaleo Davide Cozzoli[3,4] and Cinzia Giannini[1]*

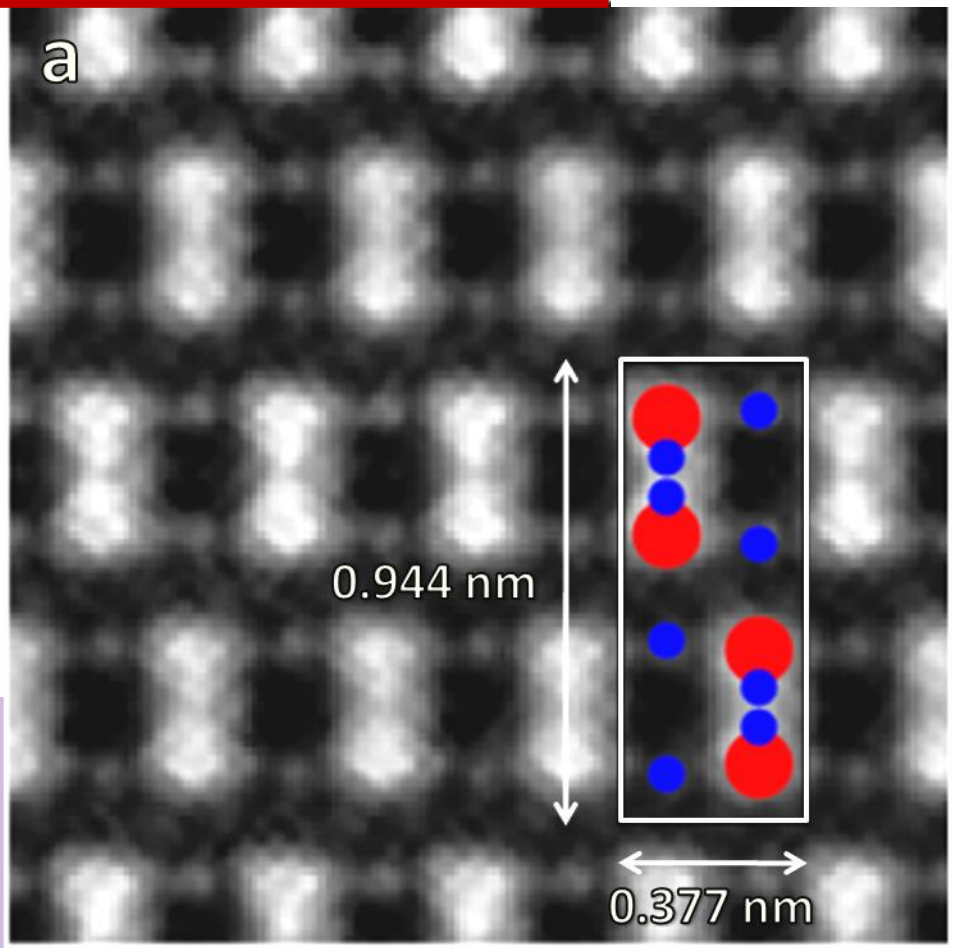

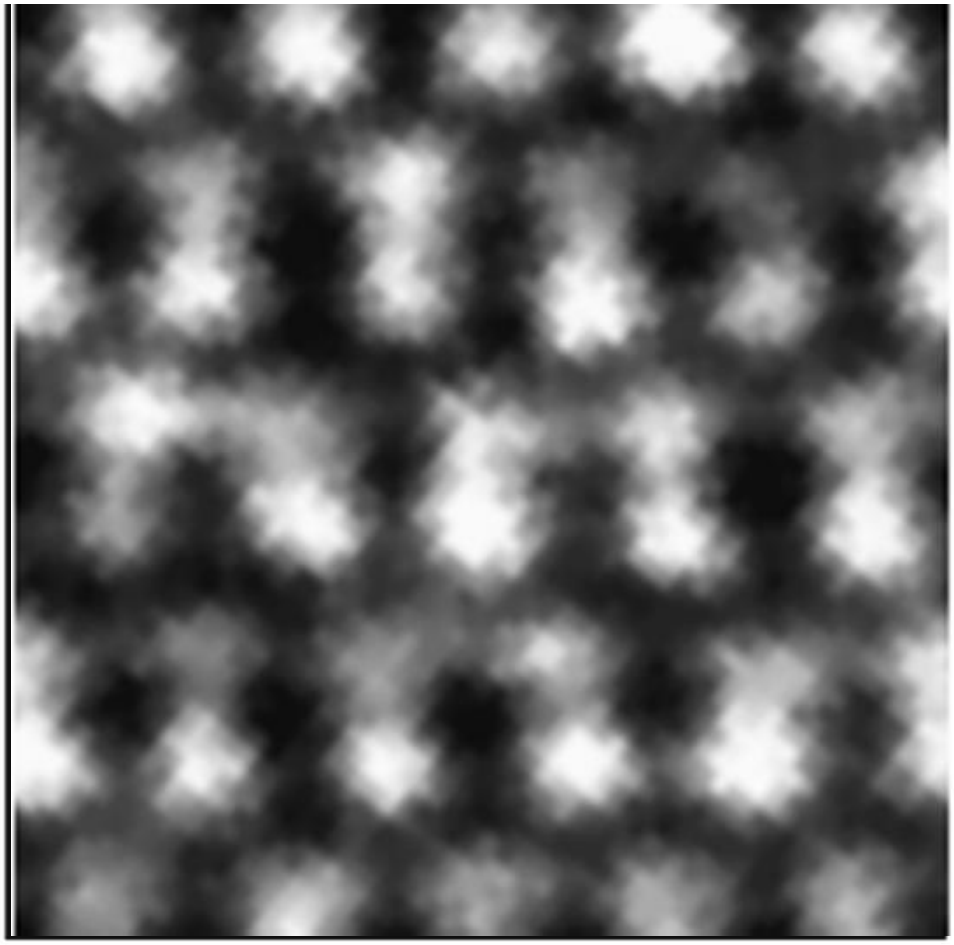

Conclusions

New materials are the foundation of major technological advances.

Examples of diffraction/imaging studies have been shown on

Nanomaterials in solutions >> SAXS/WAXS
Nanomaterials in powders, solid state >> WAXS/XRD
Nanomaterials assembled onto surfaces >> GISAXS – GIWAXS
Nanomaterials diluted in thick polymers >> Ptychography/CDI
Single Nanomaterials >> EDI